

INVESTIGATING VASCULAR PATTERNING AND REGRESSION IN KIDNEY
DEVELOPMENT AND ORGANOIDS

APPROVED BY SUPERVISORY COMMITTEE

Ondine Cleaver, Ph.D.

Denise Marciano, M.D., Ph.D.

Michael Dellinger, Ph.D.

Nikhil Munshi, M.D., Ph.D.

DEDICATION

This thesis is dedicated to all of my family, friends, and colleagues that helped me throughout my time during my Ph.D. I literally could not have done this without their support. I would like to thank my husband, Danny Ryan for moving to Texas so I could pursue this PhD and for always supporting me. I would also like to thank the following people: My parents and sisters Grace and Jane for supporting me. My friends and labmates Haley Barlow, Caitlin Maynard, Mitzy Cowdin, especially for getting me through long days in lab. All other labmates for their friendship and scientific support, including Xiaowu Gu, Neha Ahuja, Max Hiltabidle, Peter Luo, Edward Daniel, Berfin Azizoglu. Max and Mitzy specifically for helping me do experiments during the pandemic. Tezin Walji, Amrita Gohkale, Aiden Ngyuen, Phoebe Carter, Courtney Goldstein, Sarah Hanna-Addams, Alicia England, Whitney Costello, Anastasia Bobilev, Martyna Kosno and many more for their friendship and support. Edward Daniel for teaching me the kidney basics during my rotation. Maggie Brecker Cervantes for her help with organoid experiments. Chris Fourment and Amy Irby for their mentorship and teaching me about clinical research and the pharmaceutical industry. GDD program coordinator Amy Haughey. Our administrators Veronica Vilchis and Kasey Thompson for making my life easier. My previous mentors Kristin Fox, Judith Kimble, and Sarah Crittenden for preparing me for grad school and beyond. Ondine Cleaver, for mentoring me through the entire process as well as my thesis committee Denise Marciano, Mike Dellinger, and Nik Munshi. And of course my therapist Dr. Charlotte Haley.

INVESTIGATING VASCULAR PATTERNING AND REGRESSION IN KIDNEY
DEVELOPMENT AND ORGANOID

By

ANNE REGINA RYAN

DISSERTATION

Presented to the Faculty of the Graduate School of Biomedical Sciences

The University of Texas Southwestern Medical Center at Dallas

In Partial Fulfillment of the Requirements

For the Degree of

DOCTOR OF PHILOSOPHY

The University of Texas Southwestern Medical Center at Dallas

Dallas, Texas

December, 2021

INVESTIGATING VASCULAR PATTERNING AND REGRESSION IN KIDNEY DEVELOPMENT AND ORGANOID

Publication No. _____

Anne Regina Ryan, Ph.D.

The University of Texas Southwestern Medical Center at Dallas, 2021

Supervising Professor: Ondine Cleaver, Ph.D.

Chronic kidney disease (CKD) and end stage renal disease (ESRD) are increasingly frequent and devastating conditions that have driven a surge in the need for kidney transplantation. A stark shortage of organs has fueled interest in generating viable replacement tissues *ex vivo* for transplantation. One promising approach has been self-organizing organoids, which mimic developmental processes and yield multicellular, organ-specific tissues. However, a recognized roadblock to this approach is that many organoid cell types fail to acquire full maturity and function. I comprehensively assessed the vasculature in two distinct kidney organoid models as well as in explanted embryonic kidneys. Using a variety of methods, my work shows that while organoids can develop a wide range of kidney cell types, as previously shown, endothelial cells (ECs) initially arise but then rapidly regress overtime in culture. Vasculature of cultured embryonic kidneys exhibit similar regression. By contrast, engraftment of kidney organoids under the kidney capsule results in the formation of a stable, perfused vasculature that integrates into the organoid. This work demonstrates that kidney organoids offer a promising model system to define the complexities of vascular-nephron interactions, but the establishment and maintenance of a vascular network present unique challenges when grown *ex vivo*. The future of the field necessitates the inclusion of flow and perhaps additional factors into *in vitro* culture methods. Future studies investigating endothelial heterogeneity in the developing kidney will aid in forwarding our mission of creating a functional organoid vasculature.

PRIOR PUBLICATIONS

Prasad A, Porter DF, Kroll-Conner PL, Mohanty I, Ryan AR, Crittenden SL, Wickens M, Kimble J. The PUF binding landscape in metazoan germ cells. RNA. 2016 Jul;22(7):1026-43.

Daniel E, Azizoglu DB, Ryan AR, Walji TA, Chaney CP, Sutton GI, Carroll TJ, Marciano DK, Cleaver O. Spatiotemporal heterogeneity and patterning of developing renal blood vessels. 2018 Aug;21(3):617-634.

INCLUDED PUBLICATION

Ryan AR, England AR, Chaney CP, Cowdin MA, Hiltabidle M, Daniel E, Gupta AK, Oxburgh L, Carroll TJ, and Cleaver O. Vascular deficiencies in renal organoids and ex vivo kidney organogenesis. Developmental Biology. 2021 May;477:0012-1606.

LIST OF FIGURES

FIGURE 1. Process of developing personalized, transplantable kidneys for patients with kidney disease.....	4
FIGURE 2. Diagrams of nephron, filtration (left) and vasculature.	5
FIGURE 3. Model of early kidney development in the embryo.....	6
FIGURE 4. Centrally Integrated Research Network streamlines the sponsor-site relationship in clinical research trials.....	16
FIGURE 5. Activities necessary for running a clinical trial.....	16
FIGURE 6. hESC-derived kidney organoids display expected renal cell types.....	54
FIGURE 7 hESC-derived kidney organoid culture platforms.....	55
FIGURE 8. hESC-derived organoid blood vessels are sparse and lack patterning.....	56
FIGURE 9. hESC-derived organoid optimization.....	57
FIGURE 10. hESC-derived organoid vasculature regresses in culture.....	58
FIGURE 11. NZC organoids maintain epithelial and stromal cell types but suffer loss of ECs upon culture.....	59
FIGURE 12. NZC-derived kidney organoid generation.....	60
FIGURE 13. NZC organoid endothelial, stromal and epithelial cells express off-target markers.....	61
FIGURE 14. NZC-derived kidney organoids develop sparse vasculature that regresses in culture.....	62
FIGURE 15. NZC organoids display limited lumen formation.....	63
FIGURE 16. Blood vessels of explanted embryonic kidneys regress in culture.....	64
FIGURE 17. Blood vessels of explanted embryonic kidneys regress in culture.....	65
FIGURE 18. Implanted organoids display extensive vascularization.....	66
FIGURE 19. Implanted organoids display extensive vascularization.....	67
FIGURE 20. scRNA-seq comparing ECs from organoids and embryonic kidneys.....	68

FIGURE 21. scRNA-seq comparing ECs from organoids and embryonic kidneys.....	69
FIGURE 22. Macrofluidics flow chip and organoids.....	77
FIGURE 23. Microfluidics chip.....	79
FIGURE 24. Implanted organoids can cause fibrosis and transdifferentiation into chondrocytes after implantation.....	80
FIGURE 25. Yoda-1 dose-response treatment of organoids.....	81
FIGURE 26. Organoids under hypoxia.....	83
FIGURE 27. Venn diagram of gene expression analysis in adult and embryonic kidneys.....	86
FIGURE 28. Pipeline gene identification for EC heterogeneity analysis.....	86
FIGURE 29. Endothelial gene expression in embryonic kidney by zone.....	89

LIST OF TABLES

TABLE 1. Select clinical trials in CKD.....	103
TABLE 2. Human organoid EC GEO accession.....	111
TABLE 3. Human embryonic EC GEO accession.....	113
TABLE 4. Antibodies.....	114
TABLE 5. qPCR primers.....	115

LIST OF DEFINITIONS

ACE – Angiotensin-converting enzyme
ARB – Angiotensin receptor blocker
ALI – Air-liquid interface
CC3 – Cleaved caspase 3
CKD – Chronic kidney disease
DT – Diphtheria toxin
DTR – Diphtheria toxin receptor
EB – Embryoid body
EC – Endothelial cell
eGFR – Estimated glomerular filtration rate
EI – Expression index
Epithelial cadherin – E-Cad
ESA – erythropoiesis-stimulating agents
ESC – Embryonic stem cell (h- human)
ESRD – End stage renal disease
FACS – Fluorescence-activated cell sorting
FISH – Fluorescent in situ hybridization
GFP – Green fluorescent protein
GUDMAP – GenitoUrinary Development Molecular Anatomy Project
HUVECs – Human umbilical vein endothelial cells
HuNu – Human nuclear antigen
IF – Immunofluorescence
ISH – in situ hybridization
IB4 – Isolectin B4
KDIGO –
LTL – Lotus tetragonolobus
MoDTS – Mechanisms of disease and translational science
MET – Mesenchymal to epithelial transition
NIDDK – National Institute of Diabetes and Digestive and Kidney Diseases
NIH – National Institute of Health
NPC – Nephron progenitor cell
NZC – Nephrogenic zone cell
PDMS – polydimethylsiloxane
PDXL - Podocalyxin
PSC – Pluripotent stem cell (i-induced, h-human, m-mouse)
qPCR – quantitative PCR
RRT – Renal replacement therapy
SMA – Smooth muscle actin
scRNA-seq – Single cell RNA sequencing
USRDS – United States Renal Data System
VEGF – Vascular endothelial growth factor
VEGFR2 – Vascular endothelial growth factor receptor (also known as Flk1)

TABLE OF CONTENTS

LIST OF FIGURES.....	vi
LIST OF TABLES.....	viii
LIST OF DEFINITIONS.....	ix
CHAPTER ONE: Introduction.....	1
Are organoids the answer?.....	3
Mammalian kidney function and development.....	5
Vascular development.....	7
Organoids and vascularization.....	11
Perspective.....	14
CHAPTER TWO: The state of current treatments and clinical studies for chronic kidney disease.....	16
CKD causes, symptoms, and treatments.....	18
The need for new treatments and clinical trials.....	21
CHAPTER THREE: Vascular deficiencies in renal organoids and ex vivo kidney organogenesis.....	26
Results.....	29
Discussion.....	44
Figures.....	54
Figure legends.....	70
CHAPTER FOUR: future considerations, organoids require a functional vasculature.....	75
Methods of vascularization of organoids.....	75
Endothelial heterogeneity.....	85
CHAPTER FIVE: Conclusions.....	90
CHAPTER SIX: Materials and methods.....	92
BIBLIOGRAPHY.....	116

CHAPTER ONE

Introduction

Kidney disease patients need a solution

Chronic kidney disease (CKD) affects millions of people in the United States. As obesity and Type II Diabetes rates increase, so does CKD. While it is not completely understood how diabetes causes CKD, diabetes results in blood vessel damage, including in the kidney. Therefore, vascular death in the nephrons results in ischemia and nephron damage. Kidney disease is complicated in multiple ways. Kidney damage often accumulates over time, but symptoms of kidney disease are often not noticed until the kidneys only have 10% of function left. It is not possible to heal the kidney, so the clinical focus is simply preventing further damage. By the time CKD is diagnosed, many patients are close to end stage renal disease (ESRD). Once CKD has progressed to ESRD, there is no cure except a kidney transplant. Severely diseased kidneys are unable to perform the important job of filtering blood to remove waste products and maintaining fluid, salt, and acid-base homeostasis (Guyton and Hall, 2006).

Patients may be kept alive by dialysis, an external filtration system. However, this only replaces 10% of kidney function and extremely disruptive and time consuming. Additionally, while there is some effort to personalize dialysate composition, there is limited data on how this is best done, especially due to the large amounts of components. In practice, healthcare professionals often simply refer the manufacturer's guidelines. However, this lack of personalization can have dangerous consequences for patients (McGill and Weiner, 2017). Lastly, dialysis does not replace the myriad of other important kidney functions, such as vitamin D, erythropoietin, and renin production. Erythropoietin is responsible for instructing the body to produce red blood cells, resulting in CKD and dialysis patients often becoming anemic, adding to the symptoms of fatigue.

Patients may be treated with iron supplements, erythropoiesis-stimulating agents (ESAs), or blood transfusions, depending on the severity of the disease (NIDDK). More complicated is renin, an enzyme produced by the juxtaglomerular cells in the kidney that controls blood pressure through the renin-angiotensin system. This feedback mechanism can increase blood pressure by two mechanisms: The fast response is the constriction of arterioles and the slow response is to reabsorb more water and salts to increase internal fluid pressure. Alternatively, the kidneys will excrete excess water and salts to decrease pressure when it is too high. This system allows blood pressure to be maintained despite varying levels of sodium intake in the diet. Blood pressure control is especially important in CKD patients because high blood pressure is a common comorbidity of CKD and if not under control, can cause further damage to the kidney. In fact, a frequent cause of hypertension in adults is caused by partial kidney dysfunction that causes an overproduction of renin by the damaged, ischemic portion of the kidney, causing the healthy kidney to retain water and salt, increasing blood pressure (Guyton and Hall, 2006).

The survival rate of dialysis is about 5 years. Many of these patients are on the waiting list for a kidney transplant, but they are competing with 100,000 patients every year for 30,000 available kidneys. Many patients become too sick or even die before they are able to receive a life-saving transplant. If a patient is fortunate enough to receive a kidney transplant, they are not free of their illness. Even if the kidney transplant is donated by a family member, the patient is required to take immunosuppressant to prevent rejection. Immunosuppressants make patients vulnerable to communicable disease as well as some cancers that the immune system would normally have kept under check. Even with immunosuppressants, rejection can happen at any time, and a transplanted kidney only has an average lifespan of 10 years, at which point the patient will require another transplant.

Due to the limited treatments available and lack of transplants, a novel treatment is necessary. It may sound like science fiction; people have dreamed of the ability to have healthy organs available for sick patients. Biomedical scientists are working together to make that a reality. Multiple schools of thought on how to tackle this problem exist, but the overall goal is the same: design a transplantable device that allows ESRD patients to live independent, healthy lives. For this to succeed, it is necessary that nephrologists, biologists, and bioengineers work together. One effort is an NIH-funded consortium, Re-Building a Kidney, where these experts are brought together to collaborate on reaching this goal.

Are organoids the answer?

In the search for a transplantable kidney, many have looked to organoids as the solution. Organoids are 3-dimensional, self-organizing structures that differentiate into the main cell types of an organ. They can be created by directed differentiation of pluripotent stem cells or from a specific tissue's progenitors. Many organoid models exist, including liver, brain, intestine, and of course, kidneys. Organoids are an exciting new field in developmental biology and in personalized medicine. Unlike traditional cell culture, organoids allow scientists to culture complex tissues *in vitro*. Already organoids are excellent models to study disease and screen novel drugs. Enticingly, organoids can be grown from human induced pluripotent stem cells (iPSCs), meaning that tissue can be made from patients' existing cells. This will allow the transplanted tissue to avoid the immune response and freeing patient of a lifetime of immunosuppressants. If the patient has a genetic disease, the cells can be edited using CRISPR/Cas9 to correct the error and create healthy

cells. **Figure 1** demonstrates the goal of personalized medicine in kidney disease patients: iPSCs derived from patients will be used to generate an immune-matched kidney transplant.

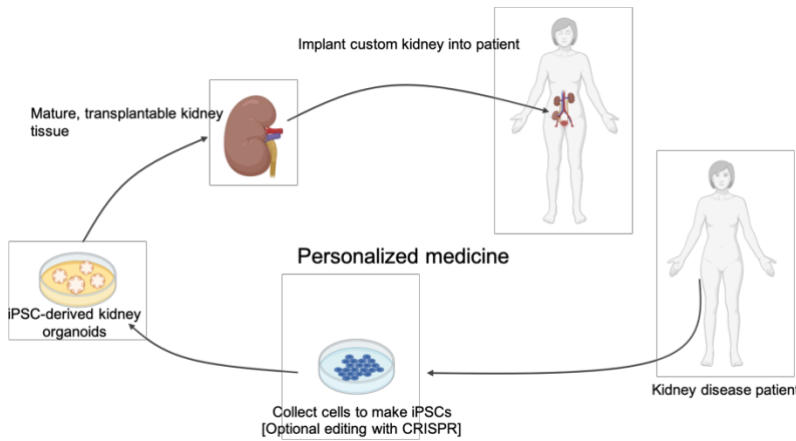


Figure 1. Process of developing personalized, transplantable kidneys for patients with kidney disease. Created using Biorender.

Despite the promising potential of organoids, the field is likely at least 20 years away from developing transplantable tissue. In order to turn organoids into transplantable organs, three

things: organization, including plumbing; nephron maturity and specification; and scalability. The most significant reason organoids are not transplantable is that while organoids form the major structures of the kidney, they are disorganized, immature, and small. The disorganization means there is no inlet or outlet to the nephrons, required for the connection to the patient's system. Once implanted, the tissue will quickly die from a lack of oxygen and nutrients if not connected to a perfused cardiovascular system. In fact, vascular dysfunction, namely renal artery stenosis, is a major cause of kidney transplant loss and patient death (Bruno et al., 2004). There is evidence of ingrowth of host vasculature into implanted organoids, but it would not be quick enough to fully vascularize a large organ. Additionally, the renal vasculature is highly patterned and functionally heterogeneous. For the kidney to function, the vasculature must form fenestrated capillary tufts in the glomeruli where affluent enters the nephron for filtration. The vasculature then leaves the glomerulus and forms the peritubular capillaries, which surround the cortical nephron, and vasa recta, which surround the loop of Henle. Peritubular capillaries are necessary for draining the nephron, absorbing secreted water and solutes. The lack of maturity in kidney organoids means

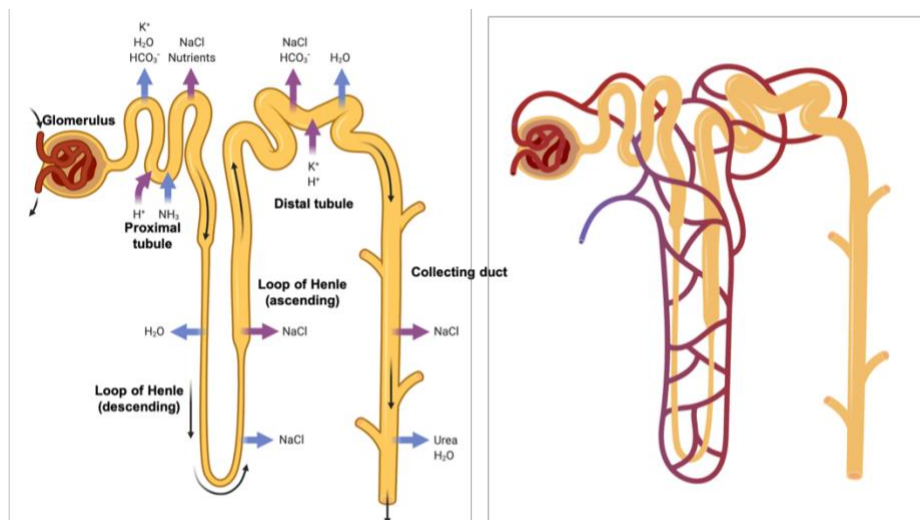
that they are not functional. Kidney organoids have a similar transcriptomic profile of a second trimester embryonic kidney (Takasato et al., 2015). There is only evidence of rudimentary function on a cellular level of the proximal tubule epithelium, but no resorption by the vasculature. Additionally, as the kidney's primary function is to filter blood, 25% of the heart's output is pumped into the kidney from the renal artery, which is a direct offshoot of the aorta. The vasculature and nephrons must be developed enough to be able to withstand the high pressure and volume of blood. Lastly, organoids are only 1-2 mm in diameter and contain less than one thousand nephrons, whereas an adult kidney contains about one million nephrons and is the size of a fist (Guyton and Hall, 2006; Takasato et al., 2015). In order to turn organoids into transplantable tissue, they will need to be much larger and properly vascularized.

Mammalian kidney function and development

The kidney is comprised of a branched network of filtration units called nephrons that aid in the removal of waste as well as maintain water and salt homeostasis. Nephrons are patterned epithelial structures, with specialized cells responsible for resorption and secretion of specific molecules (Fig. 2). Filtration starts at the glomerulus, where fluid from the circulatory system is pushed through holes, or fenestrae, in the capillary tuft. The fenestrae and podocyte foot processes work

together to create a sieve, so that cells and large

Figure 2. Diagrams of nephron, filtration (left) and vasculature (right). Filtrate flows from glomerulus through the proximal tubule, loop of Henle, distal tubule, to collecting duct. Peritubular vasculature aids in absorption of water and molecules secreted from the nephron. Biorender.



molecular weight molecules such as antibodies stay in the blood, while sugars, salts, and metabolic waste is collected into the bowman’s capsule and flows into the proximal tubule, where a majority of filtration occurs (Guyton and Hall, 2006). The filtrate moves through the nephron where necessary molecules are reabsorbed back into the peritubular capillaries, while waste continues through to the collecting duct. The effluent drains into collecting ducts, which converge into the ureter and drain into the bladder where waste is expelled as urine.

The human kidney has on average 1 million nephrons, although it varies greatly between individuals. Kidney development starts around week 5 of gestation and all nephrons are formed by birth. In the mouse, kidney development starts at embryonic day 11 (E11), continuing until around 4 days after birth (Zoetis and Hurtt, 2003).

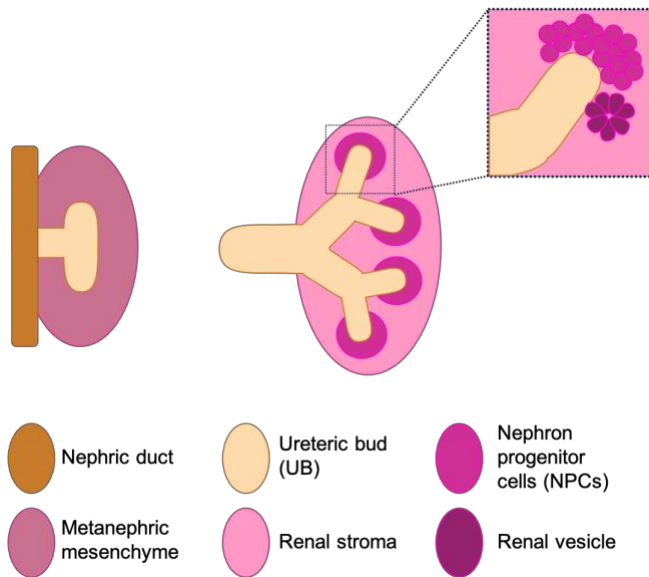


Figure 3. Model of early kidney development in the embryo. Left: ureteric budding from the nephric duct into the metanephric mesenchyme. Middle: UB branches as NPCs are maintained at the UB tips. Right: NPCs cluster underneath the NPC cap and condense to form the peritubular aggregate where the cells undergo MET to creating the renal vesicle. The renal vesicle continues to differentiate to form the nephron.

Kidney development begins from intermediate mesoderm that is located on either side of the somites. The anterior intermediate mesoderm cells undergo mesenchymal to epithelial transition (MET) to form the nephric duct (Obara-Ishihara et al., 1999). As development of the nephric duct continues caudally, three excretory organs are formed: pronephros, mesonephros, and metanephros. The pronephros and mesonephros are temporary, primitive structures. As the newer structure forms, the

more primitive structure degrades, although ducts of the mesonephros do become a part of the

male reproductive system. The metanephros, the permanent kidney, forms last. At around week 5 in the human and day E11 in the mouse, the nephric duct protrudes into the surrounding mesenchyme, which is derived from the proximal intermediate mesoderm. The budding nephric duct forms the ureteric bud (UB), which undergoes branching by planar bifurcation to form the collecting duct network. The metanephric mesenchyme gives rise to stromal progenitor cells and nephron progenitor cells (NPCs), also called the cap mesenchyme because they are present at the UB tips, forming 'caps.' As the UB branches outwards, NPCs are maintained at the UB tips, creating a nephrogenic zone on the outer layer of the developing kidney (**Fig. 3**). NPCs condense under the tip and undergo MET to form nephrons, fusing with the UB to create the connected tree (Short and Smyth, 2006). The formation of nephrons from the cap mesenchyme through reciprocal signaling with the UB has been extensively studied. (Oxburgh et al., 2004; Little et al., 2012 review.). However, there is still much to be learned about nephron development and maturation, particularly the roles played by vasculature and stroma.

Vascular development

Blood vessels develop in two ways: vasculogenesis and angiogenesis (Risau, 1997). During vasculogenesis, endothelial progenitors, or angioblasts, coalesce and form blood vessels *de novo*. Vasculogenesis occurs early in embryogenesis when angioblasts emerge from the mesoderm to form the aortae as two endothelial cords down the length of the embryo (Drake and Fleming, 2000). Next, the cords undergo tubulogenesis, opening up to form lumenized blood vessels and allowing blood flow. During embryogenesis, many blood vessels are primarily formed through vasculogenesis. Once the cardiovascular system is established, angiogenesis takes over as the primary method of new vessel formation and vascular growth. Angiogenesis is the creation of new

blood vessels from existing, pre-formed vessels. Angiogenesis can be subdivided into sprouting angiogenesis and remodeling angiogenesis (Wilting and Christ, 1996). Vessels that develop by the former mechanism sprout from currently existing vessels, while blood vessels that develop via the latter mechanism arise by either splitting an existing vessel into two (intussusception) or by fusion with adjacent vessels (anastomosis). During sprouting angiogenesis, specialized distal endothelial cells (ECs) called tip cells extend out of a pre-existing vessel and form a new vascular branch under the influence of cues in the microenvironment. After blood vessels develop, they further differentiate into different types of vessels including arteries, veins, capillaries, and lymphatic vessels. Although the cardiovascular system is arguably one of the most important organ systems in our body, we are still discovering fundamental aspects of how cells come together to form these tubular networks, especially to form complex, individualized vascular beds.

The kidney is vascularized as soon as its development begins through angiogenesis. Here, capillaries are tightly wrapped around the UB and a plexus is surrounding, but not intercalated into, the metanephric mesenchyme (Munro et al., 2017; Daniel et al., 2018). As the kidney continues to develop, so does the vasculature. Capillaries are wrapped around the maturing renal vesicle and S-shaped body in a stereotyped manner and the nephron forms. At E13.5, vascular specification begins with the formation of arteries and veins. Like UB branching, arteries branch outwards to the periphery of the developing kidney (Daniel et al., 2018). Studying this relationship between renal blood vessels and the developing nephron as well as the process of renal vascular maturation will help us to develop vascularized organoids.

Necessity of flow for blood vessel differentiation and maintenance

The requirement of blood flow for blood vessel maintenance has been known for decades. Shear stress induces many changes in ECs, influencing EC polarity, migration, proliferation, and apoptosis (Udan et al., 2013). Three well-characterized endothelial membrane proteins, platelet endothelial cell adhesion molecule-1 (PECAM-1), vascular endothelial cadherin (VE-CAD), and vascular endothelial growth factor receptor 2 (VEGFR2) form a mechanosensory complex that is responsible for EC response to flow, with PECAM-1 acting as the direct sensor (Tzima et al., 2005). The response of these proteins to shear stress results in the activation of multiple signaling cascades and pathways including ERK, SRK, AKT, NFkB, and PI3K (Tzima et al., 2005).

Disruption of flow during development, or the inability of ECs to respond to flow, results in vascular remodeling defects (Lucitti et al., 2007; Udan et al., 2013). This remodeling in response to flow is necessary for arteriovenous specification and formation for the vascular hierarchy. Particularly notable since arteries, veins, and capillaries experience different types and velocities of flow (Noble et al., 2004; Udan et al., 2013). A key element of vascular remodeling is controlled by flow: regression. Vascular regression is both a normal part of development, such as in the remodeling of the postnatal retinal vascular plexus, as well as a pathological response (Korn and Augustin, 2015). Whether pathological or developmental, regression is preempted by a cessation or blockage of flow followed by apoptosis of the downstream ECs (Meeseon et al., 1996). Therefore, not only is flow necessary for proper vascular development, it is also required for blood vessel maintenance.

Endothelial heterogeneity

Blood vessels display a remarkable variety of large and small vessels, including arteries designed to withstand high blood pressure from the heart and veins that contain valves designed to help return de-oxygenated blood through the lungs. The larger vessels join at capillary beds, where most gas and nutrient exchange happens. In addition to arteriovenous differentiation, ECs are heterogeneous structurally and transcriptionally, both between and within tissues; these phenotypes play an important role in vascular function. For example, sinusoidal ECs in the liver regulate the immune response through their fenestrations and scavenger receptors; fenestrated ECs with their unique basement membrane allow blood filtration into the nephron through the glomerulus; and the ECs in the brain have extremely low permeability to create the protective blood-brain barrier. In the kidney, the vasa recta has a unique structure that creates a slow blood flow, maintaining the concentration gradient of the medulla (Guyton and Hall, 2006).

As technology advances and single cell RNA-sequencing (scRNA-seq) studies have become commonplace, there has been an increased appreciation for transcriptional heterogeneity in all tissues and ECs are no exception (Marcu et al., 2018). As we learn more about endothelial heterogeneity in the developing and adult kidney, we can use this information to inform the creation of better, more tissue-specific organoids. The transcriptional profile of organoid ECs can indicate what vasculature organoids are able to produce—and what they aren't. In the kidney, one study utilized scRNA-seq to identify blood vessel types in the mouse kidney both during embryogenesis and in the adult (Barry et al., 2019). However, despite this incredible progress, there is still an extensive amount unknown about not just EC heterogeneity, but its developmental and functional impact. A discussion of endothelial heterogeneity in the kidney continues in Chapter 4.

Angiocrine signaling

One aspect of endothelial heterogeneity is in the cell-surface and secreted signaling molecules. There is growing evidence that endothelial cells produce angiocrine signals, diverse factors that influence neighboring cells, ranging from promoting stem cell maintenance to differentiation. For example, Rspodin3 expression in the central vein is necessary to both initially establish and maintain liver zonation (Rocha et al., 2015). In the developing brain, crosstalk between neural progenitor cells and ECs through the angiopoietin-Tie2 pathway induces TGF β 1 production by the ECs, which signals to the neural progenitors, promoting oligodendrocyte differentiation (Paredes et al., 2021). These studies show that blood vessels may be necessary to produce properly differentiated and patterned tissues *in vitro*. Additionally, crosstalk with ECs is also important in a tissue's response to stress or injury (Dumas et al., 2020). In the lung, matrix metalloproteinase 14 produced by ECs in to promote alveolarization after lung injury (Ding et al., 2011). Understanding how blood vessels respond to kidney injury and contribute to fibrosis could help discover ways to reduce scarring in improve healing. Angiocrine signaling has been investigated in many organs, but not yet in the kidney. We hypothesize that angiocrine signaling may be involved in nephron patterning, but further studies are necessary to determine if vasculature influences the developing kidney and if so, what signals are involved.

Organoids and vascularization

Takasato et al., 2015, published in Nature, was a landmark study, the first to show kidney organoids developed from human iPSCs (Takasato et al., 2015). There are multiple methods of kidney organoid generation, both from mouse embryonic kidney progenitors and pluripotent stem

cells. While there had been previous studies describing nephron progenitor differentiation *in vitro*, Takasato et al. was the first to show hiPSC-derived kidney organoids, not only with all expected cell types, but rudimentary proximal tubule function as well, as shown by dextran endocytosis by the proximal tubule. Prominent papers with methods for kidney organoid generation include Taguchi et al., 2014 (mESCs); Brown et al., 2015 (mouse embryonic kidney); Takasato et al., 2015 (hiPSCs); Freedman et al., 2015; Morizane et al., 2015; Taguchi et al., 2017; Przepiorski et al., 2018; Gupta et al., 2020 (hESCs and hiPSCs); Zeng et al., 2021 (mouse embryonic kidney); and Ryan et al., 2021 (hESCs and mouse embryonic kidney). Many of these methods share similarities and the ones in my paper Ryan et al., 2021 were derived from Takasato et al. (stem cell derived organoids), and Brown et al., 2015 (mouse embryonic nephrogenic zone cell organoids). Many of these protocols have overlapping growth factor and media components; we have found that the media additions can be distilled down to CHIR 99021 (Wnt agonist) and FGF9.

Differentiation of PSCs to kidney organoids begins with Wnt signaling activation to induce mesoderm formation. These cells further differentiate into metanephric mesenchyme, splitting off into stromal and nephron progenitor cell fates. Wnt activation is followed by FGF9 to induce MET. From here, the cells self-organize into nephron-like structures including podocytes, proximal and distal tubules, and loop of Henle (Takasato et al., 2015). Originally, it was thought that through the organoid differentiation process, both nephrons and collecting duct developed. However, this is likely due to the misattribution of collecting duct to distal tubule (Howden et al., 2021). Since this was realized, a few methods have been created to specifically develop collecting duct organoids, which can be recombined with nephron organoids (Zeng et al., 2021).

In addition to parenchyma, kidney organoids contain ECs and stroma. The exact origin of organoid angioblasts is unclear, but due to the proximity of lateral plate mesoderm and

intermediate mesoderm in the developing embryo, angioblasts are likely a non-targeted result of the differentiation process.

Embryoid bodies (EBs), the precursor to tissue-specific organoids, are simply aggregates of PSCs allowed to spontaneously differentiate by removal of stem-maintaining factors such as LIF (mouse only) or feeder cells (Kurosawa 2007). When embryoid bodies form, the stem cells differentiate into the three germ layers: mesoderm, endoderm, and ectoderm. In the embryo, angioblasts first arise from the lateral plate mesoderm; EBs form blood vessels spontaneously without the addition of any growth factors (Wang et al., 1992; Gerecht-Nir et al., 2003). These models of early embryonic development can be used as tools to study the origin of ECs, vasculogenesis, and tissue-specification of ECs (Kim et al., 2008).

As during embryogenesis, EB and organoid ECs mature over time in culture. EB ECs appear on day 3 of culture and continue to acquire expression of maturity EC genes, starting with VEGFR2, then going on to express CD31, Tie2, and then VE-Cad, followed by LVAP and CD34 (Vittet et al., 1996). This may also be seen morphologically, with ECs developing into vessel-like stages until around day 11 of culture. However, it is debated whether EB and organoid vessels are able to reach a fully mature state even with angiogenesis-promoting growth factors. The maturation of vessels by gene expression has also been shown in kidney organoids and is improved by interstitial flow (Homan et al., 2018). The importance of vasculature is often unrecognized, including in organoids. It is not uncommon for pioneer organoid publications to omit mentions of ECs. Additionally, some organoid systems such as cerebral organoids, do not appear to yield vasculature at all (Lancaster et al., 2013). As discussed in chapter 4, some organoid protocols may require the addition of ECs due to the lack of endogenous ECs. While the differentiation of

organoids follows different developmental pathways, we can use our knowledge from other systems to understand, and promote, organoid vasculature.

Perspective

As a scientist, I am driven by the fundamental question, how do cells ‘know’ how to differentiate, migrate, and form complex tissues? The cardiovascular system is often viewed as an accessory organ—simply present to support tissue survival and maintenance. It is evident however, that the vasculature is not nearly that simple. Blood vessels form an active, complex, heterogeneous system that is critical for development, not simply to provide oxygen and nutrients. My goal was to understand how. Early on in my doctoral studies, I found that there was little literature available about the renal vasculature, outside of descriptive anatomy and some studies on glomerular vasculature. To begin to address this gap, we published Daniel et al., 2018, *Spatiotemporal heterogeneity and patterning of developing renal blood vessels*. This work established vascular patterning during renal development in the embryonic mouse. In order to take this work further, higher level RNA sequencing analysis is necessary. The ongoing study of vascular heterogeneity in the embryonic kidney is outlined in Chapter 4.

There is significant research establishing how the early nephron develops and is patterned. Additionally, the function and marker gene expression profile of the differentiated nephron segments is known. However, what exactly causes this patterning is not fully understood. Organoids offer an excellent model to study tissue differentiation outside the confines of traditional *in vivo* models. When studying vasculature *in vivo*, timing is essential. Disrupting blood vessels has an immediate effect on the growth and survival of the embryo. With the organoid system, it appeared that blood vessels could be de-coupled from their role as an oxygen and nutrient supply. In particular, I was interested in studying angiocrine signaling, signals produced by ECs that

influence neighboring cells. By studying organoids outside of the cardiovascular system, we removed signals from blood circulation such as oxygen and hormones that were not directly from ECs.

As shown in this thesis, particularly in Chapter 3, organoids were not the ideal tool for studying renal vasculature. Not only is the vasculature of organoids more sparse and less organized than *in vivo*, but I found that both embryonic kidney explants in *ex vivo* culture and organoids developed vasculature, but quickly lost it. Future work in organoids is best performed under hemodynamic flow. Methods for this will be discussed in Chapter 5.

CHAPTER TWO

The state of current treatments and clinical studies for chronic kidney disease

My graduate work focused on developmental biology, studying blood vessels in developing kidneys. The basis of my thesis is the hypothesis that blood vessels produce important cues that direct nephron development. These efforts in understanding kidney development *in vivo* and *in vitro* will hopefully lead to future innovation in culturing kidney tissue in the lab for use as

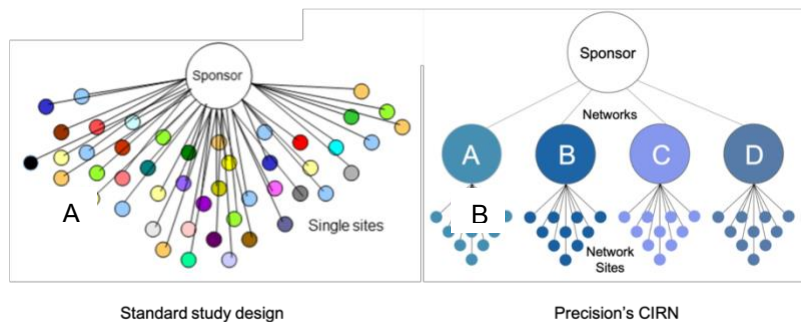


Figure 4. Centrally Integrated Research Network streamlines the sponsor-site relationship in clinical research trials. A) Standard model requires hundreds of sites, with poor communication and slow timing. B) CIRN is a carefully selected network of top research sites and sponsors. Supports sites for faster startup better site engagement.

transplantable tissue in patients with chronic kidney disease (CKD). For this project, I set off to learn about the clinical side of kidney disease in order to better understand patients' needs. First, I completed an internship from fall 2020 to spring 2021, with Precision Research. This is a new company based in Dallas, Texas that acts as a liaison between clinical research sites and the pharmaceutical companies sponsoring the research. Precision was started by an MD who worked in industry as a medical science liaison in gastroenterology. Here, he realized the challenges that come with running clinical trials; he created Precision, a centrally integrated research network (CIRN) to remove the burden from sites so healthcare providers could focus on what matters—treating patients (Fig. 4). Throughout this internship, I learned

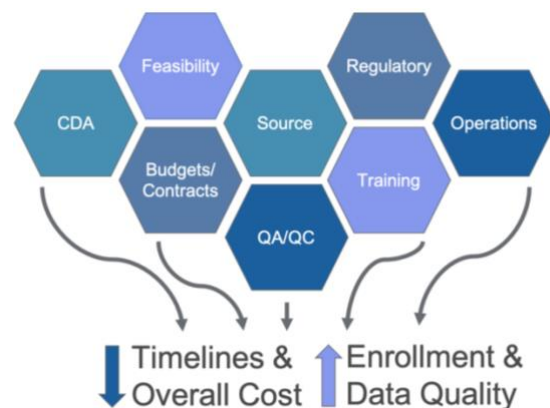


Figure 5. Activities necessary for running a clinical trial. Integrating these tasks helps streamline studies providing faster and more accurate results. CDA: confidential disclosure agreements, QA: quality assurance, QC: quality control

about the struggles of clinical trials and the immense amount of work and regulations involved in a successful trial (**Fig. 5**). Even after signing onto the study, many sites fail to recruit patients for studies. By streamlining this process, we can help patients, many who have run out of options, access novel medications more quickly. This also saves an enormous amount of time and money that is wasted setting up clinical trial sites with few enrollments, allowing drugs to come to market more quickly. My active contribution to Precision mainly consisted of aggregating information for the extensive documentation required for research sites. I also helped design pamphlets for the new neurology division of Precision to inform sponsors and potential sites, including the graphics in figures 4 and 5. During the internship, we had didactic sessions about the pharmaceutical industry and clinical trials where I gained insight into the clinical process from drug discovery to market launch. I also sat in on strategical calls with clinical research organizations and site initiation visits, learned how to identify suitable patients for studies, and attended guest lectures. Lastly, I completed a research project on multiple sclerosis, which culminated in a final presentation attended by medical science liaisons from top sponsors including Eli Lilly and Takeda.

After completing the internship, I set off to complete this research project in order to better understand CKD. This report summarizes the causes and current treatments for CKD as well as ongoing clinical trials to find novel therapeutics. Much of this report is based on information provided by the National Kidney Foundation (NKF; kidney.org); Kidney Disease: Improving Global Outcomes (KDIGO) which was started by the NKF, and is now a separate entity; and the National Institute of Diabetes and Digestive and Kidney Diseases (NIDDK)—part of the National Institute of Health (NIH)—including the United States Renal Data System (USRDS) report. These

non-profit and government organizations are fantastic sources for physicians, patients, and researchers who are interested in learning more about CKD.

CKD causes, symptoms, and treatments

Kidney disease affects roughly 1 in 7 American adults, with African Americans, Hispanics, Pacific Islanders, and seniors at an increased risk. Many people are not aware they have CKD until it becomes relatively severe due to the lack of symptoms in early stages, meaning patients could have kidney disease potentially for years before seeking treatment (NIDDK). Normally, kidneys function to filter blood and remove waste through the urine while keeping important proteins in the blood. When the filtration function does not work, patients may experience symptoms such as fatigue, swelling of the feet, frequent urination, and muscle cramping (kidney.org). The first test to assess kidney damage is likely a urinalysis for albumin. Albumin is a protein found in the blood that normally should be blocked from entering the urinary system by the kidney. However, if the kidney is damaged, this can cause albumin to slip through. Elevated levels of albumin in the urine, called albuminuria, is an indicator of kidney damage (kidney.org). The next step in diagnosing CKD is to determine how well the kidney is functioning and filtering the blood by analyzing blood creatinine levels. Creatinine is a protein waste product that results from muscle breakdown that is normally filtered out by the kidneys, therefore high levels of creatinine in the blood indicates problems with kidney function (kidney.org). Using creatinine levels and taking into account age, race, and sex, the estimated glomerular filtration rate (eGFR) may be calculated. Based on eGFR, the stage of CKD is determined. Patients in stage 1 of CKD have some kidney damage, but still have normal kidney function, with an eGFR of 90 or higher. The highest stage, stage 5, is kidney failure, with an eGFR of 15 or less. eGFR is calculated based on the blood creatinine levels

(kidney.org, NKF-KDIGO, NIDDK). As eGFR decreases, all-cause mortality increases (NKF-KDIGO; Matsushita et al., 2010).

There are various causes of CKD, including congenital defects in the kidney, inflammatory and autoimmune diseases such as lupus, polycystic kidney disease, as well as kidney damage that can occur from repeated urinary infections, kidney stones, or overuse of certain painkillers (kidney.org). However, the most common causes of CKD are diabetes and high blood pressure, present in about half of CKD patients (NIDDK). This is because both conditions can damage the blood vessels in the kidney. In fact, all CKD patients are considered at risk for cardiovascular disease, which is a significant mortality risk (NKF-KDIGO; Matsushita et al., 2010). Type II diabetes, high blood pressure, and obesity are common comorbidities in patients with CKD and put patients at greater risk of developing and progressing CKD. At present, there is no cure for CKD. The focus of clinicians is on preventing further damage to the kidneys and slowing down the progression of CKD by controlling blood pressure, diabetes, weight, and cholesterol through diet modifications and exercise (NKF-KDIGO). Medications targeting these conditions may be prescribed in addition to lifestyle changes. There are many blood pressure drugs on the market; two classes, angiotensin-converting enzyme (ACE) inhibitors and angiotensin receptor blockers (ARBs), are commonly prescribed for CKD patients and have been shown to reduce kidney damage (NIDDK). Diuretics are often prescribed for kidney patients, although they can increase the risk for acute kidney injury (NKF-KDIGO). Statins, drugs that help control cholesterol, are some of the most highly prescribed medicines in the United States. Lastly, there are multiple drugs on the market now for patients with Type II diabetes, one of the leading causes of CKD. The oldest Type II diabetes drugs are sulfanoureas, such as glipizide, that induce insulin production by the pancreas (Betonico et al., 2016). Sodium-glucose co-transporter 2 (SGLT2) inhibitors such as

Jardiance (empagliflozin) and Farxiga (dapagliflozin) reduce blood sugar in patients by stopping glucose reabsorption in the proximal tubule and have been shown to slow the progression of CKD and reduce the risk of cardiovascular death (Zinman et al., 2015; Wanner et al., 2016; Tuttle et al., 2021). Kerendia (finerenone) was recently Food and Drug Administration (FDA) approved for Type II diabetes-associated CKD patients (kerendiahcp.com, Filippatos et al., 2020). It is an oral, non-steroidal, selective mineralocorticoid receptor antagonist that inhibits inflammation and fibrosis and protects against progressive kidney and cardiovascular dysfunction (Grune et al., 2018). In addition to disease modifying treatments, medications that target specific side effects of CKD, including anemia and swelling, can also help patients.

Once CKD progresses to kidney failure, or end stage renal disease (ESRD), there is no cure except a kidney transplant. Renal filtration is supplemented through dialysis, or renal replacement therapy (RRT). There are two types, hemodialysis and peritoneal dialysis. With hemodialysis, the patient's blood is cycled through a dialysis machine that filters the blood and returns it to the patient. This is a time-consuming endeavor that is usually performed at a dialysis center, about three times a week for four hours per session (kidney.org). Peritoneal dialysis is where a dialysate flows into the abdominal cavity through a catheter and is then drained after allowing time for waste product to exchange. This setup allows patients to undergo dialysis at home, but it is not a feasible option for everyone (kidney.org). While dialysis does filter the blood, there are many other functions of the kidney that it does replace. For instance, kidneys secrete erythropoietin which controls red blood cell production, leading to many patients on dialysis being anemic. Importantly, patients undergoing dialysis only have around a 50% 5-year survival rate. Kidney disease has an incredible impact on people's quality of life and patients who progress to kidney failure have a drastically decreased lifespan. Dialysis is also an immense burden on the healthcare system, so it

is essential to discover new treatments that can improve patients' life and delay the progression to ESRD (USRDS).

The need for new treatments and clinical trials

Especially in the United States, rates of CKD are rising, highlighting the importance of finding a novel therapies (USRDS). I attended Kidney Week in 2019 (Washington, D.C.) and 2020 (virtual), an annual conference hosted by the American Society of Nephrology. This is a large meeting, attended by around 10,000 nephrology professionals, including physicians, academic scientists, and people in the pharmaceutical industry. It really stood out to me how much need there is for treatments for kidney disease. One speaker noted that with current treatments, many patients' CKD still progresses. Many drugs are not directly targeting inflammation or fibrosis in the kidney, but only affecting blood pressure and diabetes control. Additionally, many clinical trials fail. For instance, Losartan, a blood pressure drug that is used in type II diabetes patients to reduce kidney strain was found to have no difference over placebo in preventing CKD. Even if a drug is found to be effective, it takes about 12 years of testing in clinical trials and over 800 million dollars before it will be widely available for patients (DiMasi et al., 2003).

Clinical trials are necessary in order to prove the efficacy and safety of a drug or treatment for it to be approved by the FDA for public use. There are two main kinds of clinical studies: interventional and observational. Observational studies are not providing patients with an investigational treatment but can be studying the long-term effects or a mechanism of a drug that may be already FDA approved, or assessing different diagnostic methods. Interventional studies, or clinical trials, are what come to mind when thinking of clinical research: when a new treatment is being tested for safety and efficacy. Interventional studies can also be behavioral or dietary

additions or changes. There are about three times as many active interventional studies as observational. Observational studies are less risky and less expensive than interventional but are also not going to lead to a new treatment for patients. However, they are still extremely useful in order to understand how populations with different genetic backgrounds may present the disease or respond to treatments, as well as identify important diagnostic tools that could help patients begin the right treatment earlier.

Studies of new treatments first start in the lab, where drugs are tested in cell culture and animal models in pre-clinical trials. If approved for human studies, they can be tested in a small group of healthy patients to assess drug safety and metabolism. Phase II and III test the drug in patients with a specific disease for the drug. Phase III is a larger study than phase II and either compares the drug to placebo or a standard treatment to determine if the new drug is better than existing therapies. These studies show that the drug is effective for managing the disease but do not result in an unacceptable number of side-effects. Even once a drug is approved, studies may continue in order to study the long-term effects or the mechanism of a drug. Although expensive and time-consuming, the extensive clinical trial process is necessary to ensure patients are only treated with effective and safe drugs. Additionally, one drug may be part of multiple clinical trials at once. A new trial must be undergone for every indication of a disease. For instance, the drug Esbriet (pirfenidone) is approved by the FDA to treat idiopathic pulmonary fibrosis. It is now part of a phase II clinical trial in order to assess its efficacy in delaying CKD progression. A new clinical trial must also be performed for different patient populations, i.e., adult vs. pediatric. According to ClinicalTrials.gov, a clinical trials database run by the NIH, there are 3716 studies involving kidney disease, and 1165 related to CKD that have been or are being done in the United

States (12 at UT Southwestern Medical Center). 224 of the CKD studies are either currently enrolling patients or are active (clinicaltrials.gov).

There are too many ongoing clinical trials to discuss here, but a list of 54 clinical trials may be found in **Table 1**, along with the trial number, drug or device being assessed, sponsor, phase, enrollment goals, timeline, and other indications. Many drugs undergoing trials are not directly treating CKD, but aimed at treating common side-effects such as hyperphosphatemia, vitamin D deficiency, and anemia. Some treatments are simple and cost-effective, such as sodium bicarbonate (baking soda) administration to treat acidosis. During my Mechanisms of Disease and Translational Science (MoDTS) clinical internship in 2017, I learned many patients were wary of “drugs” and preferred “natural” remedies and were more open to a mix of baking soda and water than something like an antacid pill.

Biologics such as monoclonal antibodies are more commonly used now and are highly effective for many immune-mediated diseases such as inflammatory bowel disease and psoriasis. Some studies of patients with immune-mediated diseases who are taking biologics such as anti-TNF monoclonal antibodies had a lower risk of CKD progression, likely due to the anti-inflammatory effects (Sumida et al., 2018). However, these treatments have not yet been investigated directly for CKD and there are not any biologics on the market yet, but studies are beginning to investigate some. In a similar vein, Clazakizumab, an anti-IL-6 monoclonal antibody is being investigated for kidney transplant patients in order to reduce rejection, particularly in patients who have rejected a previous kidney transplant. Clazakizumab may help remove donor specific HLA antibodies to desensitize the patients and prepare for the new transplant (clinicaltrials.gov). This could help transplanted kidneys last longer and prevent patients from requiring high dose immunosuppressants.

AstraZeneca is sponsoring a phase I study (NCT04365218) of monoclonal antibody MEDI8367. The antibody binds to human integrin $\beta 8$ and inhibits its TGF β activation to reduce kidney fibrosis (Marin et al., 2020). This study will have healthy patients and patients with CKD. There are over 50 primary outcomes, including adverse events and multiple blood and urine tests to ensure the safety and tolerability of the antibody (clinicaltrials.gov). A phase I study (NCT04699032) sponsored by VectivBio AG is investigating Apraglutide, a peptide glucagon-like peptide 2 (GLP-2) analogue that acts as a GLP-2 receptor agonist. Since it promotes nutrient absorption and gut epithelium proliferation, this drug is also being investigated in short bowel system. It may have a beneficial effect on glucose metabolism and help protect against Type 2 diabetes (Amato et al., 2016).

The last interesting treatment being investigated that I would like to focus on is stem cell treatment. A phase I study by the Mayo clinic (NCT03840343 and NCT04869761) is investigating infusion of adipose-derived mesenchymal stem cells for patients with diabetic CKD. The study is mostly focusing on safety, as the primary outcomes are the number of adverse events that patients experience. Researchers will also assess kidney function by eGFR to determine if patients stayed the same, improved, or worsened. This research is based on improvement shown in animal models by injecting cells or cell products (Hickson et al., 2021). Stem cell therapy is gaining in popularity, but currently, there are not enough human studies to show that systemically injecting stem cells into a patient will cure kidney disease. Further studies both in animals and humans will be required to determine efficacy and understand mechanisms behind stem cell therapy.

Throughout my experience with MoDTS, I learned what physicians and patients go through when battling an illness. Every patient is unique, and medications are not one size fits all. We must continue to search for alternative treatments that work better, are cost effective, and are readily

accepted by patients. This is especially true for CKD as it becomes increasingly prevalent. Many new therapies are currently being investigated. However, clinical trials are time-consuming and expensive, especially due to the regulatory requirements necessary to keep participants safe. Despite the cost, both basic research and clinical trials are integral to finding new treatments and potentially a cure for CKD, which could save millions of lives.

CHAPTER THREE

Vascular deficiencies in renal organoids and *ex vivo* kidney organogenesis

Introduction

Current treatment strategies for end stage renal disease (ESRD) are largely refinements of approaches developed almost a century ago, including dialysis, supportive care, and whole kidney transplantation. For most patients, kidney transplantation is the best option; however, demand greatly surpasses the supply of available organs. For those who do ultimately receive a transplant, the average wait time for a kidney is 3–5 years and the threat of immunologic rejection is ever present (Nankivell and Alexander, 2010). Recent technological advances are providing hope for alternative sources of functional renal tissue. Current work in stem cell and regenerative medicine has the potential to provide a historic turning point in treatment possibilities and its success could provide treatment for millions of individuals with chronic kidney disease that will progress to ESRD. The last half-decade has witnessed rapid advances in stem cell technology for kidney tissue differentiation. Critical proof-of-principle generation of kidney tissue ‘in a dish’ provides viable new experimental approaches with potential for clinical application. Kidney tissue engineering and regeneration efforts have largely focused on epithelial and endothelial components, as these two cell types are responsible for much of renal filtration function. Beginning in 2015, several landmark studies established protocols to differentiate induced pluripotent stem cells (iPSCs) or embryonic stem cells (ESCs) into self-organizing organoids with the capacity to produce a wide range of kidney cell types (Morizane et al., 2015; Taguchi et al., 2014; Taguchi and Nishinakamura, 2015; Takasato et al., 2015, 2016a; Takasato and Little, 2017) Alternative techniques have also been explored, including decellularized kidney matrices and ‘organ-on-a-chip’ technologies. However, it has ultimately become clear that achieving conversion of *ex vivo* generated kidney tissue into

patient kidneys will require a full understanding of how kidney tissue develops, specifically epithelial tubules and their closely-associated interstitium, which includes both blood vessels and stroma. These approaches that recapitulate normal kidney development hold a tangible promise for generating functional replacement tissue. Despite these significant advances in tissue engineering and stem cell biology in the last decade, we have not yet achieved transplantable kidney tissue. In order to generate potentially functional replacement kidneys, the tissue must be scaled in size to fit the host and plumbed appropriately, allowing for blood filtration and urine excretion. One increasingly recognized obstacle in laboratory-created tissues, including organoids, is the difficulty of growing and maintaining a functional vasculature. Blood vessels are necessary for tissues to develop long-term and to achieve sizes beyond the limit of oxygen and nutrient diffusion. Lastly, growing evidence supports the necessity of vasculature in promoting differentiation and maturation of tissues, including the kidney (Raffi et al., 2016; Rocha et al., 2015; Rymer et al., 2014; van den Berget al., 2018; Yao et al., 2017). In fact, numerous studies have recognized this importance and shown that mimicking flow can ameliorate organoid vascularization (Homan et al., 2019; Morizane and Bonventre, 2017; Zhang et al., 2017). Despite this progress, nascent organoid vasculature still falls short. Across published protocols, organoid blood vessels generated are immature and disorganized, and our understanding of their specification, formation, and dynamics is limited. The low and transient expression of endothelial genes in kidney organoids has been shown by qPCR, but the endothelial cells (ECs) themselves have not been analyzed throughout this process (Takasato et al., 2015). In addition, it is still unclear how kidney vasculature is specified *in vivo*, how its heterogeneity might impact kidney cell types, and the dynamics of EC growth during *in vitro* culture. As the existing analysis of organoid vasculature to date has been limited, a closer look at organoid blood vessels is warranted. In this

study, we assess the dynamics, maturity, and maintenance of blood vessels in renal organoids, cultured kidneys, and implanted organoids. Using organoids generated from either human embryonic stem cells (hESCs) or mouse embryo nephrogenic zone cells (NZCs), we explore vascular structures and their growth. We show that the vasculature in both types of organoids is transient and fundamentally defective. While epithelial kidney cell types display relatively normal specification and initial patterning, the vasculature largely fails to thrive. Organoid vessels display significantly lower density and complexity than equivalent normal midgestation kidney tissue and vessels largely fail to associate with kidney epithelium. Most significantly, organoid vessels regress over time in culture. To test whether vascular regression is precipitated by initial failure of EC specification during directed differentiation of hESCs, we examine vessels in cultured embryonic kidneys and NZC-derived organoids, both of which already contain ECs. We observe significant regression in all three systems, suggesting necessity of hemodynamic flow in vessel maintenance. When organoids are implanted under the kidney capsule of adult mice, however, they are vascularized by the host. Notably, implanted organoids display capillary tufts in the glomeruli. To identify differences between ECs in lab-generated kidney tissue versus normal embryonic kidney, we analyze publicly available single cell RNA sequencing (scRNA-seq) data comparing ECs in week 8–18 human embryonic kidneys to those in human ESC and iPSC kidney organoids (day 0–34). We find that early during culture, organoid ECs have a similar transcriptional signature to embryonic ECs, but progressively diverge over the course of culture. Self-organizing models of renal development, such as organoids, offer a promising tool for studying the kidney and for engineering replacement kidney tissue; however, our work underscores critical shortcomings of organoid vasculogenesis and demonstrates the importance of developing methods to promote, maintain, and properly identify blood vessels in cultured kidney tissues.

Results

Kidney organoids generated from hESCs

To investigate blood vessels in kidney organoids, we used a previously published protocol (Takasato et al., 2016b) as a basis for differentiating hESCs. In this method, we differentiated hESCs in monolayer before collecting and aggregating cells to form organoids (Fig. 6A). We optimized the protocol by modifying the CHIR treatment length during hESC differentiation to achieve a maximal quantity of endothelial cells (ECs) while still generating a significant portion of renal structures (Fig. 7A-H). As described in (Takasato et al., 2016a), the ratio between nephrons and collecting duct in the organoids may be controlled by altering the length of CHIR treatment vs. FGF9 during the 7-day differentiation step (day -7 to day 0). A longer treatment of CHIR during hESC differentiation—and a subsequently shorter FGF9 treatment—results in organoids with a higher ratio of nephrons. Additionally, each cell line must be optimized for CHIR concentration and length to account for any variability in response to treatments (personal communication). We tested 4 μ M, 6 μ M, and 8 μ M CHIR and we assessed the effects of CHIR/FGF9 switch at day -4 or -3. Optimal organoid formation occurred with 6 μ M conditions and are shown (Fig. 8A-H). A 4-day 6 μ M CHIR treatment was selected as the standard method. After 7 days of hESC differentiation in monolayer (day-7 to day 0), we assessed differentiating cell types. E-cadherin (E-Cad)⁺ epithelium formed tubule-like structures (Fig. 6B', arrows and 6C) surrounded by Meis1/2/3⁺ stromal cells and Six2⁺ nephron progenitor cells (NPCs) (Fig. 6B). Scattered VEGFR2⁺ angioblasts (with rare co-expression of Sox17, a marker of EC specification) were observed as well (Fig. 6D). Organoids were generated by collecting the mixed population of differentiated cells from monolayers and either pipetting droplets of approximately 100,000 cells onto filters or into ultra-low attachment 96-well plates in suspension (Fig. 7I). In the first instance, organoids were

cultured on Transwell filters at the air-liquid interface (ALI), in a manner similar to typical mouse kidney explant culture (Fig. 7I, left) (Takasato et al., 2016a). These organoids were large in diameter (~2 mm) and displayed a flat pancake-shaped appearance (Fig. 7J; Fig. 9A). By contrast, when cells were cultured in low attachment plates, they self-aggregated and developed as rounded clusters (diameter of about 1mm) submerged in media (Fig. 6E and Fig. 7I, right). The low-attachment plate method with submerged organoids was chosen as it yielded more consistent organoids than Transwell organoids, as we found the latter more frequently and stochastically failed to form nephrons (Fig. 9B). Using the submerged organoid production method, we found that, as previously reported, self-organization into visible tubules could be observed after four days of culture (Fig. 6E) (Takasato et al., 2015).

hESC-derived kidney organoids contain specialized epithelium and stromal cells

We confirmed that hESC-derived kidney organoids produced the expected range of renal cell types in accordance with previous studies (Morizane et al., 2015; Takasato et al., 2015, 2016a). Using immunofluorescence, we showed that organoids developed NPCs, tubule epithelium, and stromal cells (Fig. 6F–H, Fig. 7A). Epithelial tubules stained for E-Cad; with a subset of Lotus Tetragonolobus Lectin (LTL)⁺ proximal tubules (Fig. 6F). However, in a deviation from normal kidney tissue, we found that LTL was not restricted to the apical surface of lumens as it is *in vivo* (Fig. 9F'). We also found scattered glomerulus-like structures of Podocalyxin (Podxl)⁺ podocytes (Fig. 6G). Between epithelial structures, we observed stromal cells identified by Meis1/2/3 (Fig. 6H). Hence, the hESC-derived organoid protocol altered to increase EC production still generated most expected kidney cell types, similar to previously reported protocols, but with some deviations from normal kidneys.

Vascular density in hESC-derived kidney organoids is low

We next examined the vascular structures in hESC-derived organoids at day 12, a stage previously reported to display staining for known endothelial markers (Takasato et al., 2014). Immunofluorescence for established EC markers CD31, Sox17, and VEGFR2 demonstrated the presence of positive cells at this stage (Fig. 8A–C). We found that Sox17 was the most reliable marker of ECs in the organoids. Although most presumptive ECs were Sox17⁺CD31⁺ (Fig. 8C, yellow arrow), a subset were Sox17⁺CD31⁻ (Fig. 8C, white arrows). As seen by the 3D view of the organoid (Fig. 8A, C) and in optical slices (Fig. 8B), ECs organized into thin, linear aggregates with some interconnections, suggesting a primitive plexus. Therefore, by both marker expression and morphology, these vascular structures resembled blood vessels. One striking and consistent observation, however, was that organoid vessels were distinctly sparse compared to kidneys *in vivo*. We compared the relative density by volume of vessels in normal embryonic kidneys to that in organoids and found that organoids had a significant reduction in ECs by whole mount immunofluorescent images (Fig. 8D–F). Despite selecting the most highly vascularized sections of the organoids for comparison, quantification showed hESC organoids contained less than 2% ECs by volume compared to more than an average of 20% for embryonic day 12.5 (E12.5), E13.5, and E14.5 kidneys (Fig. 8F). Together, these data showed that at day 12, the overall vascular mass in organoids was over 80% lower than in normal tissue.

Blood vessels in hESC organoids lack both patterning and lumens

We further analyzed organoid vessels to examine other aspects of renal vessels, including their physical association with kidney cell types, which is normally required for proper physiology. In

the mouse embryonic kidney, the developing renal epithelium is surrounded by a plexus of vessels (Fig. 8G) and the glomeruli consist of a complex capillary tuft enveloped by podocytes (Fig. 8H) (Daniel et al., 2018; Vaughan and Quaggin, 2008). By striking contrast, we found that kidney organoid vasculature was largely not associated or aligned with the epithelium (Fig. 8I) and organoid podocytes were not vascularized (Fig. 8J). Instead, we often observed a loose plexus of ECs extending throughout the organoid, but not surrounding epithelial structures, and only occasionally associating with podocytes (Fig. 8J, arrow). Altogether, the organoid vessels appear unstructured. Furthermore, we find that organoids have reduced vascularity and patterning, as measured by a reduced number of blood vessel branch points and fewer points of EC-epithelial contact (Fig. 9C-D). We further noted that most vascular structures in the organoids presented as either single cells or cords of single cells; most cords were not wider than an EC nucleus (Fig. 8B, K''). We assessed presence of lumens in these cords and found few identifiable open spaces (Fig. 8K'). In normal kidney tissue, capillary vessels express the sialomucin podocalyxin at their apical surface (Sawada et al., 1986), lining the lumen (Fig. 9E). This could be seen in some organoid vessels as well, although there was rarely clear apical localization (Fig. 9F-G). Finally, we assessed whether organoid vessels associated with mural cells, such as smooth muscle cells and pericytes. We carried out staining for PDGFR β and smooth muscle Actin (SMA), and while we observed PDGFR β cells, they marked much of the stroma and did not always associate with vascular structures. Additionally, some of the organoid epithelium was also PDGFR β ⁺ (Fig. 8L). Rarely, PDGFR β ⁺SMA⁺ pericytes were observed associated with a blood vessel (Fig. 9H, inset, white arrow). Not only were these cells sparse, but they were not observed after day 9 of culture (data not shown). These observations point to pericytes largely missing from organoids.

Blood vessels in hESC-derived kidney organoids are transient

We found that the vasculature in organoids displayed high variability in overall mass and pattern depending on when they were assayed. Hence, we speculated that their development might change over time in culture. To elucidate the dynamic process of vessel formation in organoids, we examined vascular structures at multiple timepoints during organoid formation. Prior to organoid aggregation, we observed the presence of scattered endothelial progenitors, or angioblasts, at day 0. These cells were positive for known endothelial marker VEGFR2 (Fig. 6D). On day 3 after aggregation, Sox17⁺ ECs were scattered throughout the organoid, with some small CD31⁺ cords (data not shown). Over the course of culture and hESC differentiation, we found increasing numbers of identifiable ECs, peaking around day 6 (Fig. 10A-B, G-H, Q-R). By day 12, however, vascular structures were beginning to decline in number (Fig. 10E-F). By day 18, organoids displayed few cells that expressed endothelial markers, with CD31 staining being diffuse and punctate (Fig. 10E-F). Quantification of ECs at these stages demonstrate that EC numbers peak at days 6–9 and decline over time afterwards (Fig. 10G-H). Attempts to increase EC mass using VEGF increased vasculature but did not prevent regression (Fig. 10I-P). In fact, differentiated hESCs cultured in EGM-2 endothelial media (which includes VEGF) were unable to form nephrons and subsequently died, indicating that optimization of organoid culture specifically for ECs was sometimes detrimental to kidney cell types (data not shown). In contrast to the vasculature, Podxl (podocytes, Fig. 3S) and E-Cad (epithelium, Fig. 10V) levels increase or stay stable through day 15 of culture. The Six2⁺ nephron progenitors also decreased quickly (Fig. 10U). Interestingly, two markers of the stroma, Meis1 and Col3a1, show differential levels throughout time in culture, with Col3a1 increasing substantially (Fig. 10T). This indicates there may be an overgrowth of stroma in organoids (Fig. 11A-B). These data are consistent with published data

(Takasato et al., 2015). To determine how vessels were regressing, we examined cleaved caspase 3 (CC3) staining in organoids at day 12. We observed significant cell death, particularly in the center of the organoid (Fig. 10W, 11C). The location of CC3 can be viewed by zoomed in virtual slices (Fig. 10X-Y, arrows). Most CC3 appears to be in the interstitium, some in ECs, and a minor amount in epithelium. These findings underscore that while ECS are present in kidney organoids, as reported in other studies, organoid vessels are generally sparse and transient, regressing relatively quickly over the course of culture.

Kidney organoids can be generated from mouse nephrogenic zone cells

After observing poor formation of vasculature in hESC-derived organoids, we reasoned that protocols designed to generate renal cell types may not be optimized to generate properly specified vascular precursors with the potential to differentiate properly. We hypothesized that blood vessels might develop better in organoids where ECs are sourced from tissue where kidney endothelium is already present. We therefore turned to an alternative method of organoid generation based on isolation and propagation of committed renal progenitors (Brown et al., 2015, 2019). In this method, we disaggregated actively proliferating cells from the cortex of the embryonic kidney, which contains ECs as well as nephron, ureteric bud, and stromal progenitor cells. As the cortex is the area of active nephrogenesis, it is referred to as the ‘nephrogenic zone’ and the cells collected from this region as nephrogenic zone cells (NZCs). Based on these methods, kidneys were isolated from mouse embryos at E17.5 and digested whole to release NZCs in the outer cortex (Fig. 12A). Only the most cortical cell layers, made up of nephron progenitor cells (NPCs), ureteric bud (UB) tips, ECs, and stromal cells, are released and isolated from the kidney using this technique (Fig. 12B). The differentiation potential of isolated NZCs was assessed using reporter mice with lineage

tracer constructs in addition to immunofluorescence. Flk1-GFP was used to identify ECs; Hoxb7Cre; RYFP confirmed the UB lineage; Six2Cre; RYFP demonstrated the NPC lineage; and Foxd1Cre; RYFP marked the stromal progenitor cell lineage (11D-G). After digestion, NZCs were either aggregated immediately to form organoids by spotting approximately 500,000 cells onto a floating membrane or cultured on monolayer to expand the population (Fig. 12A). NZCs could be maintained and passaged up to two times as a heterogeneous population of kidney progenitor cells (Fig. 12A, C-D). Similar to differentiated hESCs plated in monolayers, NZCs formed clusters of epithelial cells (Hoxb7-CreYFP⁺ UB cells) surrounded by Six2⁺ NPCs and stromal cells (Foxd1-CreYFP) (Fig. 12C and D). As previously reported (Daniel et al., 2018; Munro et al., 2017), although the NPCs in the developing kidney organize into cap-like structures, which are themselves predominantly avascular, they are surrounded by a thin layer of interstitium and ECs. Hence the isolated NZCs contain a small number of ECs that we detected using Flk1-GFP one day after plating (Fig. 11H). However, ECs experienced limited growth in monolayer and became increasingly difficult to identify, likely not surviving in culture (Fig. 11H-I). In fact, culture of human umbilical vein endothelial cells (HUVECs) in kidney organoid media resulted in cell death (data not shown). Therefore, to maximize ECs in NZC-derived organoids, we carried out organoid aggregation immediately after digestion and collection of NZCs. Like hESC-derived organoids, NZCs readily self-organized and differentiated into organoids, with tubule-like structures becoming visible in brightfield by day 4 (Fig. 12E). We next assessed the epithelial and stromal structures in NZC-derived organoids and found that NZC organoids contained ureteric and nephron epithelium, podocytes, and stromal cells (Fig. 12F–J). Whole mount immunofluorescence of NZC organoids showed a large number of E-Cad⁺ epithelial tubules and Podxl⁺ podocytes (Fig. 12F). Sectioned organoids (Fig. 12G–J) showed Aqp1⁺ proximal tubule and descending loop

of Henle and NPHS1⁺ podocytes (Fig. 12G), LTL⁺ proximal tubule and Umod⁺ loop of Henle (Fig. 12H), a stromal population throughout the organoid marked by the protein Meis1/2/3 (12I), and collecting duct marked by Aqp3 and pan-cytokeratin (Fig. 12J). These findings demonstrate the ability of embryonic NZCs to form organoids with a range of kidney cell types.

NZC-derived organoids contain intermediate ‘off-target’ vascular cell types

To analyze organoid vasculature, we generated NZC organoids from the kidneys of Flk1-GFP reporter mice. Interestingly, however, we identified discrepancies between vascular cell type specific reporters and immunofluorescence. In particular, we observed relatively few Flk1-GFP⁺ ECs in NZC organoids. By contrast, although CD31 could be seen in EC cords, it was also patchy throughout large regions of the organoid (Fig. 14A). We investigated these cells further and found that NZC organoids contained two distinct populations of presumptive ECs; one located on the filter side and one at the ALI. ECs along the ALI were rare but often organized into cords (Fig. 13A, yellow arrows), while those at the filter interface were abundant and disorganized (Fig. 13A, white arrows). Co-staining for the endothelial marker EMCN and the stromal marker Meis1/2/3 demonstrated that these more abundant cells were positive for both stromal and EC markers, while the cells at the organoid ALI exclusively expressed EC markers (Fig. 13B). To trace the origins of these ‘endothelial’ cells in organoids, we used genetic lineage tracing. Surprisingly, we found that NZC organoids displayed EC marker expression in cells that had originated from both stromal and NPC progenitors (Fig. 13C-D). Co-expression of stromal and EC markers led us to further investigate whether the double positive cells were due to aberrant expression of endothelial genes by stromal cells. We used the Foxd1Cre; RYFP/Terminator mouse to generate organoids derived solely from nephrogenic stromal cells (Fig. 13C) (Guo et al.,2013). This mouse contained a

transgenic diphtheria toxin receptor (DTR) flanked by LoxP sites at the Rosa26 locus. Following Cre recombination in Foxd1-expressing stromal progenitors, the DTR was deleted and those cells were resistant to diphtheria toxin (DT). Following isolation, NZCs in culture were treated with DT *in vitro* to kill all non-stromal cells, resulting in an organoid made exclusively from stromal-lineage cells. Unexpectedly, these ‘stroma only’ organoids contained CD31⁺ cells that were derived from the stromal lineage (Fig. S4C). These cells resembled the filter-side CD31 and EMCN-expressing cells that we deemed to not be true ECs. Similarly, we observed that NPCs, normally fated to become epithelium, also inappropriately expressed stromal and endothelial markers in wildtype organoids, as demonstrated by triple positive cells (YFP⁺EMCN⁺Meis1/2/3⁺) in Six2Cre; RosaYFP traced organoids (Fig. 13D). In accordance with observations above, these triple positive cells localized to the filter region of the organoid and did not appear to form nephrons or EC cords. In addition to alternative progenitor lineages, cells in NZC organoids aberrantly co-expressed markers of multiple differentiated cell types. For instance, we observed organoid tubules that were double positive for cytokeratin, a marker of collecting duct, and LTL, a marker of proximal tubule (Fig. 13F). These two types of tubules normally originate from different cell lineages (UB and NPCs, respectively) and are not known to be co-expressed in any kidney cell types *in vivo*. We hypothesized that ectopic gene expression was an artifact of organoid culture. Therefore, we examined whether ectopic gene expression could also be observed in hESC organoids as well. Interestingly, immunofluorescence suggested that hESC organoids did not display an overlap in protein expression between ECs or NPCs and stromal markers (Fig. 13G-H). These data suggest that cells in organoids, particularly in NZCs, have relatively plastic identities or differentiation status. This underscores the importance of using multiple independent methods to validate cell

type authenticity, including multiple molecular markers, cell and tissue morphology, and functionality tests.

Vasculature of NZC-derived organoids is scarce and deficient

We further analyzed vasculature structures in NZC-derived organoids to establish whether initial inclusion of bona fide ECs would yield a more robust organoid vasculature (Fig. 14A). Like the vasculature in hESC-derived organoids, on rare occasions, larger vessels developed that contained partial lumens (Fig. 15A-C). However, most vessels presented as EC cords, with no distinguishable central luminal space. We visualized the lack of lumens using virtual section view (Fig. 14B, B0yellow arrow). In contrast to the EC cords of hESC organoids, some ECs did appear to polarize, suggesting an initial step towards lumen formation, as shown by the presence of Podxl and Icam2 at the apical membrane between ECs (Fig. 14D, 15A). Most NZC organoid vascular structures, however, largely failed to invade the glomerulus or form a capillary tuft within the podocytes (Fig. 14B, B', white arrow). Beyond morphological abnormalities, we found that ECs in organoids were highly variable in other respects, including overall vascular mass. To address the issue of EC mass, we analyzed a large number of organoids and systematically measured the vascular content based on immunofluorescence expression of EC markers and expected morphology. Fig. 14E shows three day 7 NZC organoids from one experiment with vastly different vascularization levels. These were classified as Class I, II or III as indicated, from low to high vasculature, as well as a score of 0 for no identifiable ECs. Over 200 NZC organoids were evaluated and scored, showing that NZC organoids were distributed across all four scores, with a skewing towards a score of 0 or 1 (Fig. 14E'). In addition to variability, much like the hESC-derived organoids, NZC-derived organoids demonstrated substantial vascular regression over the course of their time in culture. The Flk1-GFP reporter allowed us to track ECs over time within a single organoid (Fig. 14C). On day 1, the

day after NZC aggregation, single ECs could be identified as GFP⁺ punctae (day 1, arrows). These cells proliferated and elongated, forming cords by day 3. Shortly thereafter, however, the EC cords began to shrink, often leaving behind only a few ECs, or sometimes none at all (day 7, arrows). Cell death of NZC organoid vasculature is seen by CC3 immunofluorescence (Fig. 11J-K). These data not only highlight the high level of variability in NZC organoid ECs, but it underscores the overall low vascularity of the organoids. These findings suggest that the paucity of ECs observed in ESC derived organoids is not an effect of inappropriate reprogramming to an endothelial progenitor state but rather a consequence of culture conditions.

Vasculature of explanted embryonic kidneys

Based on studies showing the dependence of vascular maintenance on shear stress from blood flow, both *in vivo* and in organoid culture (Langille and O'Donnell 1986; Meeson et al., 1996; Ando and Yamamoto, 2009; Homan et al., 2019; Korn and Augustin, 2015; Langille and O'Donnell, 1986; Meeson et al., 1996), we speculated that vessels in both hESC- and NZC-derived organoids were largely sparse and lacked lumens due to the absence of hemodynamic flow in culture. This idea has been tested in other settings, and experimental data suggests flow can potentiate kidney organoid vessels (Homan et al., 2019). To further examine this possibility, we explanted normal embryonic kidney tissues and cultured them on filters (Ihermann-Hella and Kuure, 2019; Rak-Raszewska et al., 2015) in the absence of flow. These organs have all the requisite progenitor cell types of the mature organ and also contain the proper 3D patterning, allowing us to directly test the impact of loss of blood flow on vascular maintenance. As expected, the vascularity of explanted E12.5 embryonic kidneys at the start of *ex vivo* culture was much

higher than that of either NZC or hESC organoids (Fig. 17C). However, over the 3–6 day course of culture, established blood vessels quickly regressed (Fig. 17A). A comparison of whole mount immunofluorescence of explanted kidneys with their age-matched embryonic kidneys (one day *in vitro* is roughly equal to half a day of *in vivo* development) showed that explanted kidneys at days 3 and 6 had significantly less vasculature (Fig. 16A–D, 17C–G). However, NPCs were maintained and the UB continued to branch (Fig. 16A–D, 17F–G). Live imaging of Flk1-GFP in E12.5 kidney explants showed the dynamic nature of these vessels, including regression (Fig. 16E–F, 17A–B). Areas of vessels, and sometimes entire branches, were observed to fall apart around day 3 (Fig. 16F, extended data video). Cleaved caspase 3 staining showed that ECs underwent programmed cell death to an extent not observed in normal embryonic kidney tissues (Fig. 16G–I). Additionally, there was increased death in the center of the explant in non-vascularized tissues, a phenomenon observed in organoids as well. To determine whether EC regression was due to a lack of necessary angiogenic signaling, we treated the explants with a high amount of VEGF (200 ng/ml) to promote EC growth. VEGF-treated explants did not exhibit differences in EC regression compared to controls (Fig. 16J and K). Together, these findings further suggest the possibility that blood flow is a key factor in the differentiation and maintenance of *ex vivo* blood vessels.

Organoid implantation ameliorates vascularization

Given that all kidney tissues, both from *in vivo* or *in vitro* sources, displayed regression of the vasculature upon culture, we asked whether providing flow would prevent loss of vascularity in organoids. Recent studies using bioengineered flow platforms show that providing flow improved maintenance of blood vessels (Homan et al., 2019). Engraftment of organoids under the kidney capsule of immunocompromised mice has been shown as an alternative method of introducing

flow (van den Berg et al., 2018). We thus carried out implantation of hiPSC-derived organoids under the kidney capsule, as previously shown (Gupta et al., 2019). Organoids were found to be well-vascularized 3 weeks after implantation, with a total organoid age of 30 days, well after we would expect the vasculature to have regressed (Fig. 18). The implanted organoids grow and expand in mass at the surface of the kidney (Fig. 18A and B). We found that CD31⁺ blood vessels populated both the organoid and the interface between the host and organoid (Fig. 18C). To determine whether the vessels were derived from the host or the graft, we stained for Human Nuclear Antigen (HuNu). Surprisingly, the vasculature in the organoid was negative for HuNu, demonstrating that it was entirely populated from invading host vasculature (Fig. 18D and E). In addition, injection of isolectin B4 (IB4), which binds to perfused ECs upon systemic vascular injection, showed that blood flowing from the host was indeed reaching and penetrating the organoid (Fig. 18E and F). Unlike in the non-implanted organoids, we observed structures resembling glomerular capillary tufts within clusters of podocytes in the implanted organoids. Additionally, these capillaries were IB4⁺, suggesting circulation from host to well-developed glomeruli was occurring in implanted organoids (Fig. 18G). These findings demonstrate that hiPSC organoids have the capacity to form perfused, vascularized glomeruli, a major step in developing functional nephrons. However, this was not universal as we found a portion of unperfused vessels. While most vessels were EMCN⁺CD31⁺IB4⁺triple positive, EMCN⁻CD31⁺ vessels were left unperfused (Fig. 18H, arrow, Fig. 19D). Conversely, these organoids only contained EMCN⁻CD31⁺ vasculature preceding implantation (Fig. 19C), demonstrating a difference in vessel maturation or identity upon perfusion. Therefore, further investigation into organoid vasculature heterogeneity and dynamics before and after engraftment will be of great interest to the field.

scRNA-seq of endothelial cells in organoids and human embryonic kidneys

To perform a comprehensive comparison of the vasculature in human embryonic kidneys (eECs) and human ESC and iPSC organoids (oECs), we compiled and compared scRNA-seq data from multiple published sources. GEO accession information for these data sets can be found in Tables 2 and 3 in the supplemental data. Uniform Manifold Approximation and Projection (UMAP) plots show the clustering of ECs in relation to the other cells in the embryonic kidneys (Fig. 21D) and organoids (Fig. 21A and C). First, we analyzed the percentage of ECs in the total cell population at each time point of organoid development (Fig. 20A-B). We discovered that there were two peaks where oECs were at their highest, at day 14 and day 25. It is important to note that these timepoints do not directly correspond with our protocol, for which the corresponding days would be day 7 and day 18 respectively. This is due to the days including the monolayer differentiation step. The two EC peaks do not indicate a transient death and reemergence of vasculature in organoids. Instead, they likely represent differences in the lifecycles oECs in organoids derived from ESCs versus iPSCs; organoids derived from the two cell types appear to generate different amounts of ECs that peak at different times. We inferred this because the clusters do not completely overlap, as seen in the UMAP in Fig. 21B. In fact, iPSC organoid ECs show an individual cluster that does not contain hESC ECs at all, meaning that there is a level of transcriptional divergence between organoids of different cell sources. Regardless of these differences, however, all organoids analyzed still demonstrate the pattern we observed where ECs emerge, proliferate for a short period, then regress. Next, we assessed endothelial gene expression in the embryonic kidneys and iPSC organoids. The heatmap in Fig. 20C illustrates this analysis. We find EC signature genes present in both eECs and oECs, including canonical endothelial genes such as EMCN, EGFL7, ANXA2, ARHGAP29, and COL41A. Surprisingly, we found an overall similarity of the eEC and

oEC populations, showing that despite our findings of vascular deficiencies in organoids, oECs are transcriptionally similar to normal kidney ECs at early stages. On the other hand, oECs from day 14 organoids are more similar to the eECs than the oECs at later timepoints. This indicates that day 14 is both a peak in EC mass as well as in EC transcriptional similarity. Overall, there were not large differences between eECs at the different time points during the 8–18 week gestational period observed, although some time points display differential clustering (Fig. S8F). Our previous work (Daniel et al., 2018) described endothelial heterogeneity during mouse renal development. These data demonstrate similar findings, that most ECs have a baseline expression of a number of pan-endothelial genes, while displaying distinct individual profiles. Multiple genes that encode ribosomal proteins such as RPS28 and RPL36 were identified in the eEC set. This indicates that the two sets of cells are so transcriptionally similar that housekeeping genes are being marked as upregulated. Interestingly, despite filtering out cells with high mitochondrial gene expression—indicative of cellular stress—the most consistently expressed gene in the ECs was HSPB1. This could mean ECs are particularly sensitive to the stress induced by the cell extraction process (Adam et al., 2017; O'Flanagan et al., 2019). In addition, a significant number of differentially expressed canonical EC genes in the eECs were omitted from the heatmap analysis due to discrepancies in quality control for the oEC population. These include PLVAP, APLNR, CDH5, TIE1, VEGFR1 and VEGFR2 (Fig. 20D). Consequently, most of the genes included in the heatmap were not known to be EC-specific. This could further illustrate the insufficiencies of organoid vasculature, but further analysis will be necessary to determine this definitively. Altogether, the data support the observations that organoid vasculature first develops normally and begins to mature but then degrades over time.

Discussion

In this study, we report in detail limitations of cultured kidney tissue blood vessel formation and maintenance. We analyze the vasculature generated using two distinct kidney organoid protocols—one which generates kidney cell types via directed differentiation of hESCs, and the other which isolates primary cells from the nephrogenic zone, including ECs, from developing mouse kidneys. In both cases, the endothelium is initially present and vascular cords form. However, in both protocols, we identify deviations from normal blood vessel development. First, organoid blood vessel morphology is abnormal in that vessels form few continuous lumens, indicating roadblocks in their functional differentiation. Second, organoid ECs can express non-endothelial markers (in NZC-derived organoids), such as stromal marker *Meis1/2/3*. This calls into question both their identity and our ability to recognize bona fide blood vessels without careful analysis of multiple markers. Third, while they are dynamic, similar to developing *in vivo* vessels, they are not stable, and we find that the vascular network in organoids inevitably regresses over time in culture. We propose that this is due to the absence of blood flow, as even cultures of intact embryonic kidneys exhibit this regression. Organoids implanted under the kidney capsule, by contrast, maintain complex vascular networks perfused by blood. Interestingly, these perfused organoid vessels are entirely derived from the host mouse vessels and display arteriovenous defects, as vessels associated with glomeruli stain for the venous marker (vessels entering and exiting the glomeruli are normally arterial). Lastly, transcriptomic analysis of ECs from hPSC organoids are relatively similar in gene expression to human embryonic kidney ECs early during their culture. It is likely that regression of organoid vessels over the course of culture exacerbates transcriptional differences observed at later stages.

While organoids have extraordinary potential for developmental biology studies and for personalized medicine, this study paints a cautionary tale regarding our ability to evaluate the vasculature of tissues generated *ex vivo*. Reliable blood vessel identification relies on a combination of standard vascular features, including multiple EC markers, vessel morphology, and patterning relative to other tissue structures. Although organoid ECs display some expected characteristics, we find that all three of these parameters are mostly abnormal in organoids.

Vascular deficiencies and regression in kidney organoids

We propose that in order for organoid systems to prove useful in therapeutic applications as functional *ex vivo*-grown tissue, they must contain blood vessels that are mature, perfused, and organized along the nephron. We show that organoid blood vessels display fundamental defects in both morphology and differentiation status. Despite source of origin or protocol used, organoid blood vessels regress over time in static culture significantly more rapidly than other organoid cell types. Therefore, methods have to be developed to further optimize, expand, and maintain blood vessels for them to perdure in culture, especially for the time it takes for a human kidney to develop *in vivo* (Hinchliffe et al., 1991; McMahon, 2016). In addition to limited vasculature, we find that NZC organoids have strikingly variable EC content. While hESC organoids were more consistent, they have noticeable batch variability, as noted in previous studies (Phipson et al., 2019). These are additional considerations that must be taken into account in organoid research and support the importance of large-batch analysis of scRNA-seq data that utilizes data from multiple datasets and labs.

Our findings point to some critical limitations of kidney organoid vasculature, which may prove applicable across different fields of organoid studies. In fact, cerebral organoids do not

appear to contain ECs (Lancaster et al., 2013), although groups are trying to address this deficiency by adding exogenous ECs or expressing vascular transcription factors (Cakir et al., 2019; Shi et al., 2020a). Based on our findings, this could be due to the long culture times of these organoids of 75 days or more. Intestinal organoids, previously thought to not develop a significant vasculature as well, have recently been shown to contain a small population of ECs that arises and quickly disappears, similar to what we observe (Holloway et al., 2020; Spence et al., 2011). Previous studies in kidney organoids have also described the presence of varying amounts of vasculature. Some publications do not show any ECs, but most have at least a small amount of vasculature (Freedman et al., 2015; Kumar Gupta et al., 2020; Morizane et al., 2015; Takasato et al., 2015).

The reason for the dearth of vasculature, and the key to solving it, have thus far been unknown. However, the improvement of organoid vascularization has been tackled by multiple labs using a variety of methods. For instance, there has been progress in creating vascularized cerebral organoids by the addition of HUVECs or ECs differentiated from iPSCs in addition to engraftment (Pham et al., 2018; Shi et al., 2020b). HUVECs expressing ectopic ETV2 have been shown to have a remarkable ability to adapt tissue-specific identity and form stable, perfusable vessels that can colonize organoids (Palikuqi et al., 2020). Another recent study found a notable improvement in human intestinal organoid vasculature presence and maintenance through specific growth factor addition (Holloway et al., 2020). One study demonstrated that VEGF addition to kidney organoids appeared to drastically increase the endothelial population by immunofluorescence, but transcriptionally these cells appeared in the stromal cluster, raising the possibility of parallels with our observations of off-target cell types in NZC organoids and the importance of multi-marker EC verification (Czerniecki et al., 2018). We found that the addition

of VEGF in static culture is not sufficient to block or reverse vascular regression in explants, although it may increase vasculature in the short term.

Another tantalizing approach to address vascular deficiencies might involve hypoxia, a known inducer of angiogenesis. It is known that embryonic *in vivo* blood vessels initially undergo vasculogenesis under markedly hypoxic conditions. In our experiments, we note that submerged organoids tend to fare better than organoids grown at the air-liquid interface, suggesting that elevated oxygen levels present in standard cell culture incubators may suppress vessel growth. However, investigation into the effects of hypo- and hyperoxia in kidney explant culture have thus far not demonstrated a clear benefit (Loughna et al., 1998; Rymer et al., 2014). Future studies will be needed to investigate this line of inquiry.

Together, our experiments highlight the complexities in blood vessel growth and maintenance in cultured tissues; the solution to improving *ex vivo* vasculature is therefore unlikely to rely on a single factor. *In vivo*, beyond hypoxia and VEGF signaling, there are many factors that regulate vascular stability, such as the ECM and factors provided by pericytes, and macrophages. In fact, we observed few pericytes (PDGFR β , SMA anti-body) and could not detect macrophages (data not shown, NG2 or F4-80 antibody), suggesting these cell types do not differentiate in organoids. While we cannot rule out the possibility that disruption of the normal 3D cellular environment of the kidney, likely inherent in any organoid model, might impact vascular maturation, we argue that kidney cell types self-organize relatively efficiently and cannot fully explain the vascular abnormalities observed. Additionally, these factors—ECM, pericytes, and macrophages—are already present in kidney explants, which still experience extensive vascular regression (Hoeffel et al., 2015). Therefore, we propose that hemodynamic flow is likely a prerequisite for maintaining vasculature in kidney organoids. Once a stable organoid vasculature

has been achieved, the field may focus on the other important aspects of endothelium in the kidney. These studies show that while organoids may have defective vasculature, we are already making progress toward understanding and improving vascularization of cultured kidney tissue.

Implantation of organoids for perfusion

Why are blood vessels in vitro generally fragile and unstable? Our study suggests that one possibility is that the absence of blood flow results in vessel regression. Blood vessels are known to be sensitive to changes in hemodynamic stress (Ando and Yamamoto, 2009), so we tested whether tissues cultured in the absence of flow would lose their vascularity. We show that hESC-derived organoid vessels regress after about 12 days in culture. Similarly, despite containing ECs derived from an existing, functional vascular network, NZC-derived organoids experience an even more rapid loss of vessels in under a week. This may be due to the initially smaller number of ECs or perhaps the angioblasts produced through hESC differentiation are more resilient in culture than ECs from pre-formed vessels. To further test how acutely lack of blood flow impairs blood vessels, we challenged the established vasculature of embryonic kidneys explanted and cultured ex vivo and observed rapid regression and apoptotic cell death in static culture. Therefore, regardless of whether vessels formed de novo via vasculogenesis in organoids or via angiogenesis in embryonic kidneys, ECs regress in static culture. Our observations support recent studies that ameliorate organoid vasculature using microfluidics or engraftment (Homan et al., 2019; Kloth et al., 1993; Van den Berge et al., 2018).

We show that organoid implantation under the kidney capsule resulted in higher levels of vascularization than expected at the comparable 30-day culture time. Remarkably, capillaries even invade into podocyte clusters and form perfused, glomeruli-like capillary tufts. Strikingly, all the

vasculature in the implanted organoid appeared to be primarily derived from the host. It was shown in a lymph-node engraftment model that this is progressive over 8 weeks (Kloth et al., 1993). In contrast, other studies have shown anastomosis of host and organoid vasculature (van den Berg et al., 2018). The real challenge ahead is to optimize transplantation efficiency and better understand the behavior and qualities of ECs in engrafted organoids and how to promote anastomosis with host vessels. Further analysis of the heterogeneity and maturity of vessels growing after implantation, as well as their arteriovenous differentiation, will be of particular interest to the fields of vascular biology and tissue engineering alike. Not only is vasculature maintained in the organoid upon implantation and perfusion, but organoids display improved maturation of epithelium (Homan et al., 2019; Kumar Gupta et al., 2020; van den Berg et al., 2018). Is this due to increased oxygenation, nutrient availability, signals from the ECs themselves, or a combination thereof? We hypothesize that ECs produce angiocrine signals that are important for kidney development and maturation, but this remains to be answered.

Blood vessel organization and patterning

In addition to the challenge of maintaining ECs in cultured organoids, optimization of kidney vessel patterning and regional specialization will be needed. In our previous work (Daniel et al., 2018), we described the spatial patterning of embryonic kidney vasculature. Recent studies further emphasize the striking heterogeneity of the vasculature along the differentiated nephron (Barry et al., 2019). While the full array of mechanisms that maintain the physical relationship between ECs and the developing nephron is not yet fully understood, it is likely that EC-nephron crosstalk has a role in ensuring proper differentiation of both tissues. This specificity is likely important for renal development and maintenance due to paracrine signals produced by ECs. Called ‘angiocrine

signaling,' ECs have been observed to influence tissue growth, maintenance, and patterning in many tissues including the lung, brain, pancreas, and liver (Jakab and Augustin, 2020; Magenheimer et al., 2011; Rafii et al., 2016; Rocha et al., 2015). Additionally, EC heterogeneity, both phenotypically and transcriptionally, is necessary for nephron function and adaptations to the environment and stress (Aird, 2007; Barry et al., 2019; Ding et al., 2011; Dumas et al., 2020; Garlanda and Dejana, 1997; Kumar Gupta et al., 2020; Molema and Aird, 2012; Nolan et al., 2013; Ottone et al., 2014). Although active angiocrine signals in the kidney have yet to be identified, there are indications that blood vessels are involved in NPC maintenance and disruption of vasculature through Sox17 and Sox18 deletion results in medullary hypoplasia (Matsui et al., 2006; Rymer et al., 2014). As shown in intestinal organoids (Holloway et al., 2020), scRNA-seq data can provide clues to receptor-ligand pathways active in ECs and surrounding cells. Future analysis will seek to identify pathways possibly altered in organoids.

It is clear that nephron vasculature must be properly organized and differentiated into an arterial-capillary-venous system, as well as distinct renal EC types, to assure function of the kidney as a whole. However, even in the most highly vascularized organoids, the ECs are not uniformly distributed, have defective branching, and do not closely associate with nephrons or podocytes. In hESC organoids, we noticed heterogeneity in the vasculature that may be an indicator of a progression towards vascular maturity, with VEGFR2 marking angioblasts, the emergence of Sox17 expression indicating a slightly more mature EC (Matsui et al., 2006), then CD31 only appearing once cords begin to form. This is demonstrated by the VEGFR2⁺Sox17⁻ ECs on monolayer on day 0, indicating that there are only immature angioblasts present. 3 days after aggregation, ECs are mostly CD31⁻Sox17⁺, but as the organoid develops, CD31⁺Sox17⁺ cords form. A similar hierarchy was described in Homan et al. (2019). Some organoid vessels also

demonstrated maturity by the presence of Podxl and the emergence of lumens. A deeper understanding of endothelial maturity, identity, and heterogeneity is possible via scRNA-seq data analysis, which promises to move this field forward.

Evaluating organoid vasculature

How similar or different are organoid vessels from in vivo kidney vessels? How can we recognize properly differentiated kidney ECs? Our scRNA-seq transcriptional analysis combining numerous datasets identifies striking similarity between organoid ECs and human embryonic kidney ECs. Therefore, while not entirely differentiated or patterned, organoid ECs show a potential to become functional kidney ECs. This is corroborated by a pseudotime analysis of scRNA-seq of day 10, 12, and 14-day organoids suggesting maturation of immature ECs into arterial and venous-like fates (Low et al., 2019). Notably, day 14 organoids are much more like the eECs, while the day 26 oECs have much lower similarity and EC gene expression in general. This further highlights our point that while vasculature may be present initially in organoids, it degrades both physically and transcriptionally.

The investigation into organoid vasculature through scRNA-seq brings about the often debated subject—what defines an endothelial cell? How can we definitively identify an angioblast or an endothelial cell within an organoid or cultured kidney tissue? How can we conclusively determine whether it contributes to a functional blood vessel? We have shown that gene expression of a few canonical markers is not sufficient, yet it is a method universally relied upon. ScRNA-seq is a powerful tool that reveals insights into cell fate and differentiation beyond what can be learned through classic methods such as antibody staining or quantitative PCR. However, we show that transcriptional signatures, particularly in organoids, may not provide definitive identification of

bona fide ECs. Our study demonstrates that to validate blood vessels and other cell types, expression of multiple genes along with morphological features and ultimately function must be assessed to properly recognize vessels within engineered tissues.

We put forth that additional efforts will be required in future organoid studies to ensure that regionally specific, organotypic vasculature must differentiate in conjunction with their associated epithelia. The presence of ECs alone does not ensure functional engineered tissue vascularization. Further analysis, characterization, and understanding of organoid endothelium will be needed, and this may be facilitated using gene lists generated from scRNA-seq analysis. These types of efforts will likely provide needed insight into the successes and deficiencies of organoid vasculature and give direction for its advancement.

The promise of organoids

An explosion in organoid research has resulted in related publications increasing 10-fold within the last decade alone. With dozens of protocols developed for generating various tissue types, many of these studies still largely ignore the associated vasculature despite its central importance for organ survival and function. Additionally, our understanding of blood vessels and ECs themselves is experiencing a renaissance, particularly in the light of scRNA-seq which has provided new insights into organotypic EC heterogeneity. We propose that a more dedicated focus on the vasculature during organ development is essential and that directing more attention to blood vessels in organoid cultures and laboratory generated tissues will be crucial to achieving functional tissues for transplantation.

Our work highlights the importance of context during vessel formation and maintenance, both in vivo and in engineered tissues (Homan et al., 2019). Further work will be needed to generate regionally specific blood vessels, which we propose actively support epithelial development and the maintenance of a functional endothelial-epithelial association throughout the filtration process. While endothelial crosstalk has been implicated in the development and maintenance of multiple tissues (Cleaver and Melton, 2003), there is still much to be discovered in the kidney on that front. Bioinformatics and scRNA-seq data will provide more insight into the insufficiencies of organoid vasculature and provide candidate targets to try to support maturation and maintenance.

In this study, we have systematically investigated blood vessels in kidney ex vivo model systems, uncovering underappreciated (or previously unevaluated) challenges in the use of organoids and cultured tissues with respect to their vasculature. Organoids ultimately have the capability to form tissue-specific, mature vasculature, but we must develop ways to overcome the vascular deficiencies in ex vivo kidney tissues we have described. Together, our investigation into organoid vasculature underscores the engineering challenges ahead and cautions the field to properly evaluate in vitro ECs, as they are particularly susceptible to misidentification, immaturity, and regression.

Fig. 6. hESC-derived kidney organoids display expected renal cell types.

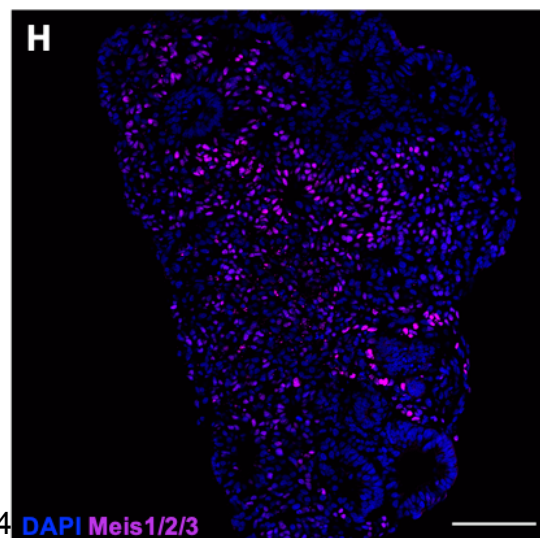
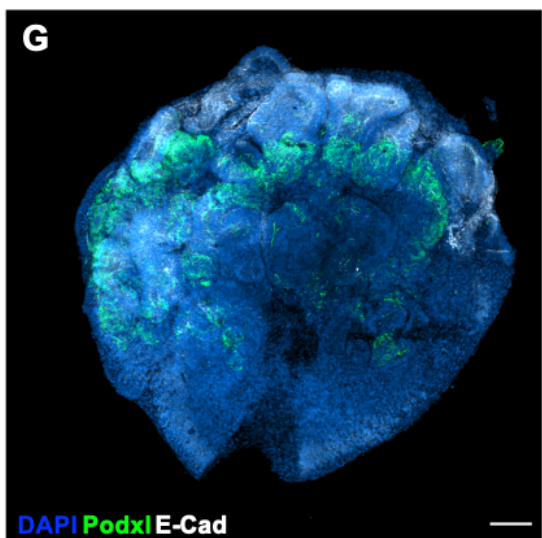
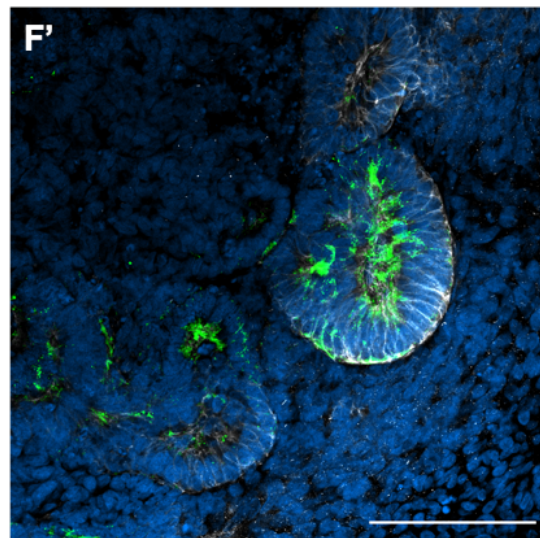
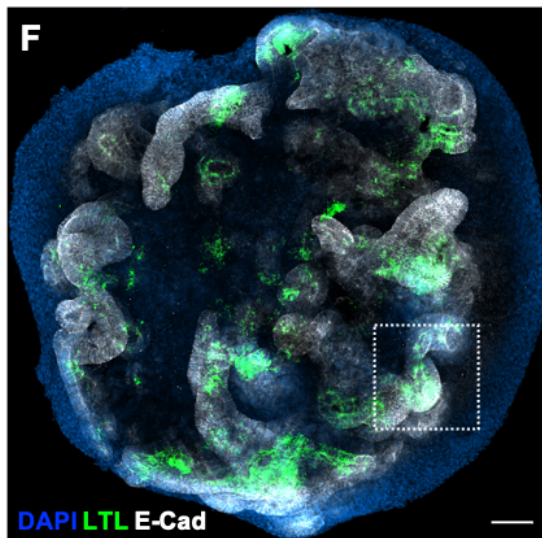
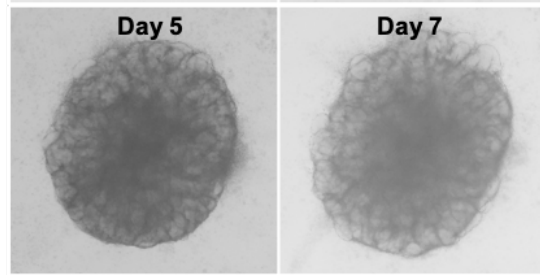
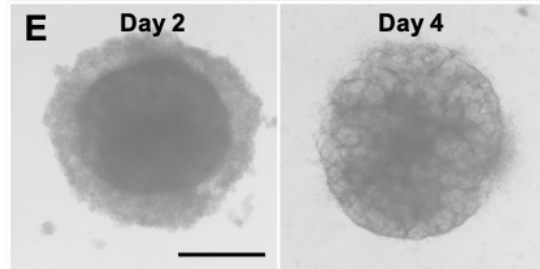
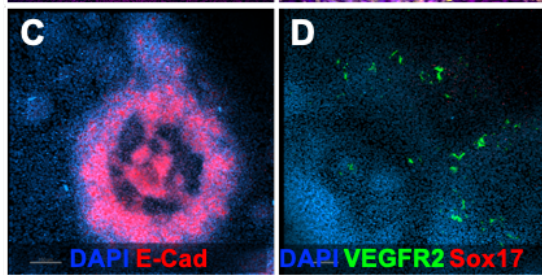
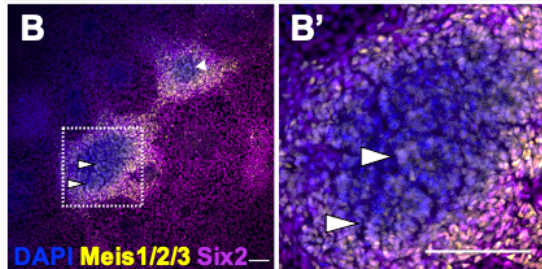
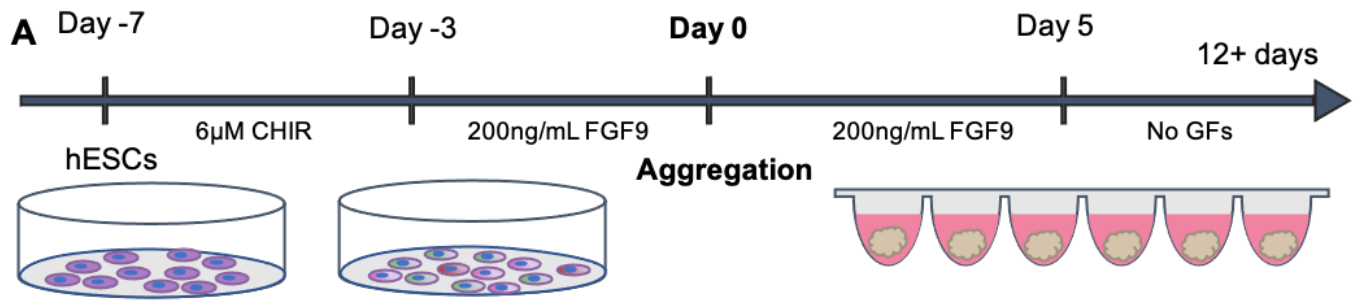


Fig. 7. hESC-derived kidney organoid optimization and culture platforms.

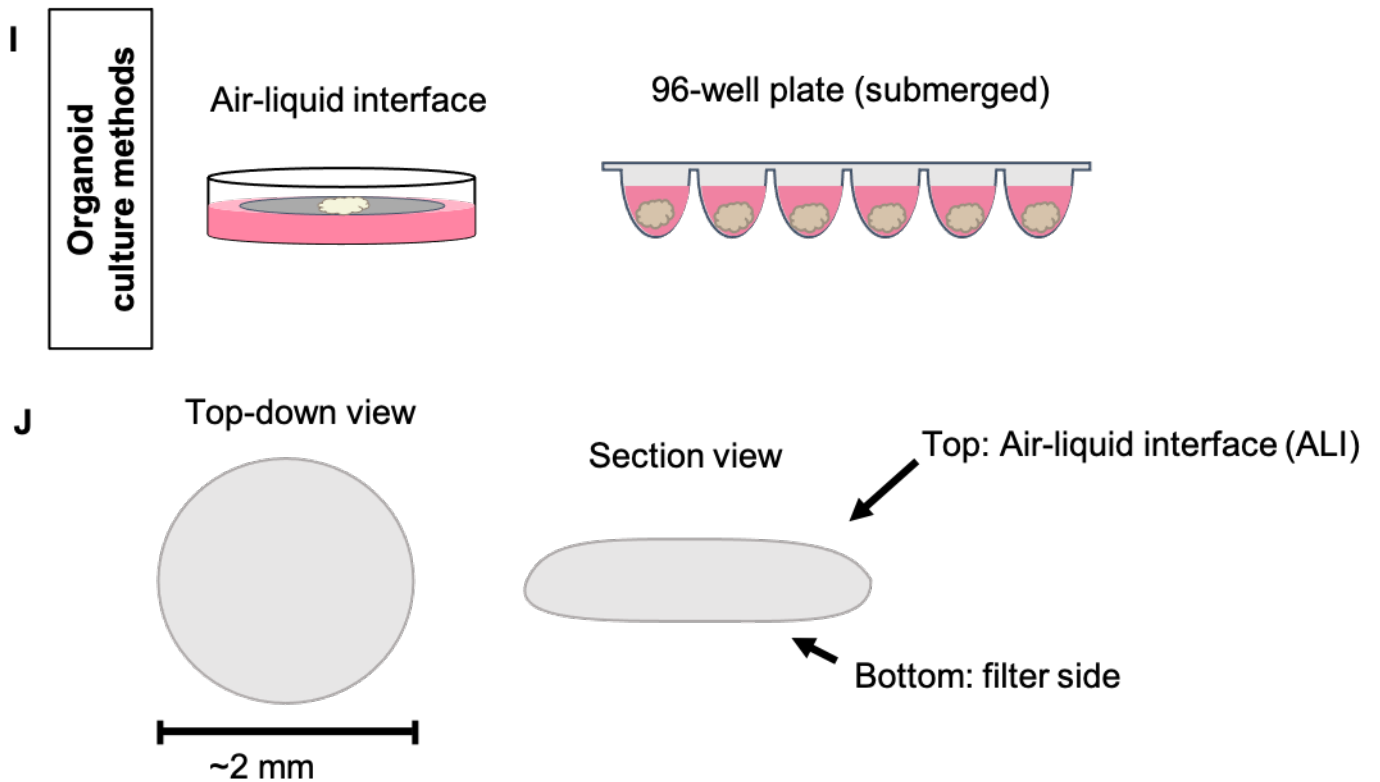
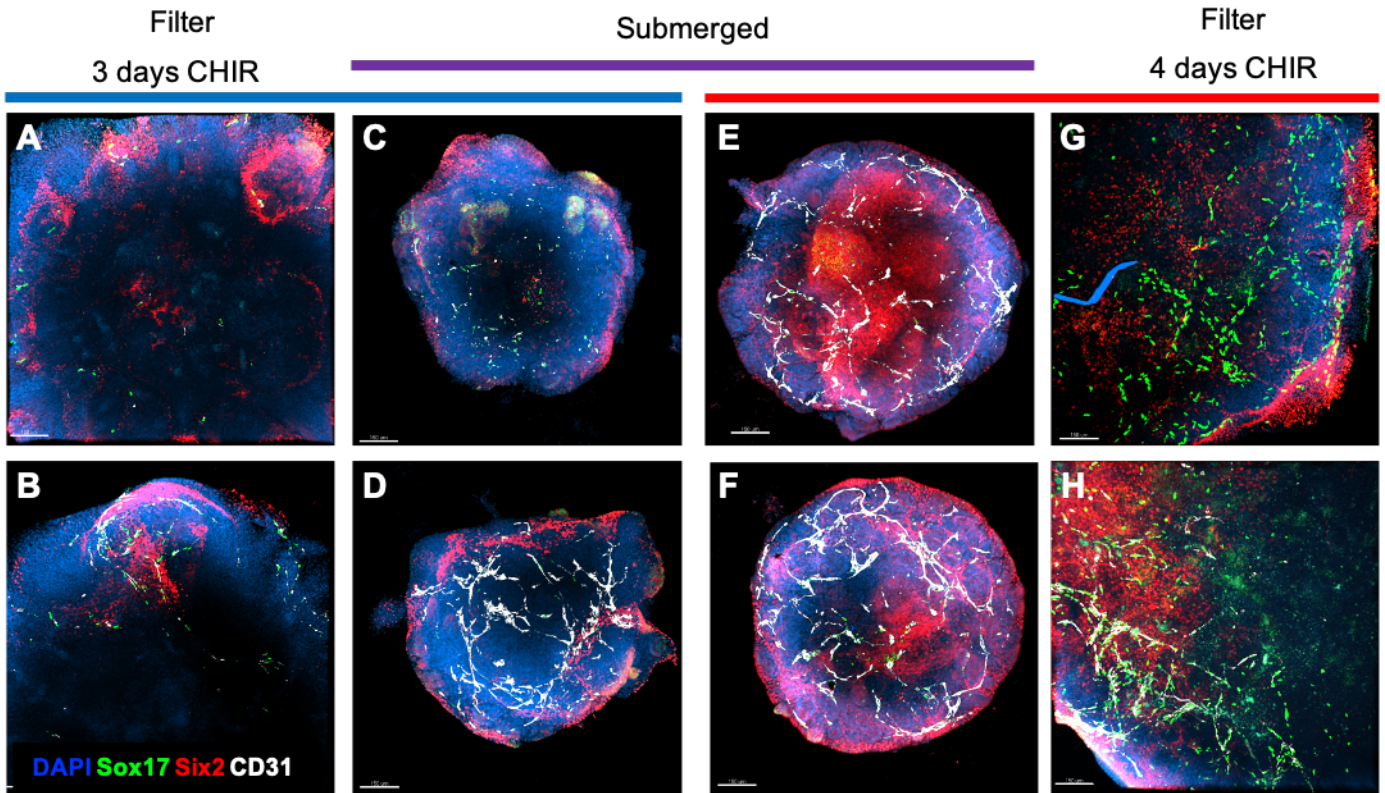


Fig. 8. hESC-derived organoid blood vessels are sparse and lack patterning.

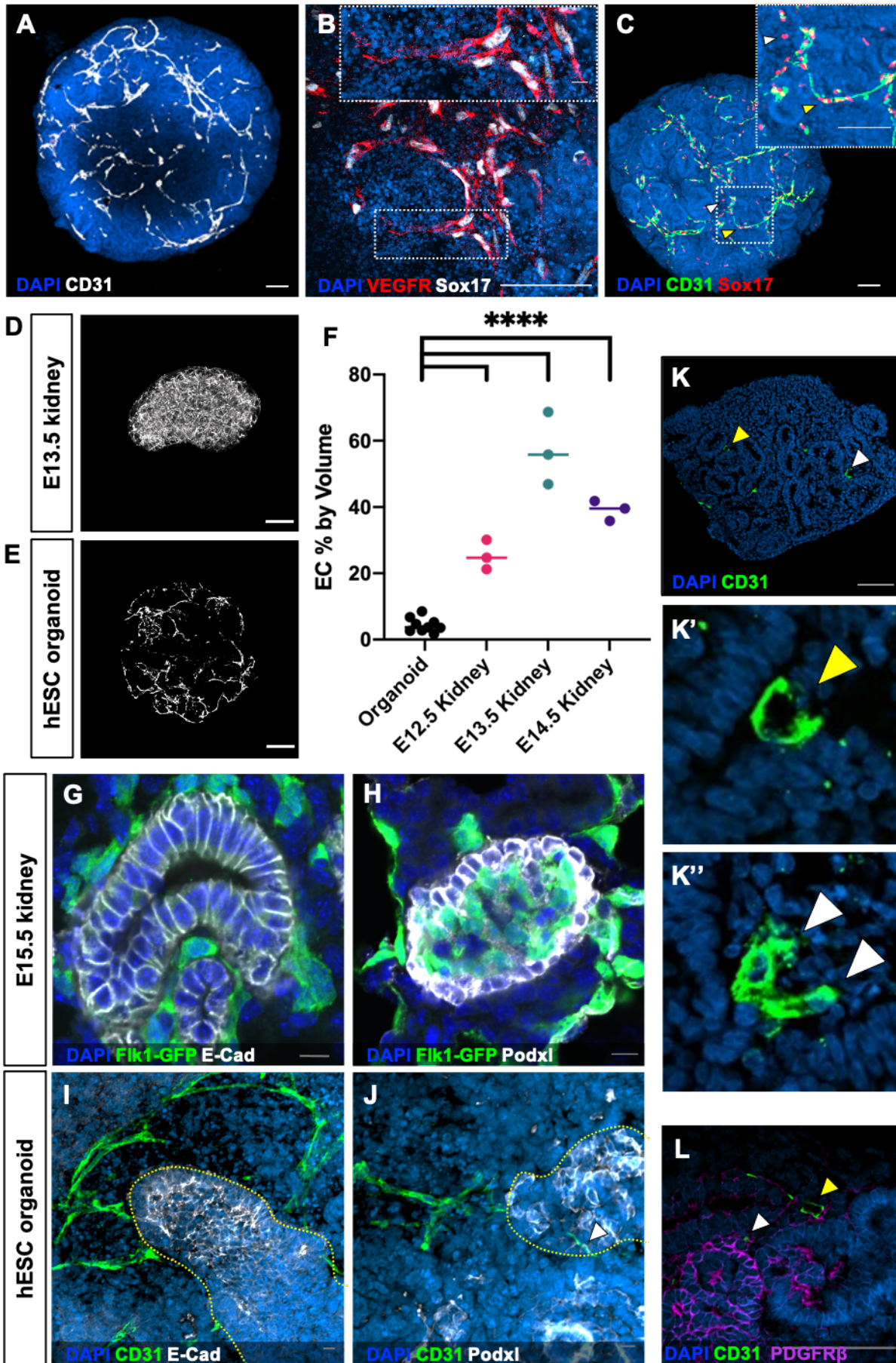


Fig. 9. hESC-derived kidney organoids culture variability, EC patterning, polarity, and mural cells.

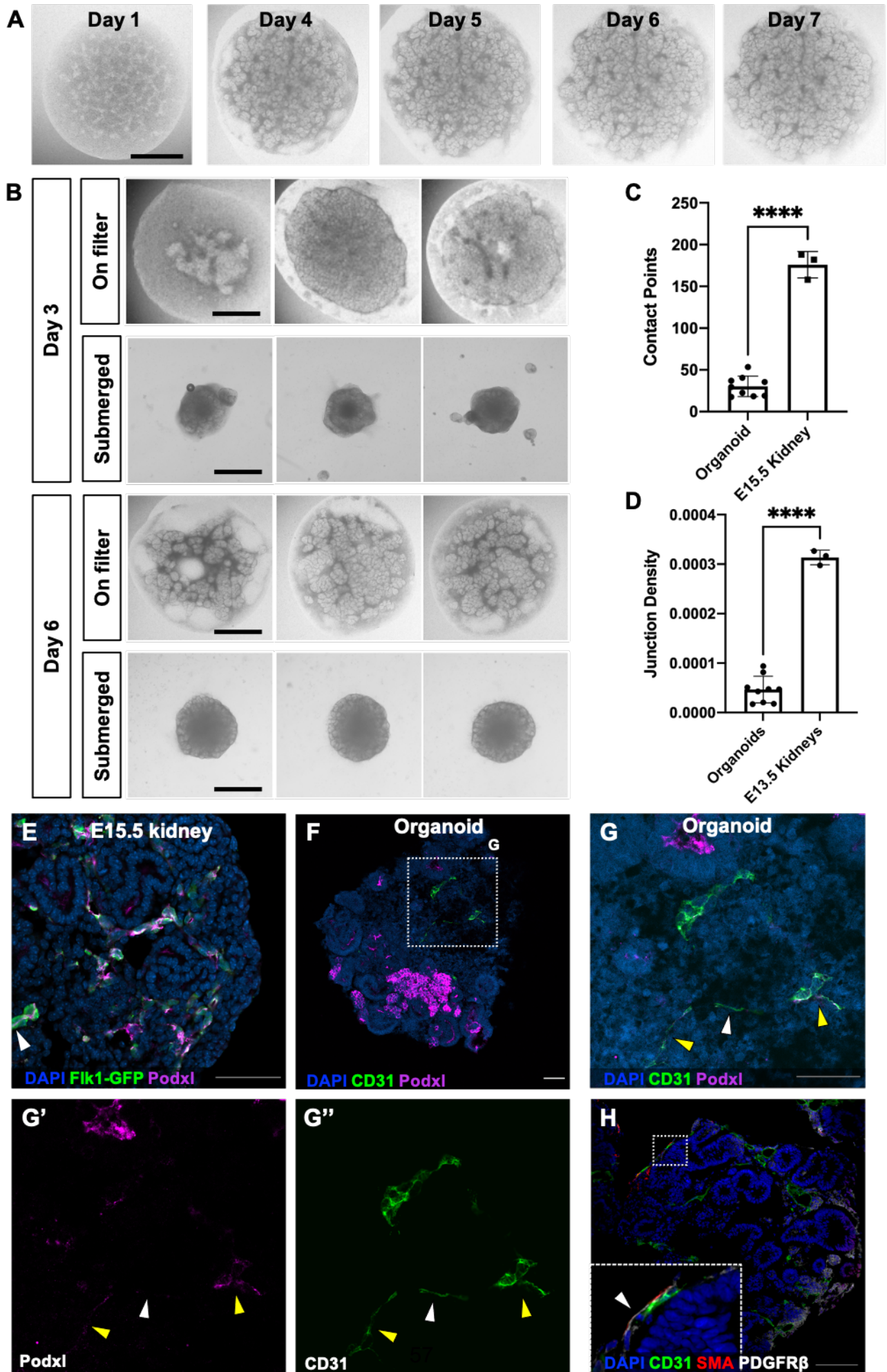


Fig. 10. hESC-derived organoid vasculature regresses in culture

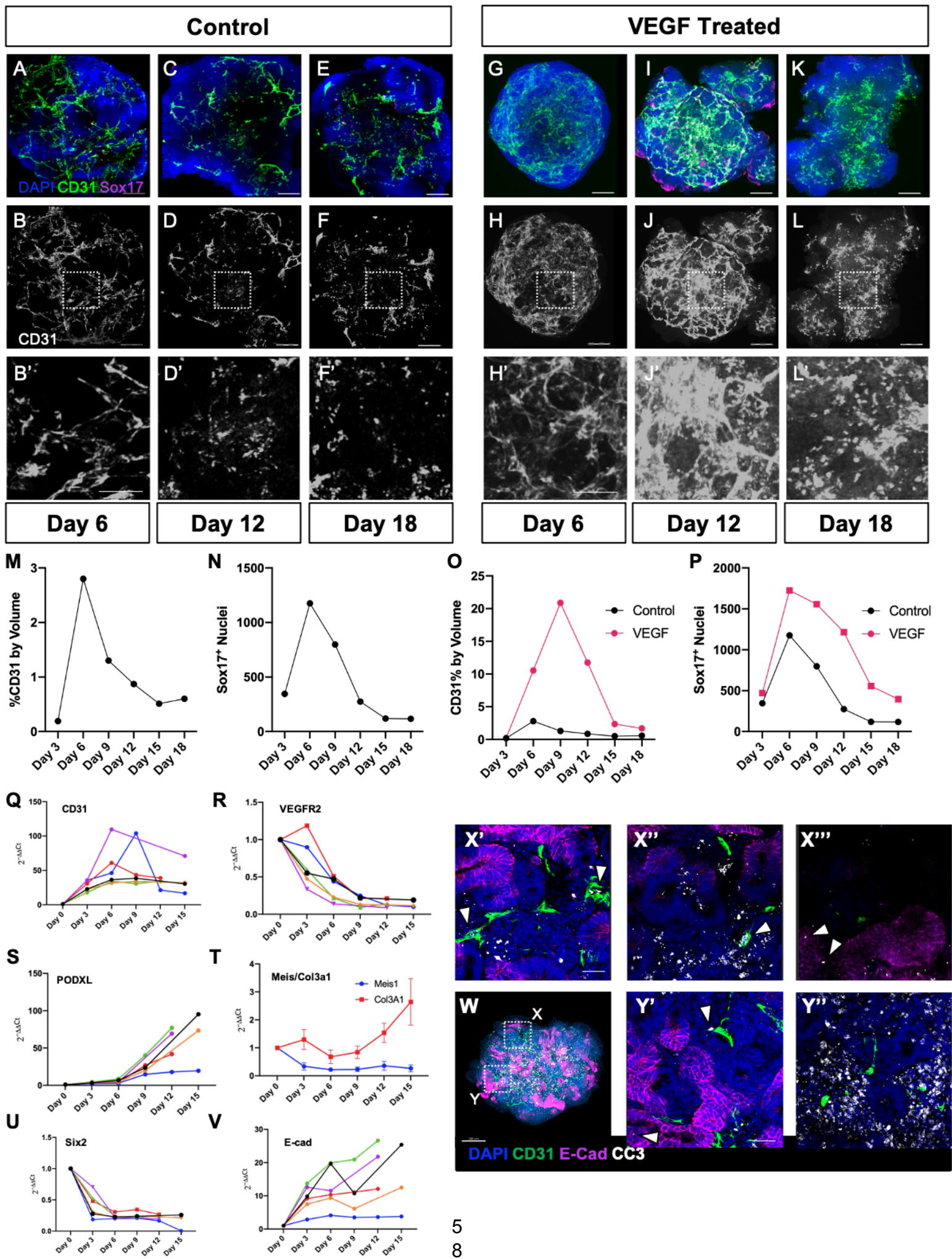


Fig. 11. NZC organoids maintain epithelial and stromal cell types but suffer significant loss of endothelial cells upon culture.

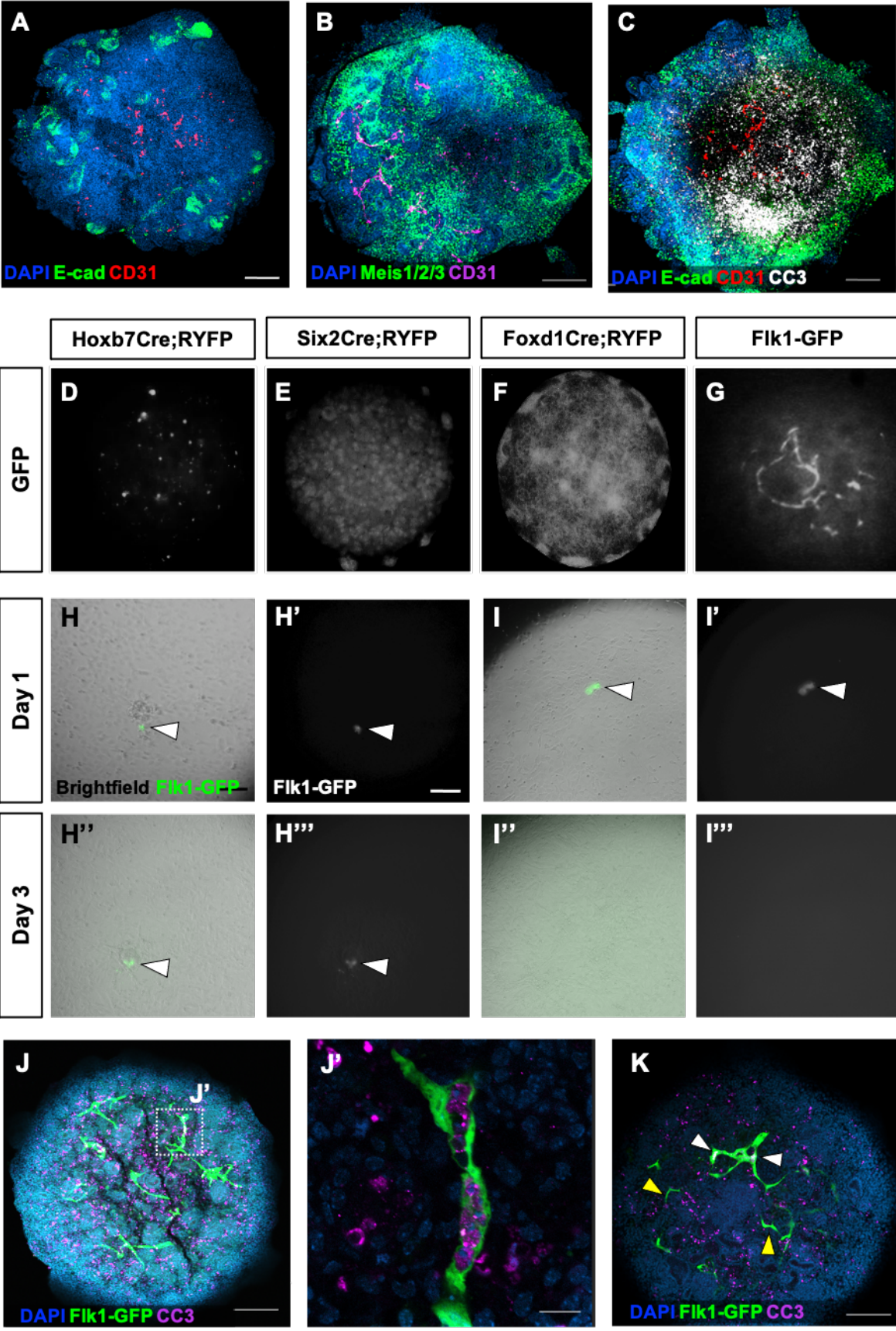


Fig. 12. NZC-derived kidney organoid generation.

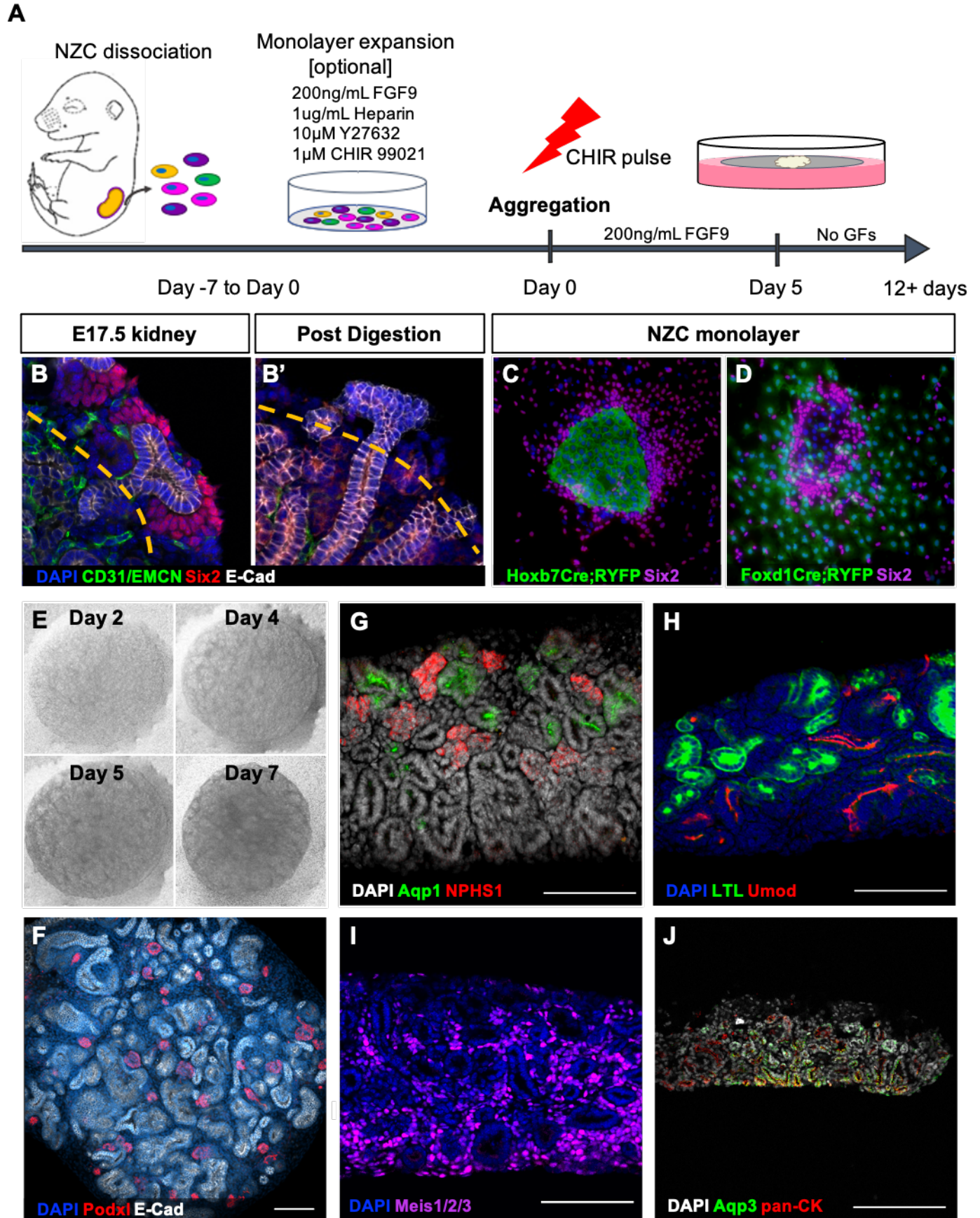


Fig. 13. NZC organoid endothelial, stromal and epithelial cells express off-target markers.

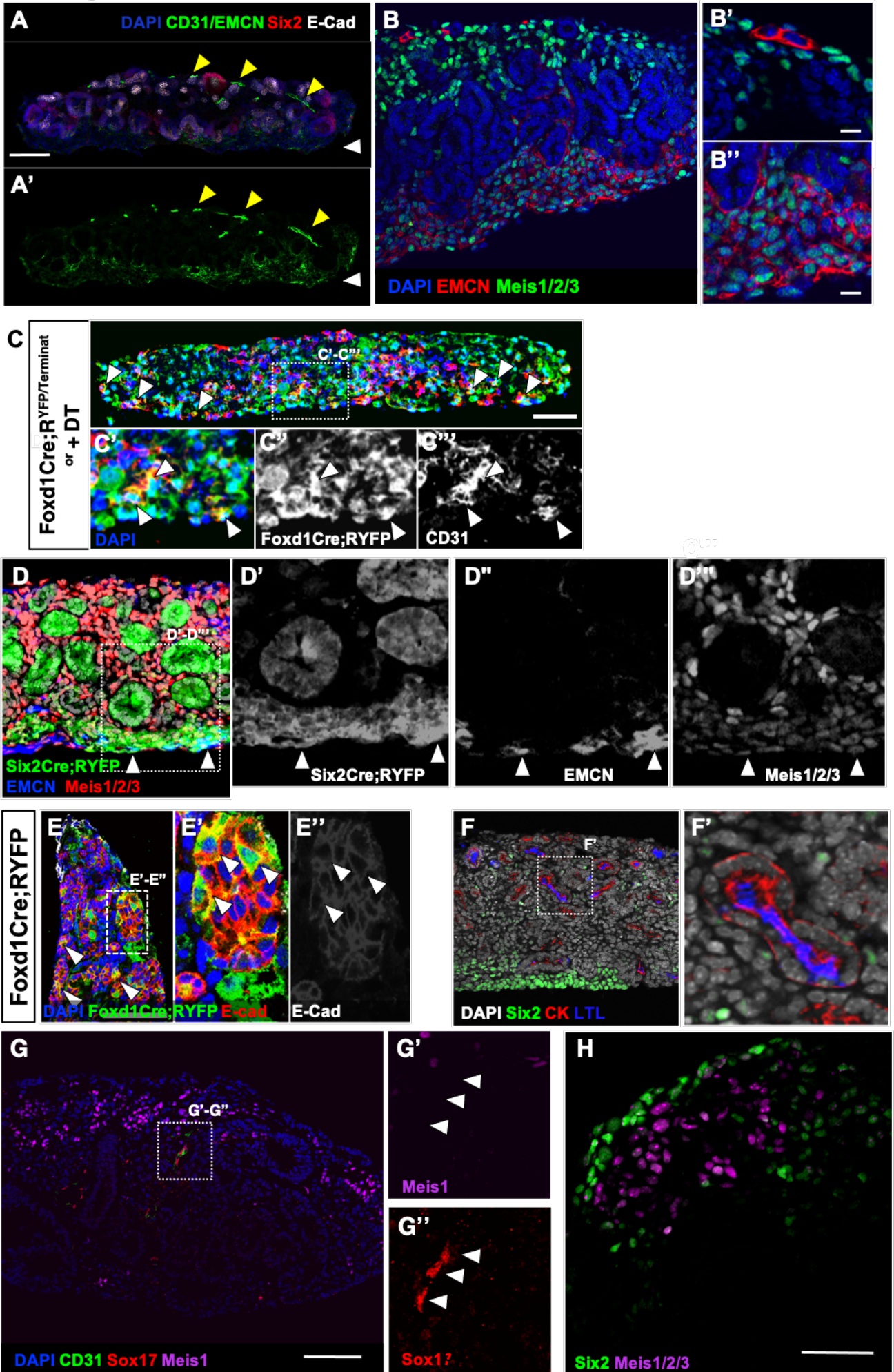


Fig. 14. NZC-derived kidney organoids develop sparse vasculature that regresses in culture.

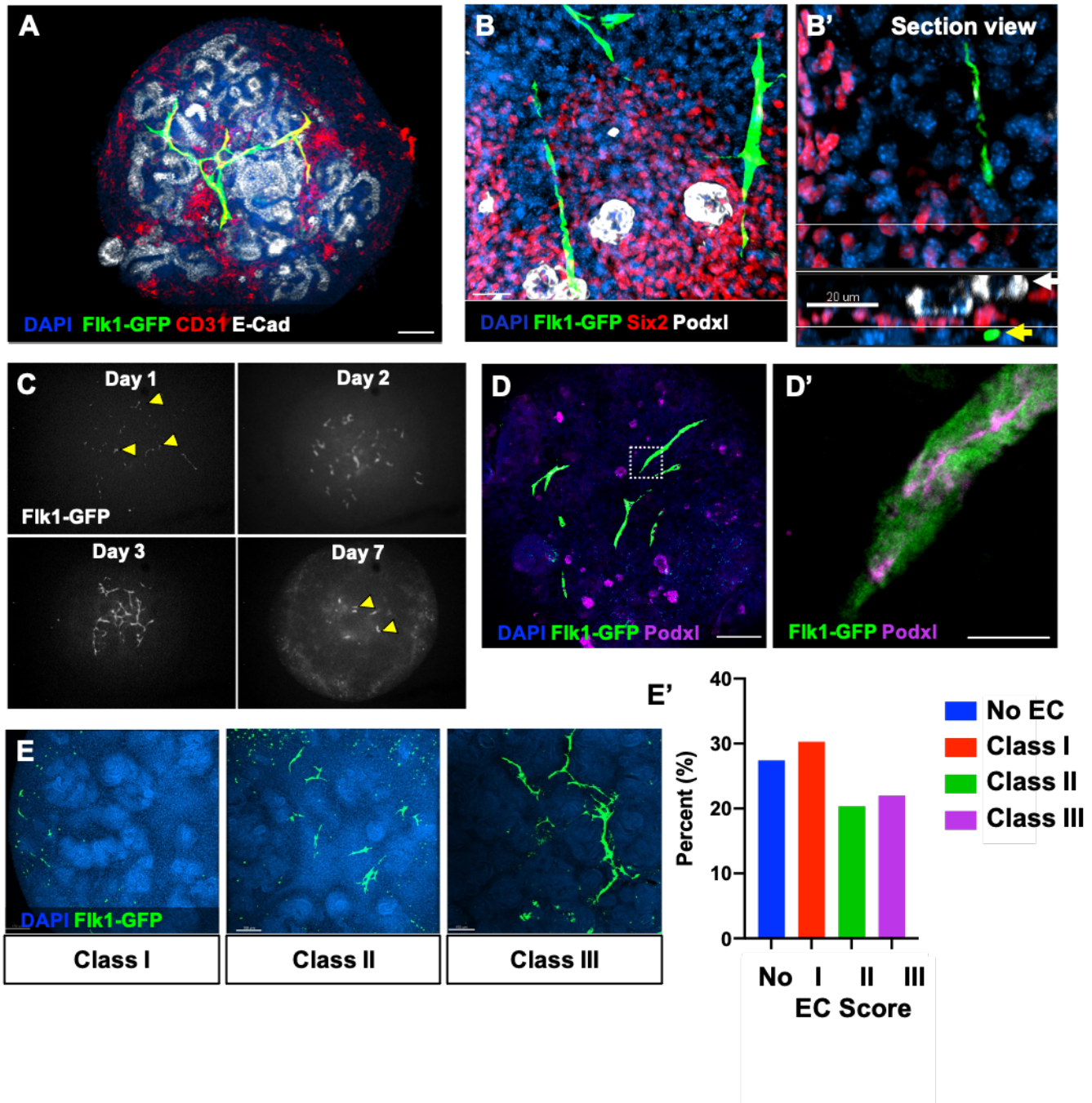


Fig. 15. NZC organoids display limited lumen formation.

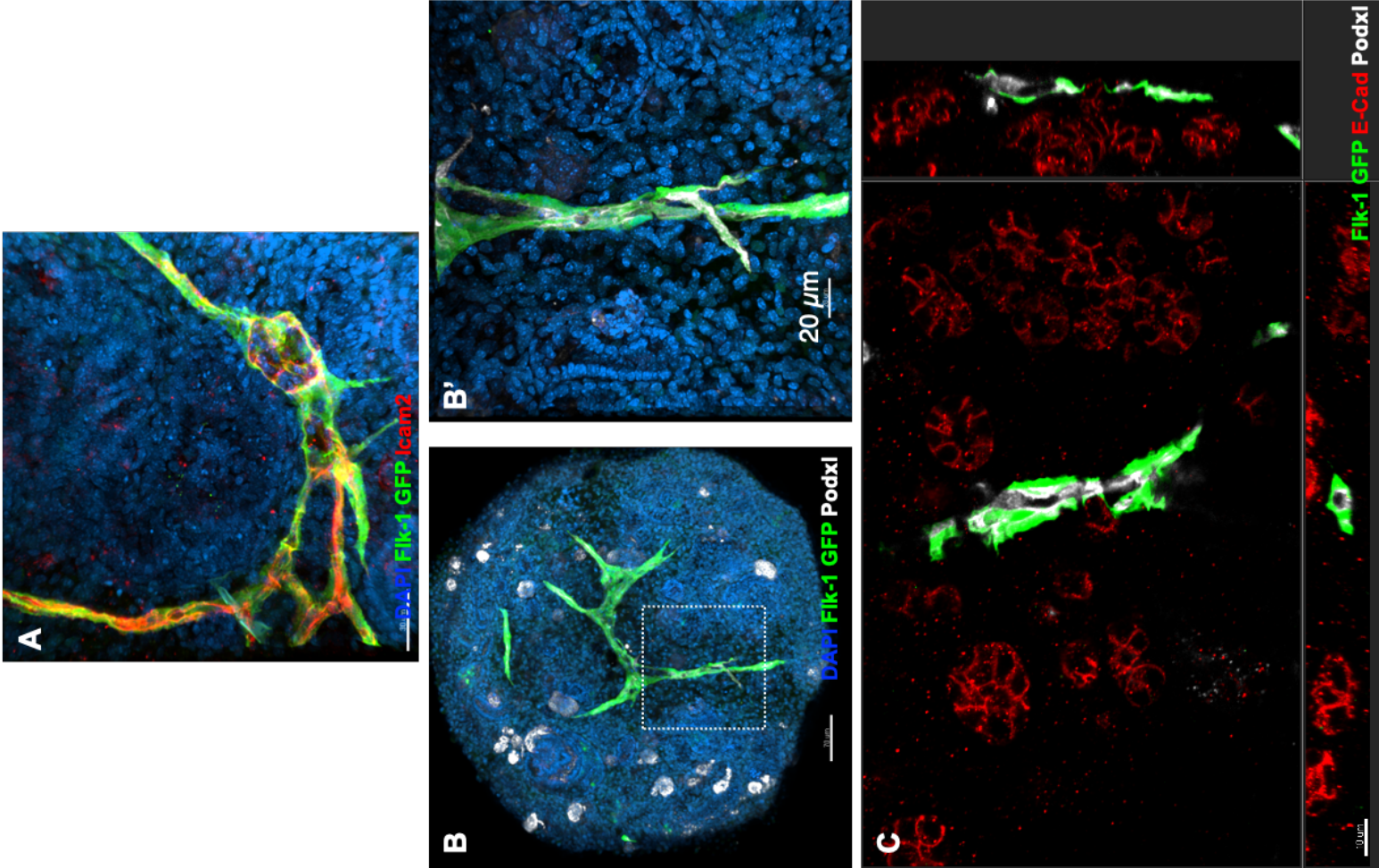


Fig. 16. Blood vessels of explanted embryonic kidneys regress in culture.

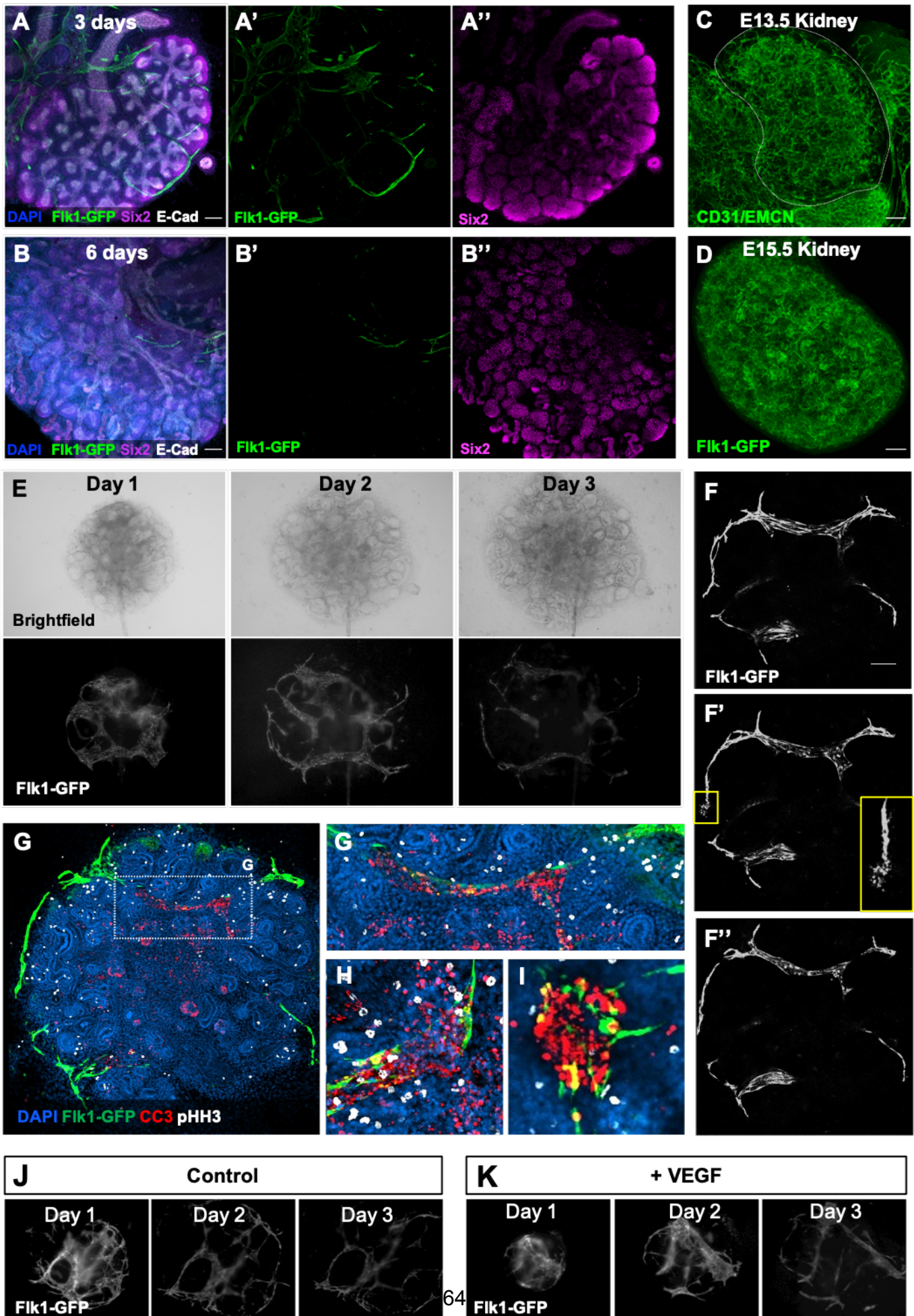


Fig. 17. Blood vessels of explanted embryonic kidneys regress in culture.

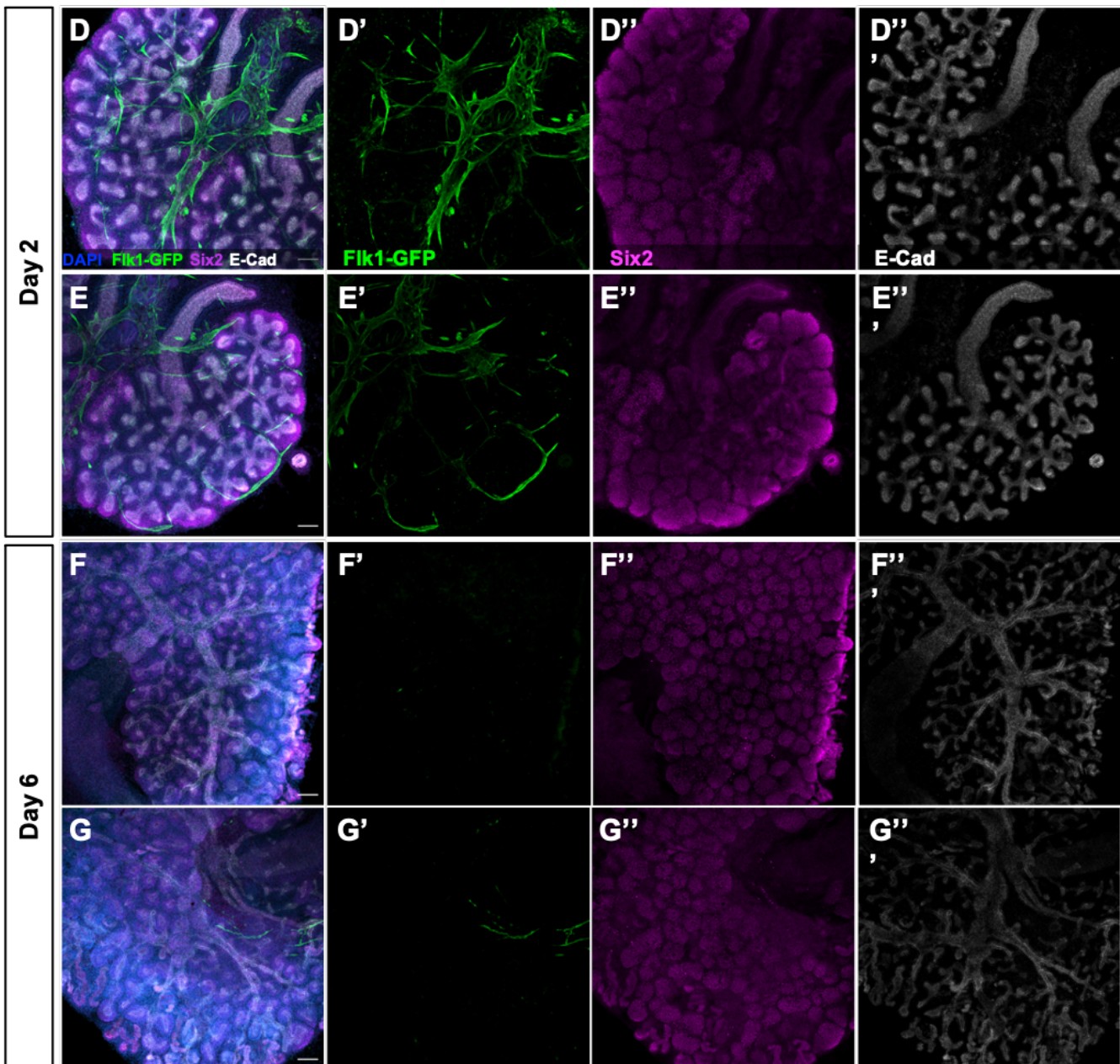
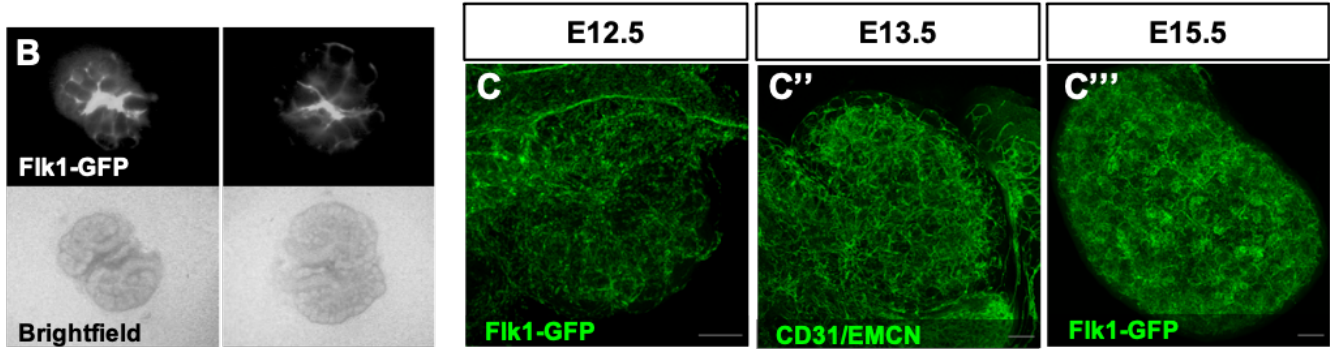
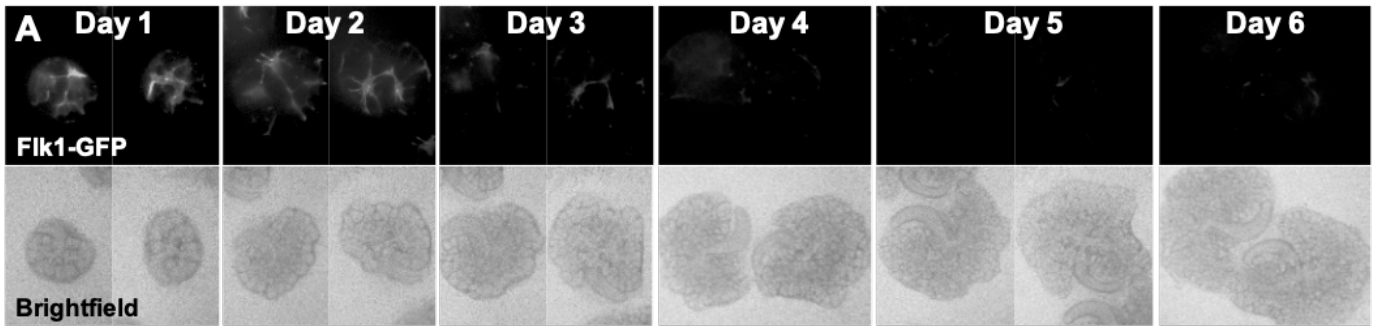


Fig. 18. Implanted organoids display extensive vascularization.

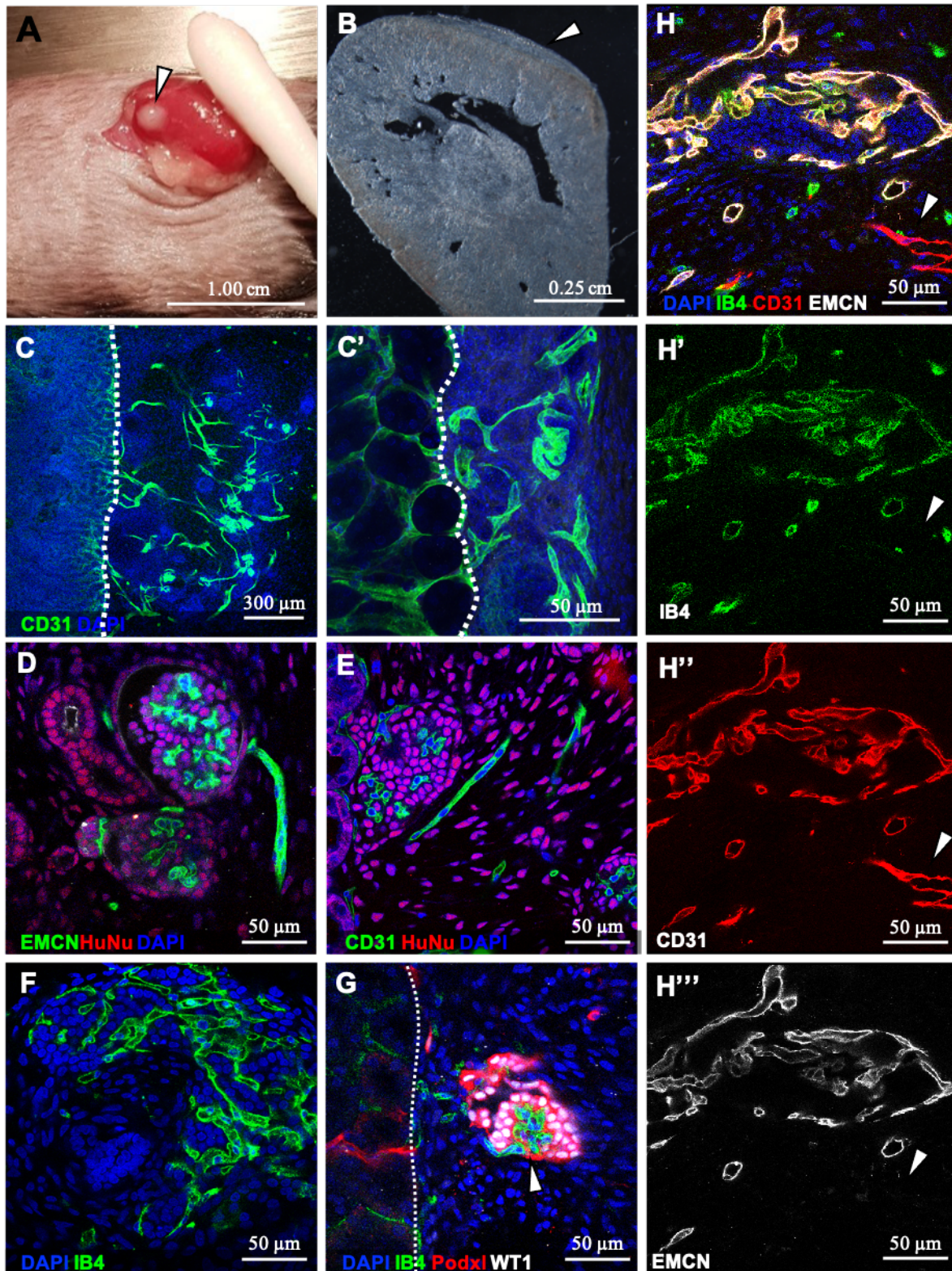


Fig. 19. Implanted organoids display extensive vascularization.

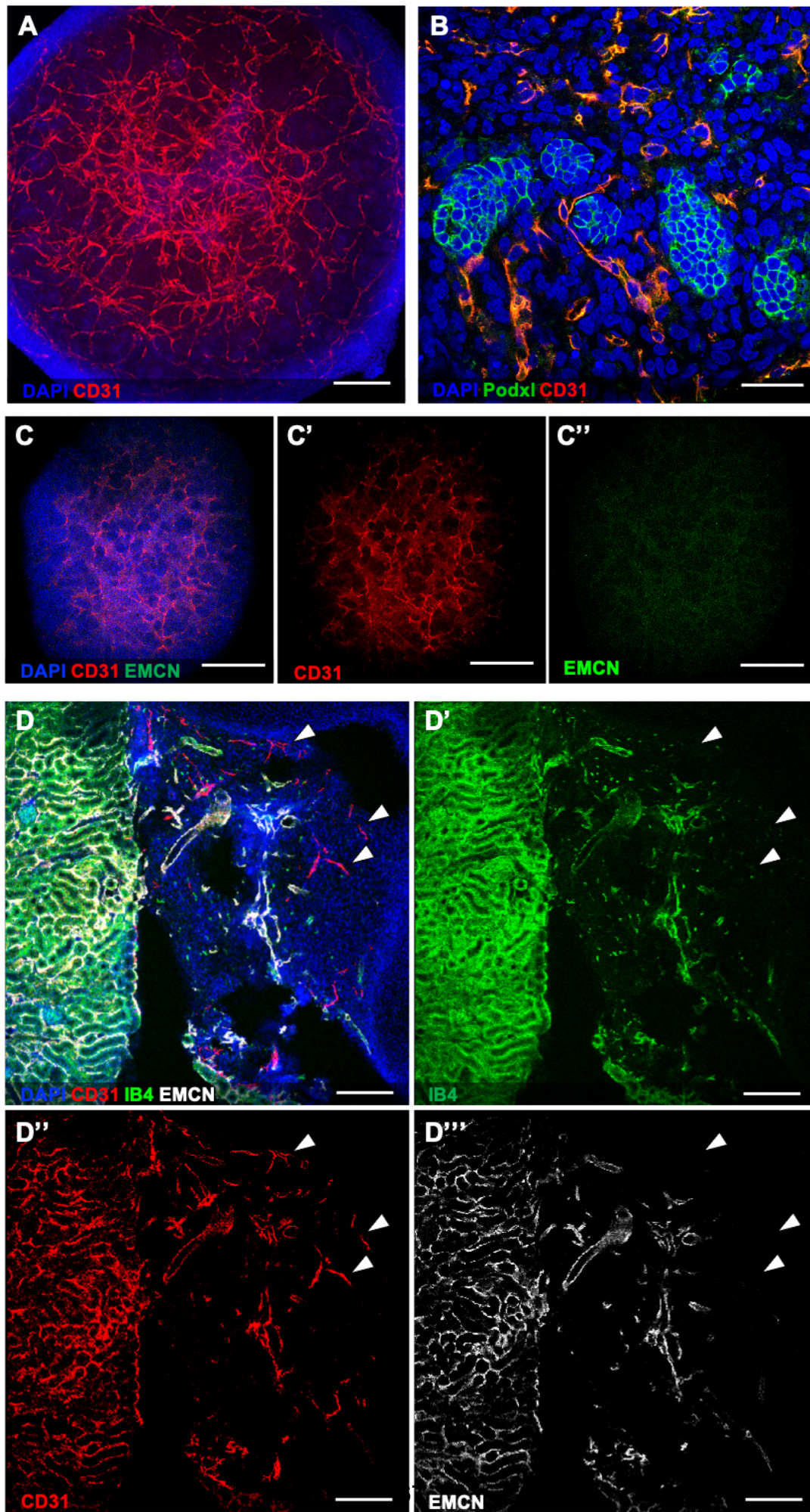
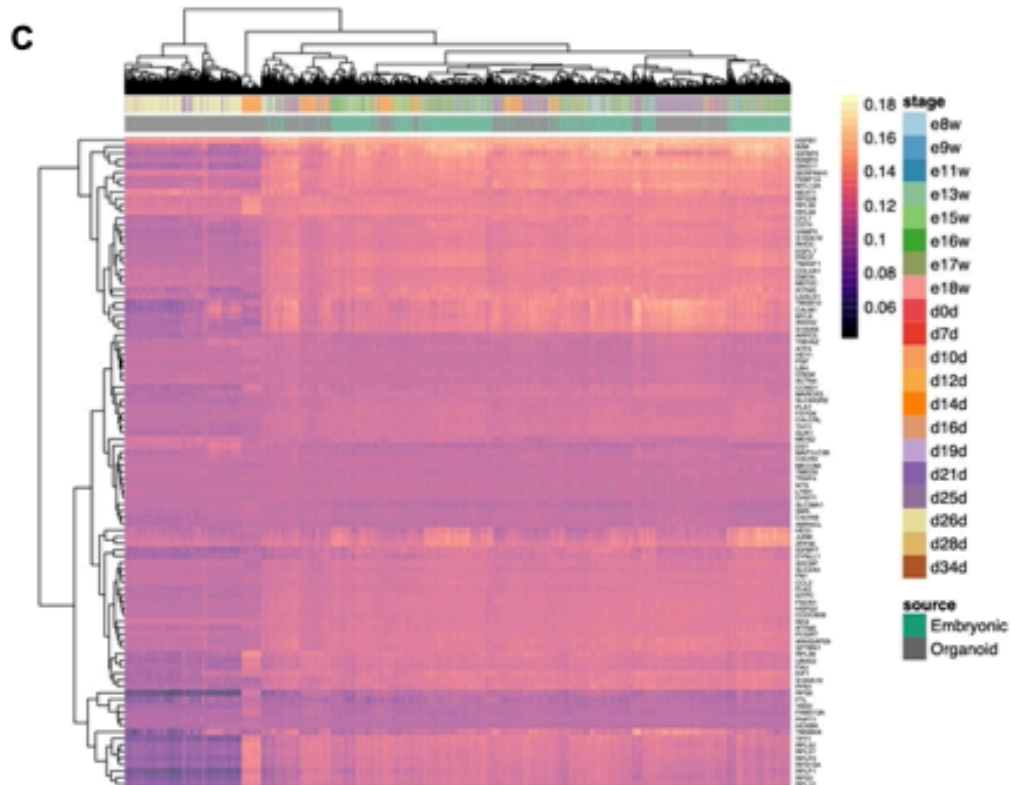
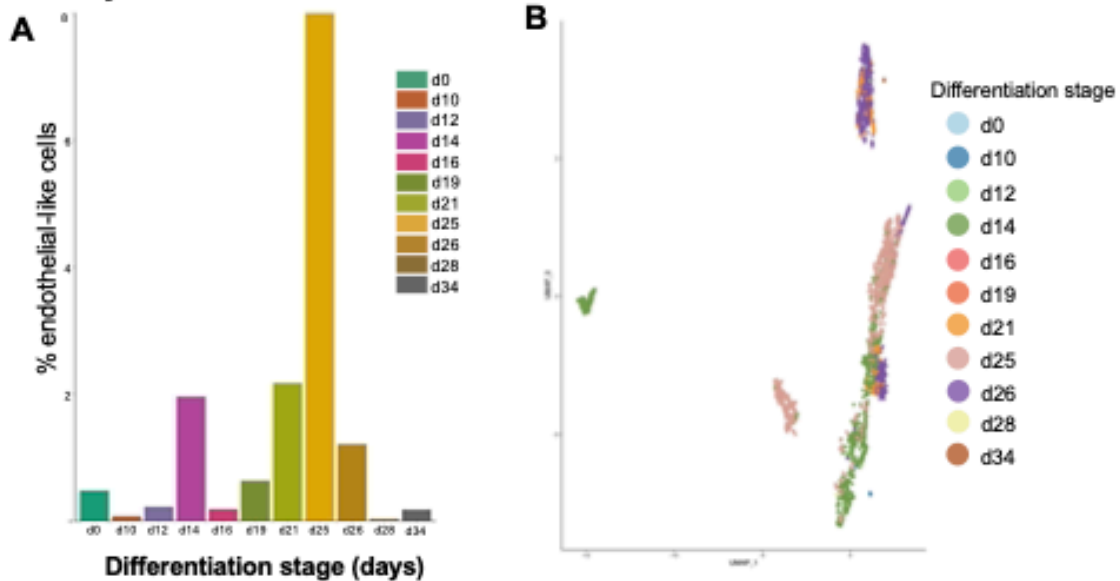


Fig. 20. scRNA-seq comparing ECs in organoids and embryonic kidneys



D Differentially expressed EC genes

eECs & oECs	Embryonic kidney ECs	eECs (Omitted)	Organoid ECs
ANAX2	IGFBP5	PLVAP	PGF
EGFL7	IGFBP7	SDPR	HEY1
EMCN		APLNR	HYAL2
ARHGAP29		ESAM	CHST1

Fig. 21. scRNA-seq comparing ECs from organoids and embryonic kidneys

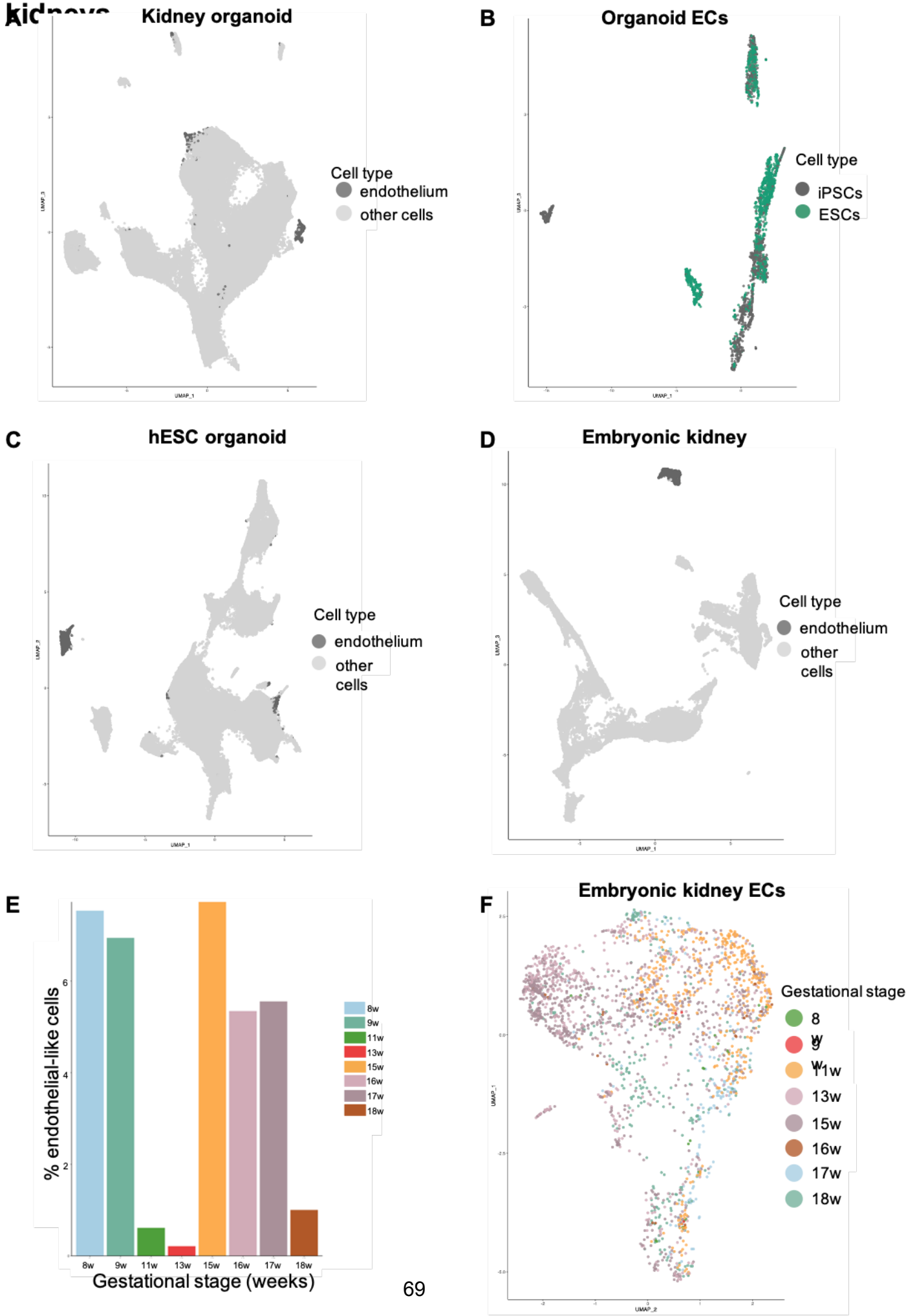


Figure legends

Figure 6. hESC-derived kidney organoids display expected renal cell types. **A)** Schematic and timeline of human embryonic stem cell (hESC) kidney organoid protocol. H9 ESCs were cultured in TeSR-E6 with 6 μ M CHIR, with a switch to 200 ng/ml Fgf9 at day -3. On day 0, the differentiated cells were aggregated and placed into an ultra-low attachment 96-well plate with 200 ng/ml FGF9 for 5 days before being switched to growth-factor free media. **B-D)** Immunofluorescence of day 0 differentiated hESCs. 150 μ m scale bars. **B)** Accumulations of cells with Meis1/2/3⁺ stroma surrounded by Six2⁺ NPCs. Cells in the middle forming tubule-like rings as seen by DAPI (arrows). **C)** Formation of E-Cad⁺ epithelial structures. **D)** VEGFR2⁺Sox17⁻ angioblasts. **E)** Brightfield images of hESC organoids 2–7 days after aggregation. 0.5 mm scale bar. **F-G)** Immunofluorescence of day 12 hESC organoids demonstrating **F)** E-Cad⁺ epithelium and LTL⁺ proximal tubules and **G)** Podxl⁺ podocytes. **H)** Paraffin section of Meis1/2/3⁺ stroma. 100 μ m scale bars. DAPI marks nuclei. N \geq 3 from at least 3 independent experiments.

Fig. 7. hESC-derived kidney organoid culture platforms. **A-H)** Representative images of organoids 12 days after aggregation comparing results of CHIR timing optimization during differentiation days -7-0 and ALI/submerged culture conditions. Whole mount immunofluorescence of DAPI, Six2, Sox17, and CD31. **A-D)** blue line: CHIR/FGF9 switch on day -4 of differentiation. **E-H)** red line: CHIR/FGF9 switch on day -3. **A, B, G, and H)** cultured on Transwells at the ALI. **C-F)** submerged in 96 well format. Sox17⁺CD31⁺ ECs and Six2⁺ NPCs. **I)** Diagram demonstrating the two organoid culture methods: Air-liquid interface (ALI) on a Transwell filter (left) and submerged in an ultra low-attachment 96 well plate (right). **J)** Cartoon showing the viewpoint of a filter-cultured organoid when examined through whole mount immunofluorescence and viewed from above (left) or sectioned (right). Representative immunofluorescence images were derived from n \geq 3 organoids.

Figure 8. hESC-derived organoid blood vessels are sparse and lack patterning. **A)** Whole mount immunofluorescence of a day 12 organoid demonstrating a network of CD31⁺ ECs. **B)** Virtual slice of Sox17⁺VEGFR2⁺ ECs. 100 μ m scale, inset 10 μ m scale. **C)** Whole mount immunofluorescence of CD31⁺Sox17⁺ ECs in a day 12 hESC organoid (yellow arrow). CD31⁺Sox17⁺ cells are indicated with white arrows. 100 μ m scale. **D-F)** Comparison of vascular volume by whole mount immunofluorescence staining of embryonic kidneys and hESC organoids. **D)** 3D view of an E13.5 mouse kidney stained with EMCN. 100 μ m scale. **E)** 3D view of an hESC organoid stained with CD31. 100 μ m scale. **F)** A graph quantifying the percent volume of ECs in a whole mount image comparing 3 embryonic kidneys at E12.5, 13.5, and 14.5 with 9 organoids from 3 independent experiments. One-way ANOVA performed. **** adjusted p value < 0.0001. EC % volume is not significantly different between kidneys. **G)** E-Cad⁺ tubule surrounded by Flk-1 GFP⁺ ECs in a E15.5 kidney. 10 μ m scale. **H)** E15.5 glomerulus formed by a Flk-1 GFP⁺ capillary tuft surrounded by Podxl⁺ podocytes. 10 μ m scale. **I)** Epithelial tubule (E-Cad, dotted line) is not surrounded by ECs (CD31) in the hESC organoid. 10 μ m scale. **J)** ECs (CD31) did not invade hESC organoid glomerulus (Podxl). 10 μ m scale. **K)** Immunofluorescence on a section of a day 12 hESC organoid stained for ECs with CD31. 100 μ m scale. Yellow arrow (**K'**) points to a lumenized blood vessel. White arrow (**K''**) are cords without lumens. **L)** Immunofluorescence of a day 12 hESC organoid on section stained with CD31 and PDGFR β . White arrow points to a single EC or EC cord surrounded by PDGFR β ⁺ cells. Yellow arrow points to a lumenized vessel without PDGFR β coverage. 100 μ m scale. DAPI marks nuclei. Representative immunofluorescence images were derived from n \geq 3 organoids from at least 3 different experiments.

Figure 9. hESC-derived organoid optimization. **A)** Brightfield microscopy images of hESC organoid differentiation at the ALI, days 1–7. **B)** Demonstration of the organoid variability when cultured at the ALI (rows 1 and 3) compared to submerged in the 96 well format (rows 2 and 4). Rows 1 and 2 are on day 3; rows 3 and 4 are on day 6. 0.5 mm scale bars. **C)** Quantification of contact points between ECs and E-Cad⁺ epithelial structures by area. **D)** Branching index, quantification of blood vessel junction density, comparing 9 organoids from 3 experiments to 3 E15.5 kidneys. **D-E)** Unpaired Student's *t*-test was performed. **** adjusted p value < 0.0001. **E)** Immunofluorescence of an E15.5 kidney showing Podxl in the apical surface of Flk1-GFP⁺ capillaries. 50 μ m scale. **F)** Immunofluorescence of CD31⁺ blood vessels in an hESC organoid. **G)** Zoom into image in (F) with Podxl (**G'**) and CD31 (**G''**) channels separated. Some cords express Podxl on the apical membrane (yellow arrow) and some do not (white arrow). 50 μ m scale. **H)** Immunofluorescence of an hESC organoid section stained with CD31, PDGFR β , and SMA. Arrow points to PDGFR β ⁺SMA⁺ cell in contact with a CD31⁺ EC. 100 μ m scale. Representative immunofluorescence images were derived from n \geq 3 organoids from at least 2 different experiments.

Figure 10. hESC-derived organoid vasculature regresses in culture. **A-F)** Whole mount immunofluorescence of hESC organoids with CD31 and Sox17 on days 6–18. DAPI mark nuclei. 200 μm scale. Zoomed in areas are marked with a white box. **G-H)** Quantification of day 3–18 images by percent volume of CD31 (**G**) and Sox17⁺ nuclei (**H**). **H–N)** vasculature of VEGF-treated organoids by whole mount immunofluorescence (**I–N**) and quantified by percent volume of CD31 (**O**) and Sox17⁺ nuclei (**P**) compared to control treated data (**G–H**). **Q–V)** qPCR data of 6 different organoid experiments (by color) showing relative gene expression relative to day 0 before aggregation to day 15. **Q)** CD31, **R)** VEGFR2, **S)** Podxl, **T)** Meis1 and Col3a1 **U)** Six2, and **V)** E-Cad. **W–Y)** Cell death in organoids shown by cleaved caspase 3 (CC3), with CD31 and E-Cad. **W)** Whole mount immunofluorescence of a day 12 organoid. 200 μm scale. **X–Y)** Selected virtual slices of regions of (**W**). Arrows point to cell-specific CC3. 30 μm scales. DAPI marks nuclei. Representative immunofluorescence images were derived from $n \geq 3$ organoids from at least 2 different experiments.

Figure 11. NZC organoids maintain epithelial and stromal cell types but suffer loss of ECs upon culture. **A–C)** 3D view of a day 18 hESC organoids stained with DAPI, CD31, and E-Cad, (**A and C**) Meis1/2/3 (**B**), and Cleaved Caspase 3 (CC3) (**C**). 105 μm scales. **D–G)** Live images of NZC organoids expressing GFP: Hoxb7Cre; RYFP (ureteric bud lineage, **D**), Six2Cre; RYFP (NPC lineage, **E**), Foxd1Cre; RYFP (stromal progenitor cell lineage, **F**), and Flk1-GFP (ECs, **G**). **H–I)** Live images of NZCs isolated from Flk1-GFP⁺ embryos after 1 day (top row, **H and H'**, **I and I'**) and 3 days (bottom row, **H'' and H'''** and **I'' and I'''**) of NZC culture on monolayer. 100 μm scale. Color balance is adjusted for clarity. **J)** Whole mount immunofluorescence of an NZC organoid 2 days after aggregation stained with DAPI, Flk1-GFP, and CC3. 200 μm scale. **J'** shows close up of a vessel with large amounts of CC3. 10 μm scale. **K)** Whole mount immunofluorescence of an NZC organoid 3 days after aggregation stained with DAPI, Flk1-GFP, and CC3. 100 μm scale.

Figure 12. NZC-derived kidney organoid generation. **A)** Schematic and timeline of NZC-derived organoid protocol. A heterogeneous population of nephrogenic zone cells (NZCs), including stromal cells, nephron progenitor cells (NPCs), endothelial cells (ECs), and ureteric bud (UB) tip cells, are isolated from embryonic mouse kidneys. NZCs may be expanded on monolayer for up to 2 passages to increase the organoid yield or proceed directly to the aggregation step. Organoids are aggregated on a filter floating on APEL2 media then treated with a 1 h CHIR pulse before culture with 200 ng/ml FGF9 for 5 days before being switched to growth-factor free media. Mouse illustration from <http://www.emouseatlas.org> **B)** Immunofluorescence of an E17.5 mouse kidney with E-Cad⁺ UB, Six2⁺ NPCs, and CD31/EMCN⁺ ECs. The nephrogenic zone is demarcated with a yellow dotted line. **B')** After pancreatin and collagenase A digestion, the NPCs, ECs, and stromal cells of the nephrogenic zone are no longer present. **C–D)** Immunofluorescence showing the NZCs after monolayer culture. **C)** Foxd1Cre; YFP + stromal cells, Six2⁺ NPCs and **D)** Hoxb7Cre; YFP + UB cells. **E)** Brightfield images of NZC organoids 2–7 days after aggregation. **F–J)** Immunofluorescence of various kidney cell types present in NZC organoids. **F)** Whole mount immunofluorescence of an NZC organoid with E-Cad⁺ epithelium. 80 μm scale. **G–J)** Immunofluorescence of sectioned NZC organoids, oriented with the air-liquid interface on top displaying Aqp1⁺ proximal tubule and descending loop of Henle and NPHS1⁺ podocytes (**G**), LTL⁺ proximal tubule and Umod⁺ loop of Henle (**H**), Meis1/2/3⁺ stroma (**I**), and Aqp3⁺ and pan-cytokeratin⁺ UB (**J**). G–H 100 μm scale. DAPI marks nuclei. Representative immunofluorescence images shown in A–C were derived from $n \geq 3$ organoids from at least 2 different litters.

Figure 13. NZC organoid endothelial, stromal and epithelial cells express off-target markers. **A–F)** Immunofluorescence on section of an NZC organoid. **A)** ECs are marked by CD31/EMCN, NPCs by Six2, epithelium by E-Cad, and nuclei by DAPI. Yellow arrowheads point to morphologically distinct ECs. White arrow points to CD31⁺EMCN⁺ cells on filter side of NZC organoid. 100 μm scale bar. $N > 3$ **B)** Stroma is marked by Meis1/2/3, ECs by EMCN, and nuclei by DAPI. 50 μm scale. $N = 6$ from two experiments **B')** Zoom in of EMCN⁺Meis1/2/3⁺ ECs on the air-liquid interface. 10 μm scale **B'')** Zoom in of Meis⁺EMCN⁺ cells on the filter side. 10 μm scale **C)** Foxd1Cre; RYFP/terminator + DTA 'stroma only' NZC organoid. Stroma lineage is shown with YFP, ECs by CD31, and nuclei by DAPI. Arrows point to YFP⁺CD31⁺ cells. **D)** Six2Cre; RYFP NZC organoid, NPC lineage shown by YFP, ECs by CD31, and stroma by Meis1/2/3. Arrows point to triple positive cells. **E)** Stroma lineage is marked by Foxd1Cre; RYFP, epithelium by E-Cad, and nuclei by DAPI. YFP⁺E-Cad⁺ cells marked with arrows. **F)** NZC organoid with LTL⁺ (Proximal tubule) and Cytokeratin (CK)⁺ tubules. Six2⁺ NPCs at the ALI. **G)** Immunofluorescence of a sectioned hESC organoid with CD31⁺Sox17⁺Meis1⁻ ECs and Meis1⁺ stromal cells. 100 μm scale. **H)** Immunofluorescence of a sectioned hESC organoid with Six2⁺Meis1/2/3⁻ NPCs and Six2⁻Meis1/2/3⁺ stromal cells. 50 μm scale.

Figure 14. NZC-derived kidney organoids develop sparse vasculature that regresses in culture. A-D) Whole mount immunofluorescence of NZC organoids. **A)** A small Flk1-GFP⁺CD31⁺ vascular plexus at the air-liquid interface. E-Cad⁺ epithelium and additional CD31⁺ cells are present. 80 μ m scale. **B)** Flk1-GFP⁺ ECs and Podxl⁺ podocytes visualized by 3D and section view. White arrow: podocytes. Yellow arrow: Cross section view of an EC cord lacking a lumen. 20 μ m scale. **C)** Live images of Flk1-GFP in NZC organoids from days 1–7. Yellow arrows point to ECs. **D)** Endothelial cord is formed by polarized ECs expressing Podxl at the apical surface. No open lumen is visible. **E)** Three NZC organoids varying levels of vascularization from a single experiment scored as I, II, and III by level of vasculature. 150 μ m scale bar. **E')** Graph of EC score quantification of 244 organoids. DAPI marks nuclei. Representative immunofluorescence images shown in A-C were derived from n = 3 organoids from at least 2 different litters.

Figure 15. NZC organoids display limited lumen formation. Whole mount immunofluorescence of NZC organoids showing **A)** A small Flk-1 GFP⁺Icam2⁺ vascular plexus, **B)** A large Flk1-GFP⁺Podxl⁺ vessel with micro lumens and **C)** A single Flk1-GFP⁺Podxl⁺ vessel on section view with a clear luminal space.

Figure 16. Blood vessels of explanted embryonic kidneys regress in culture. A-B) Whole mount immunofluorescence of explanted E12.5 kidneys after 3 (**A**) and 6 (**B**) days of culture. ECs are marked by Flk1-GFP, NPCs by Six2, and nephrons and ureteric bud by E-Cad. **C-D)** Whole mount immunofluorescence of **C)** E13.5 kidney stained with CD31 and EMCN for ECs and **D)** an E15.5 kidney stained for Flk1-GFP ECs **E-G)** Explanted E12.5 kidney on glass for live imaging. **E)** Brightfield and Flk1-GFP after 1–3 days of culture. **F)** Live imaging of Flk1-GFP over 12 h. **G-I)** Whole mount immunofluorescence of Flk1-GFP⁺ ECs, Cleaved Caspase 3 (CC3)⁺ apoptosing cells, and Phospho-histone H3 (pHH3)⁺ proliferating cells. **J-K)** Live images of explanted E12.5 kidneys in brightfield and Flk1-GFP. **J)** Control and **K)** treated with 200 ng/ml VEGF. 100 μ m scale bars. DAPI marks nuclei. Representative immunofluorescence images were derived from n = 3 explants.

Figure 17. Blood vessels of explanted embryonic kidneys regress in culture. A-B) Live images of Flk1-GFP E12.5 kidney explants over 6 (**A**) and 2 (**B**) days. **C)** Whole mount immunofluorescence of Flk1-GFP ECs in embryonic mouse kidneys at E12.5 plus E13.5 and E15.5 as seen in Fig. 6C and D. **D-G)** Whole mount immunofluorescence of explanted E12.5 kidneys after 3 (**D-E**) and 6 (**F-G**) days of culture. ECs are marked by Flk1-GFP, NPCs by Six2, and nephrons and ureteric bud by E-Cad. Representative immunofluorescence images were derived from n = 3 explants.

Fig. 18. Implanted organoids display extensive vascularization. hiPSC organoids developed using methods from Kumar Gupta et al. (2020), 3 weeks after engraftment under the kidney capsule of NSG mice. **A)** Cluster of organoids under the kidney capsule after 3 weeks, arrow. 1 cm scale. **B)** Section of adult kidney showing growth of implanted organoids under the capsule, arrow. 2.5 mm scale. **C)** Mouse-specific antibody CD31⁺ vessels were visible at the interface between the host and organoid (dotted white line) 300 μ m (**C**) and 50 μ m (**C'**) scale. **D)** EMCN⁺ and **E)** CD31⁺ ECs in the organoid are HuNu⁻. **F-H)** Vessels display perfusion as per isolectin B4 (IB4) visible following injection into mouse host. **G)** IB4⁺ perfused capillary tuft in a Podxl⁺WT1⁺ glomerulus (arrow). **H)** Most perfused vessels are EMCN⁺CD31⁺ and non-perfused vessel (arrow) is EMCN⁻CD31⁺. D-H 50 μ m scale. DAPI marks nuclei. Representative images shown here were derived from n = 6 NSG mice.

Figure 19. Implanted organoids display extensive vascularization. hiPSC organoids developed using methods from Gupta et al. (2020). **A)** Whole mount CD31 immunofluorescence of an organoid on day 18 of differentiation. **B)** Immunofluorescence of an organoid showing interaction between CD31⁺ ECs and clusters of Podxl⁺ podocytes. **C)** Whole mount immunofluorescence of an organoid with EMCN⁻CD31⁺ ECs. **D)** Implanted organoid with perfused EMCN⁺CD31⁺ blood vessels and EMCN⁻CD31⁺ non-perfused vessels, arrows. Perfusion shown by IB4. 300 μ m scale bars. Representative immunofluorescence images shown in A-C were derived from n = 3 independent biological replicates. Representative images shown in D were derived from n = 6 NSG mice.

Figure 20. scRNA-seq comparing ECs from organoids and embryonic kidneys. Analysis of scRNA-seq datasets of organoids and human embryonic kidney tissue from multiple publications. Organoids were differentiated using multiple protocols and ESC or PSC lines. Differentiation stages (days 0, 10, 12, 14, 16, 19, 21, 25, 26, 28, and 34 of organoid culture) do not correspond with methods used in previous figures. **A)** Histogram of EC percentage in organoid samples by day. **B)** UMAP of oECs color-coded by day. **C)** Heat map of 100 genes differentially expressed in eECs and oECs. Combines the top 50 genes differentially expressed in both eECs and oECs in comparison to other cells plus the top 25 genes highly expressed individually in eEC and oEC populations. Genes are grouped by cell

expression similarity. Left to right, cells are grouped by gene expression similarity. eECs are indicated in green, and oECs are grey, with color coding above referring to stage. **D)** Differentially expressed endothelial genes in eECs and oECs.

Figure 21. scRNA-seq comparing ECs from organoids and embryonic kidneys. **A)** UMAP showing clustering of kidney hESC and hiPSC organoid ECs (oECs) against non-ECs. **B)** UMAP of kidney organoid EC cluster color-coded by cell source. hiPSCs, grey, hESCs, green. **C)** UMAP showing clustering of kidney hESC organoid ECs against non-endothelial cells. **D)** UMAP showing clustering of embryonic kidney ECs (eECs) against non-ECs. **E)** Histogram showing the percentage of ECs in embryonic samples by gestational stage. **F)** UMAP of human embryonic kidney EC cluster, color-coded by gestational time point.

Future considerations

CHAPTER FOUR

ORGANOIDS REQUIRE A FUNCTIONAL VASCULATURE

Vascularization of organoids increases maturity

A vascular network is no doubt required for the function and survival of tissues. Additionally, it is now evident that vascularization of also increases tissue maturation. For instance, the addition of ECs to cerebral organoids results in neuronal action potentials (Cakir et al., 2019) and vascularization of kidney organoids leads to podocyte maturity and proximal tubule polarity and ciliation (van den Berg et al., 2018; Homan et al., 2018). The importance of vasculature in creating a mature tissue has been recognized, and protocols are being established in order to achieve vascularized tissue. Below, we discuss current methods for creating and maintaining organoid vasculature as well as evaluating their strengths and weaknesses.

Methods for vascularization of organoids

Vascularization through addition of endothelial cells

Cerebral organoids are avascular (Lancaster et al., 2013); this may be due to the differentiation protocol not yielding to ECs or the regression of vasculature due to the long culture time of cerebral organoids. In order to overcome the lack of blood vessels, ECs have been added to the mixture of cells. Various forms of ECs have been added, including HUVECs and differentiated hESCs (Pham et al., 2018; Cakir et al., 2019; Shi et al., 2020). As discussed above, ECs are heterogeneous and tissue specific. Even in organoids, the endogenous vasculature has been shown to be transcriptionally similar to ECs in vivo. Therefore, it is inadvisable to use HUVECs or other EC lines to create vasculature in organoids because it will not match the tissue. Additionally, ECs lose

their unique properties once cultured (Lacorre et al., 2004; Israely et al., 2014). However, it has been shown that expression of endothelial transcription factor ETV-2 in ECs gives them the plasticity to adapt to a new environment (Palikuqi et al., 2020). ETV-2 expression, even transient, appears to revert ECs into an angiogenic state that allows them to form a network of stable vessels. In fact, overexpression of ETV-2 in hESCs is sufficient to differentiate into ECs (Cakir et al., 2019; Morita et al., 2015).

In vitro flow studies

Regression of vasculature has been noted in multiple organoid systems where organoids are cultured under static conditions (Takasato et al., 2015; Holloway et al., 2020; Ryan et al., 2021). Blood flow contributes two important functions: 1. Provides ECs and surrounding tissues with oxygen and nutrients while removing metabolic waste and 2. Exerts shear stress on the ECs, resulting in production of survival and differentiation signals. Hence, organoid vasculature regresses due to the lack of hemodynamic flow in standard culture conditions. In order to develop organoids with a stable vasculature, hemodynamic flow must be provided. There are two ways of doing this: through *in vitro* fluidics systems and through implantation into a host animal.

Microfluidics

Adding hemodynamic flow to *in vitro* tissue can be done using microfluidics, engineered devices that produce the flow of liquid, colloquially known as ‘tissue on a chip.’ There are many variations of these tools, with their own specific objectives and advantages. A simple way to introduce flow into organoids is by orbital shaker or spinner flask bioreactor. This creates flow in a circular motion by moving all the fluid. While most studies focus on the hemodynamic flow within a vessel, even

interstitial flow induces sprouting of ECs (Song and Munn, 2011). Orbital shakers are a standard part of the Lancaster et al., 2013 protocol to prevent necrosis in cerebral organoids, although vasculature is not present. Przepiorski et al., 2019 uses a bioreactor to generate hiPSC-derived kidney organoids, but there does not appear to be a significant improvement in vasculature over other organoid culture systems.

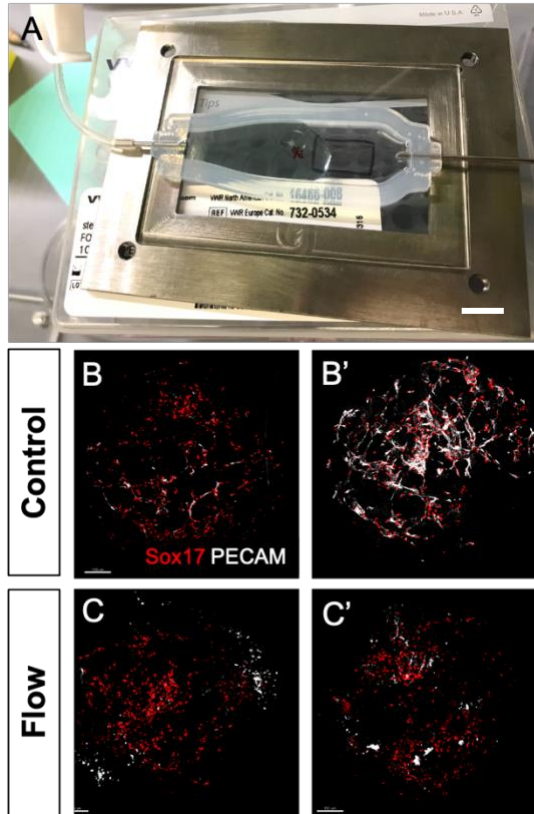


Figure 22. Macrofluidics flow chip and organoids. A) Flow chip, 1cm scale. B-C) Whole mount IF of organoids under control conditions (B) or under flow (C) days 6-12 at 2.79 ml/min at 5 mbar pressure. Results are inconclusive. 150µm scale.

A ‘macrofluidics’ device applies shear stress to as many as 100 organoids at once (Homan et al., 2018). Most of the flow is around and over the organoids, although some fluid moves through the vessels as well. This method has only been used with kidney organoids, but it can likely be used with multiple types. We received the materials for the Homan et al., 2019 device through a collaboration with the Lewis Lab (Fig. 22). Of note, there is not yet clear evidence that the improvement of vasculature from this type of flow is due to an increase in oxygenation and nutrients or the physical effects of hemodynamic flow on the ECs. I have used this device to introduce flow onto both hESC organoids and kidney explants, but did not observe an improvement

in vasculature. This could be due to differences in the pump used and flow settings or inconsistencies in the ‘gelbrin’ matrix when recreated in my hands. The published work is

remarkably promising, so likely with further troubleshooting we will be able to recreate their success.

Bioreactors may stabilize organoid vasculature, but in order to create a functional kidney tissue, the culture system will have a vasculature with an inlet and outlet. One such microfluidics chip was generated to create a *de novo* capillary bed with unidirectional flow through lumenized blood vessels (Moya et al., 2013). We hypothesized that this would be the perfect model to develop vascularized organoids. Not only could we create a *de novo* network of perfused vasculature in the organoid, but the inlet and outlet would allow us to test renal function

Bioreactors may stabilize organoid vasculature, but in order to create a functional kidney tissue, the culture system will have a vasculature with an inlet and outlet. One such microfluidics chip was generated to create a *de novo* capillary bed with unidirectional flow through lumenized blood vessels (Moya et al., 2013; Wang et al., 2016). We hypothesized that this would be the perfect model to develop vascularized organoids. Not only could we create a *de novo* network of perfused vasculature in the organoid, but the inlet and outlet would allow us to test renal filtration. Through a collaboration with the Schmidtke Lab at UT Southwestern, we used the published design in order to develop a similar microfluidics chip (Fig. 23). Similar to the chip in figure 22, we encountered difficulties in recreating the published results. After 7 days of culture under flow, while we expected a capillary network, instead a PECAM⁺ monolayer of HUVECs had formed. We realized that once again, a significant amount of troubleshooting will be necessary in order to achieve the desired results, but it could be a significant step forward in organoids.

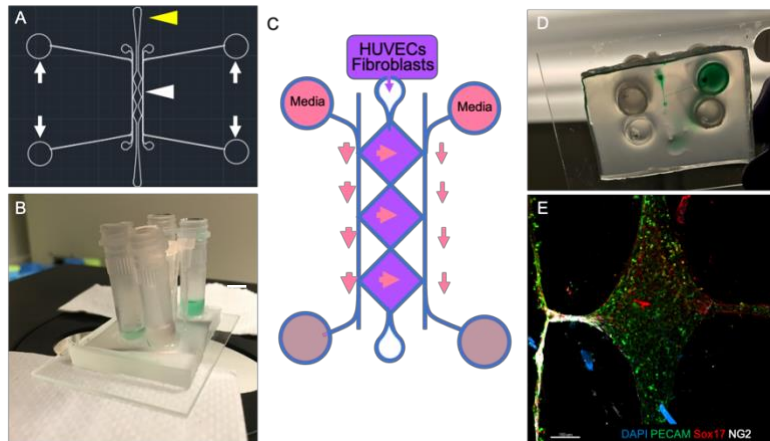


Figure 23. Microfluidics chip. **A)** PDMS stamp designed by Kevin Lam using Wang et al., 2016 for reference. White arrows, media reservoir placement. White arrowhead, tissue chambers. Yellow arrowhead, cell port. 100 μ m height channels. 2mm scale. **B)** Side view of the chip with green water in reservoirs. **C)** Model of media and cells in the chip. HUVECs and human lung fibroblasts are seeded into the tissue chamber in a mixture of fibrinogen with polymerization activated by thrombin. Media (pink) is added to the top two reservoirs at a 3:1 ratio, which flows to the lower two reservoirs. This creates interstitial flow across the tissue chambers. **D)** View from beneath the microfluidics chip with green water in one reservoir, demonstrating flow. Leakage can be observed. **E)** IF of HUVECs and fibroblasts after 7 days. 100 μ m scale.

Implantation

Many researchers have achieved organoid vascularization through implanting organoids into immunocompromised mice, allowing for host blood vessel invasion into the organoid. The most widely used method for implantation is under the kidney capsule of an adult mouse, due to the relative accessibility of the area

and the capsule holding the implanted tissue in place. Within weeks, vasculature from the host invades into the organoid tissue implantation results in significant growth of the organoids and maturation of the tissue, including architecturally (Finkbeiner et al., 2015; Chen et al., 2018; van den Berg et al., 2018). Organoids implanted at earlier time points in culture have been shown to demonstrate better growth (Bantounas et al., 2018). Additionally, the presence of pre-implantation vasculature may increase the level of host invasion (Cakir et al., 2019). VEGF knockout mESCs implanted into nude mice do not form teratomas as readily as wildtype cells and have less vascularization, demonstrating the importance of endogenous VEGF in blood vessel recruitment after implantation (Ferrara et al., 1996).

The vasculature resulting from implantation has been shown to have two results. Either the host vasculature anastomoses with the existing organoid vasculature present, creating hybrid

vessels, or the host vasculature entirely takes over the organoid, with the graft vasculature disappearing over time (van den Berg et al., 2018; Francipane et al., 2019). However, these phenomena are not necessarily mutually exclusive, and more studies on the dynamics between the host and graft ECs will shed light on this process. ECs migrate against the direction of flow; therefore, they may simply be diluted out by the host ECs (Sprague et al., 1997). Alternatively, deficiencies in organoid ECs not yet identified may result in them being out competed by host vessels if anastomosis, and therefore blood flow, is not quickly established.

Drawbacks of implantation include the expense and difficulty of the technique. Immunocompromised mice are expensive to obtain and house. This method also diminishes the *in vitro* advantages that organoids provide over *in vivo* models. Additionally, the surgery can result in an overgrowth of scar tissue, stroma, and other unwanted cell types such as cartilage (Przepiorski et al., 2019; Gupta et al., 2020). Most studies of implanted organoids focus on the successful experiments and appear to even zoom in on the healthy organoids and crop out fibrosis.

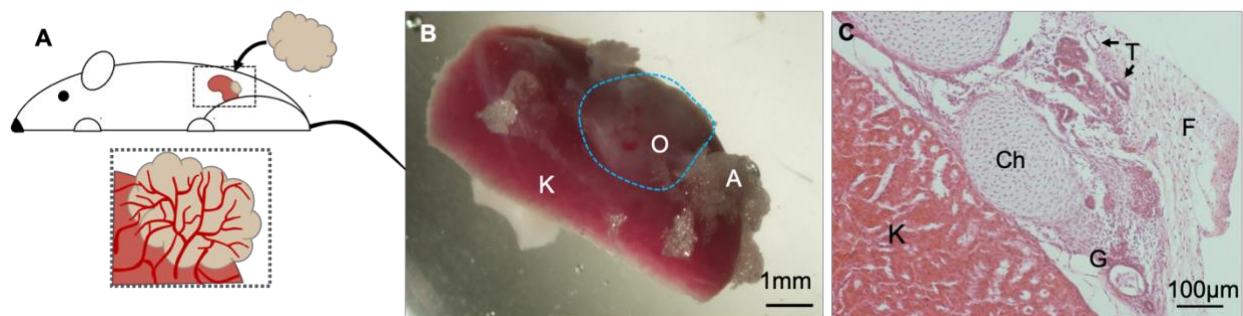


Figure 24. Implanted organoids can cause fibrosis and transdifferentiation into chondrocytes after implantation. A) Model of implantation of kidney organoids into an immunocompromised mouse and resulting vascularization by the host. B) Image of a section of adult kidney 4 weeks after organoid transplant. C) H & E showing the interface between implanted organoids and host kidney. O: organoids, K: host kidney, A: adipose tissue, F: fibrosis, Ch: chondrocytes, T: tubules, G: glomerulus.

Imitating the effects of flow using Yoda-1

Since it is clear from numerous studies that vasculature requires flow, but we had trouble with microfluidics, we decided to look into an alternative method to imitate flow. Piezo-1 is mechanosensory ion channel. It is necessary for endothelial response to flow and particularly important for vascular development and remodeling. In fact, the Piezo1 endothelial knockout is embryonic lethal (Renade et al., 2014). Yoda-1, a Piezo1 agonist, has been shown to activate *Icam1* and *Vcam1* expression in a concentration-dependent manner, reaching similar levels as 5 dyn/cm² shear stress at 2 μ M Yoda-1 (Davies et al., 2019). A Yoda-1 dose response experiment with hESC organoids is shown in **Figure 25**. At the highest dose used in Davies et al., 2019 of 2 μ M Yoda-1, organoids displayed significantly more vasculature by PECAM⁺ percent area. Further experiments will be necessary in order to determine if Yoda-1 treatment expands the longevity of vasculature and how it affects the epithelium.

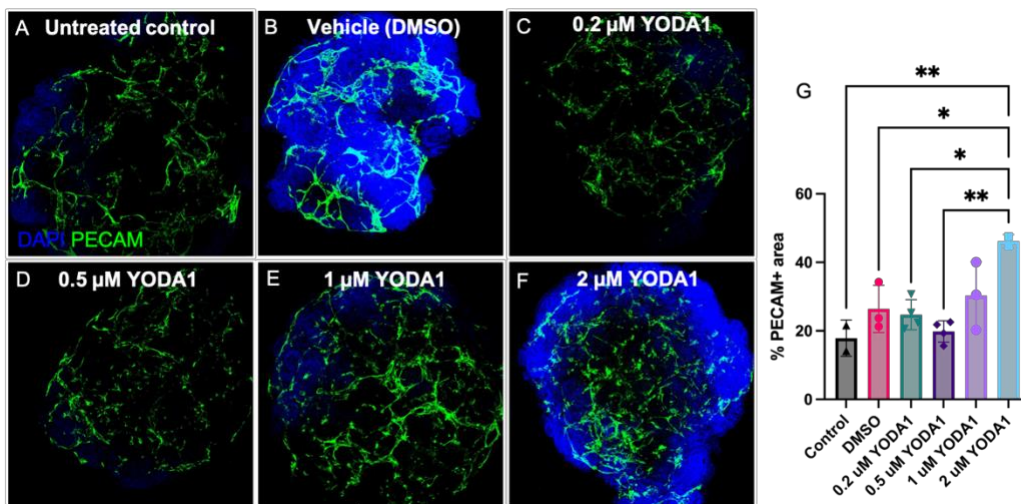


Figure 25. Yoda-1 dose-response treatment of organoids. A-F) Whole mount IF of hESC organoids stained with DAPI and PECAM. G) Graph of percent PECAM by organoid area. Only 2 μ M Yoda-1 has significantly more PECAM than controls.

Alternative pathways to promote blood vessel maturation and maintenance

While considerable attention has been placed on the necessity of flow for vascular maintenance and maturation, the vasculature must be stabilized before flow can be established. Here we discuss signaling pathways that may be activated for this purpose. The addition of pro-angiogenic factors and pro-maintenance (anti-regression) are being assessed as a tool for increasing and maintaining vasculature before flow can be established. The addition of VEGF increases EC number in EBs, with a significant improvement using a growth factor (GF) 'cocktail' that increased cell number overall in addition to a specific upregulation of ECs and hematopoietic cells. These GFs include VEGF, FGF2, IL-6, and EPO. There has been success in both increasing and maintaining the vasculature in intestinal organoids through the addition of VEGF, BMP4, and FGF2 (Holloway et al., 2020.) VEGF signaling is necessary for vascular development. Organoids and embryoid bodies contain endogenous VEGF signaling; VEGF knockout mESCs fail to form any ECs or vascular-like structures in embryoid bodies (Ferrara et al., 1996). Additionally, endogenous VEGF expression is necessary for the association of ECs and epithelium, however addition of VEGF to the culture can disrupt this relationship (Homan et al., 2018).

Hypoxia, or low oxygen, is a well-known inducer of angiogenesis. Low oxygen levels induce hypoxia inducible factors (HIFs) which turn on a number of genes including angiogenic factors such as VEGF (Liu et al., 1995; Krock et al., 2011). This results in blood vessels sprouting into the hypoxic region to provide oxygen to the ischemic tissue (Shweiki et al., 1992). Hypoxia-induced angiogenesis is integral to both physiological processes such as wound healing as well as pathological phenomena like tumorigenesis. *In utero*, the embryo experiences an environment that is around 3% oxygen. However, cell culture is performed at ambient oxygen levels of 20%. In fact,

standard cell culture should be referred to as ‘hyperoxia’ and 3-9% O₂ as ‘normoxia’ or ‘physoxia’ since it is closer to physiological levels (Ivanovic, 2009; Carreau et al., 2011). I hypothesized that hypoxia would maintain organoid vascularization by induce angiogenesis. Additionally, I hypothesized that there would be more NPCs due to the lack of perfused vasculature in the NPC caps and evidence that oxygenation induces nephron differentiation (Rymer et al., 2014; Daniel et al., 2018). I tested the effects of hypoxia on organoids by culturing them in a hypoxia chamber at 3% oxygen. The organoids shown in Figure 26 were cultured in 3% oxygen from days 5-9, around the peak of organoid vasculature. Strikingly, the hypoxia-treated organoids were much smaller. This is consistent with a study on the effect of oxygen levels in tumor spheroids, which were cultured in ultra low-attachment 96 well plates, same as our organoid system. They showed that the spheroids were smaller with less proliferation when cultured at 5% oxygen. Importantly, the spheroids in 5% oxygen did not have a necrotic core that was seen under the normoxia condition and in our kidney organoids (Gomes et al., 2016). Even more surprising, the organoids contained almost no Six2⁺ NPCs and had a completely different organization than organoids in standard culture. The hypoxia-treated organoids had a completely different organization, with E-Cad⁺ epithelium in the middle of the organoid, with mesenchyme and ECs on the outside. There did not appear to be an increase in vascularity of the hypoxia-treated organoids, but this experiment must be repeated in order to better understand the effect of low oxygen on kidney organoids.

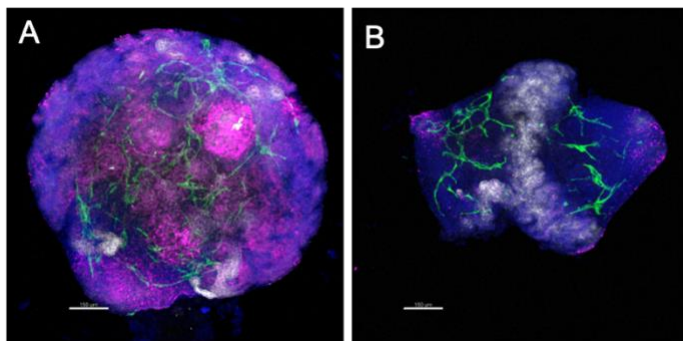


Figure 26. Organoids under hypoxia. A-B) Whole mount IF of day 9 hESC organoids with DAPI, PECAM, Six2, and E-Cad. A) Cultured under standard conditions and B) cultured under 3% oxygen from day 5-9. 150 μ m scale.

In vivo, many signals that are important for vessel stability and

maintenance come from supportive cell types, pericytes and macrophages, as well as extracellular matrix (ECM). Pericytes are the cells that architecturally and environmentally support blood vessels. Not only do pericytes provide vessels with physical support and ECM, but they also create biochemical signals that stabilize vessels, and their recruitment is necessary for vessel maturation. EC-pericyte communicate in multiple ways including the Angiopoietin-Tie, VEGF-VEGR2, and TGF β signaling, (Dickson et al., 1995; Armulik et al., 2005; Wakui et al., 2006; Chatterjee and Naik, 2012). Early vascular plexuses are initially formed ‘naked’ and require VEGF for maintenance (Alon et al., 1995). Once remodeling is finished, the vessels then recruit pericytes, marking VEGF-independent stability and maturation. Disruption of the EC-pericyte relationship results in aberrant remodeling of the capillary plexus, including regression and breaking of the vessels (Benjamin et al., 1998). Pericytes vary depending on vessel type, from the smooth muscle actin (SMA) tightly covering arteries to more spread out pericytes of the capillaries and veins. Pericytes are heterogeneous like ECs; notably, pericytes have disputed origins, and may differentiate from various sources, including mesenchyme and macrophages in a tissue-specific manner (Muller et al., 2008; Yamamoto et al., 2017; Yamakazi and Mukoyama, 2018). In organoids, pericytes appear to develop along with ECs, as they are prominent in blood vessel organoids (Embryoid bodies contain a small amount of Desmin⁺ and α -SMA⁺, two types of pericytes. However, they are not closely associated with the CD31⁺ ECs. VEGF treatment increases the number of ECs and pericytes present while also increasing pericyte-EC association (Hagedorn et al., 2004).

Macrophages are also essential for regulating angiogenesis, vascular regression, and anastomosis. In order to recreate the diverse population of cells in the brain, organoids have been made by combining precursors of the various cell types present, including

microglial/macrophage precursors and ECs in cerebral organoids, or Kupffer cells—specialized macrophages—and ECs in liver organoids (Schwartz et al., 2015; Rennert et al., 2015). Embryoid bodies produce CD34⁺CD35⁺ hematopoietic cells which can be induced to form mature macrophages through treatment with cytokines IL3, SCF and M-CSF (Wiles and Keller 1991; Subramanian et al., 2009).

Blood vessel development and maintenance is complicated, requiring both physical signals from shear stress and biochemical signals provided by the surrounding pericytes, stroma, and parenchyma. Further, we are still working to understand even fundamental aspects of vascular biology. Therefore, recreating a healthy vasculature *in vitro* is a difficult challenge. Likely, one specific factor will not be enough to create a functional vasculature in organoids. Through trial and error, we can incorporate our extensive knowledge of blood vessels into the organoid system as we continue to learn more about blood vessel dynamics.

Endothelial heterogeneity

In order to create properly vascularized organoids, it is necessary to know what the vasculature should look like. Blood vessel anatomy in the adult kidney is well established, but we still have much to learn about transcriptional identity of the renal vasculature during development (Aird 2007; Molema and Aird, 2012; Dumas et al., 2021). We previously assessed heterogeneity of ECs in mouse renal development by examining many known EC genes, helping us understand how the embryonic kidney is vascularized (Daniel et al., 2018). Many studies have added to our knowledge to EC heterogeneity, especially with the advancement of scRNA-seq (Barry et al., 2019; Dumas et al., 2020). Despite the growing number of published scRNA-seq studies, we noticed that many

lacked substantial *in vivo* validation of gene expression. We set off to aggregate various renal

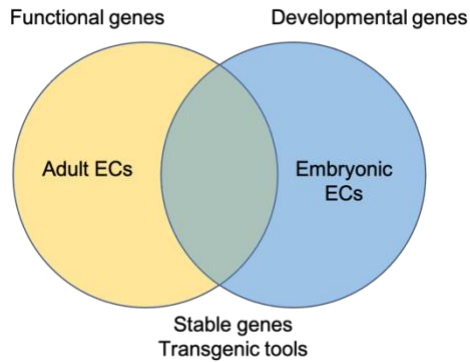


Figure 27. Venn diagram of gene expression analysis in adult and embryonic kidneys. Genes expressed by ECs in both adult and embryonic kidneys may be potential candidates for developing transgenic reporters and knockouts to examine kidney or region-specific genes.

RNA-seq studies to compare the results and determine if they are consistent with each other and understand how *in silico* data represents *in vivo*, asking questions such as how many types of ECs are present in the kidney? Are we able to identify spatial heterogeneity or renal specific EC genes with scRNA-seq? Angiocrine signals? This knowledge will aid in our understanding of renal vasculature and potentially lead to genetic tools. Our idea was that assessing EC heterogeneity, especially

over different stages could help us in multiple ways (Fig. 27). Genes expressed only during embryogenesis could be important molecular determinants of vascular and kidney development, including angiocrine signals. Genes expressed during later developmental stages and adulthood are likely genes important for endothelial function in renal filtration and resorption. Genes that are expressed in both embryonic and adult ECs but are only in renal ECs or regionally specific in the kidney could be used to create reporter or Cre lines to investigate specific vasculature.

The analysis pipeline is shown in Figure 28. Lists of genes sorted by cluster from RNA-seq experiments are first assessed by Genepaint, a database of E14.5 embryo ISHs. We hypothesized

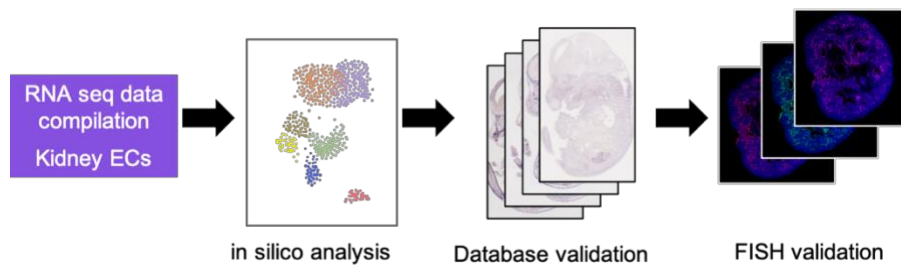


Figure 28. Pipeline gene identification for EC heterogeneity analysis.

that kidney ECs could be divided spatially into 5 zones: Cortical, outer medullary, inner medullary, arteries,

and glomeruli (Fig. 29). The genes that are present in the kidney and appear endothelial are then searched through other gene and protein expression databases, including GUDMAP (human embryonic kidney), Kidney Cell Explorer (adult kidney), Kidney Interactive Transcriptomics (adult mouse kidney), Betsholtz Brain Database (adult mouse brain and lung), and Tabula Muris (adult mouse kidney), Allen Brain Atlas (mouse embryo), Human Protein Atlas (adult human) (McMahon et al., 2008; Harding et al., 2008; He et al., 2018; Vanlandewijck et al., 2018). In order to identify priority genes, we created a scoring system, the Expression Index (EI). For each database, genes will be given a score based on expression level and specificity between 1-4. A score of 1 is given for expression in ECs only in kidney or in a specific kidney region, 2 for expression in ECs and other cells, 3 for genes not expressed in kidney ECs, kidney but in ECs in other tissues/organs, and a score of 4 for genes that are not expressed in ECs or have ubiquitous expression. The average of these scores is the EI, and lower scored genes are prioritized for further study and validation. The selected genes will be analyzed by fluorescent in situ hybridization (FISH) on E18.5 kidneys. While validating scRNA-seq data through many databases is time consuming, it is still less time consuming than performing FISH in the lab, and this extensive corroboration has shown itself to be crucial. Many genes that are identified as highly expressed through sequencing end up not being EC-specific, or in ECs at all. Figure 29 shows genes identified as ECs specific to a kidney region by Genepaint, but through GUDMAP, it was shown that they are likely not endothelial. If we had continued with FISH validation simply based on the Genepaint ISH, we would likely have wasted our time.

I am currently setting up an experiment in order to perform single nuclear RNA sequencing (sNuc-seq). One issue we have encountered when analyzing published scRNA-seq data is that the number of ECs is low, since only around 2% of cells are ECs. With such few cells, it is more

difficult to remove noise and extrapolate biologically meaningful information. Additionally, ECs are tightly wrapped by mural cells *in vivo*, so when performing traditional scRNA-seq, ECs are often accompanied by fragments of mural cells, convoluting the data. Therefore, we determined that by isolating nuclei, we could avoid this problem. Using a Flk-1::H2B-YFP reporter mouse, we are isolating nuclei from E18.5 mouse kidneys and collecting the YFP⁺ EC nuclei with Fluorescence-activated cell sorting (FACS) with assistance from the UT Southwestern FACS core (Fraser et al., 2005; Habib et al., 2017). 10x RNA sequencing will then be performed by the McDermott Center Sequencing Core.

The goal is that by combining published scRNA-seq data with our planned sNuc-seq will have an abundance of genes to analyze. Ideally, we will be able to create a map of kidney vasculature gene expression as well as identify interesting candidates for future studies of kidney blood vessel development.

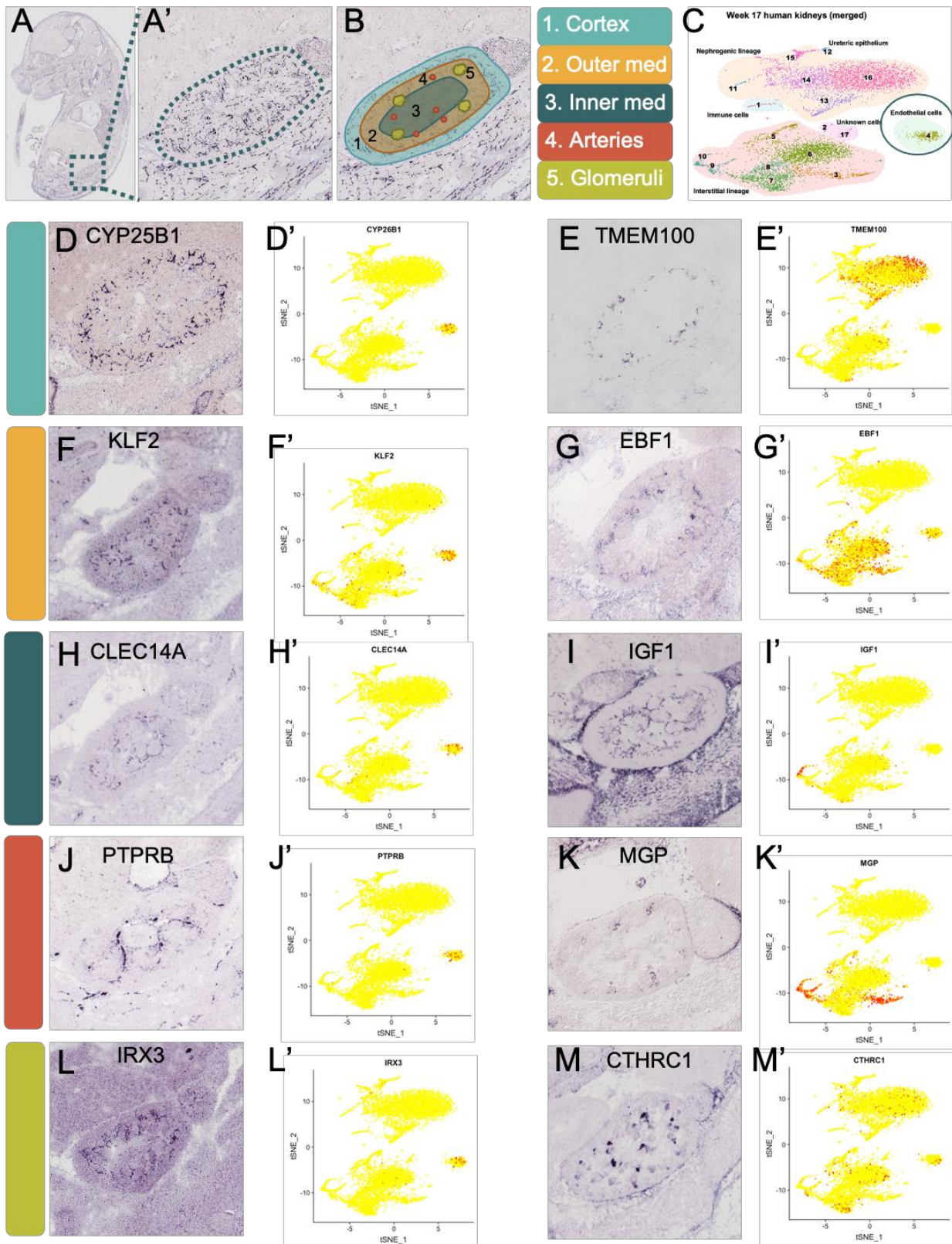


Figure 29. Endothelial gene expression in embryonic kidney by zone. A) PECAM1 expression in an E14.5 mouse embryo kidney (A'). B) Five zones of kidney vasculature. C) GUDMAP tSNE of acRNA-seq clustering, ECs circled. D-M) Genepaint image of ISH and gene expression overlay on tSNE. Images from Genepaint and GUDMAP

CHAPTER FIVE CONCLUSIONS

Necessity for in vitro kidney tissue

Millions of people in the United States have some form of chronic kidney disease and numbers are rising due to obesity and type 2 diabetes. CKD treatment focuses on controlling weight, blood pressure, and diabetes both through both lifestyle changes and drugs. While these methods have been shown to be effective in delaying CKD onset, it is not a cure, and lost kidney function cannot be repaired. When patients reach kidney failure, they rely on dialysis unless they are able to receive a kidney transplant. Unfortunately, the number of available kidney transplants is unable to support the number of patients in need. Transplants also come with the risk of rejection and require constant immunosuppression, which comes with its own risks. Clinical trials are ongoing to search for CKD treatments, but the efficacy is yet to be determined. While new treatments such as stem cell transplants are enticing, we do not know enough to determine how, or if, they work.

To combat the lack of transplantable kidneys and the complications that come with donor transplants, we have set out to find an alternative. With the surge in stem cell technology in recent years, it has become a feasible goal to develop transplantable kidneys from patients' own cells. Through a relatively simple process, we are able to turn human iPSCs into rudimentary kidney tissue. With further research, we hope to turn organoids into mature, functional, transplantable tissue.

The challenges of organoid culture

Despite immense progress in less than a decade, many challenges exist in the organoid field. As shown in this thesis, there is a particularly evident problem with organoid vasculature, particularly

its maintenance and maturity. While not as egregious as the changes in vasculature, we also noted regression of epithelium and an expansion of the stroma by day 18. Preventing the degradation of organoid tissue

With many methods generated to form organoids, it is unclear what makes the ‘best’ organoid. Additionally, there is significant variability between organoids, particularly for different batches and even the same cells can drift over time (Phipson et al., 2019). Compounding on this problem, there is no certified list of attributes that are agreed upon by the field to decisively determine if an organoid is a ‘success.’ Currently, the best estimation available is by gene expression of hallmark genes through antibody staining, RNA sequencing, or qPCR. Continuation of basic developmental biology studies, like our investigation into renal endothelial heterogeneity, are integral to establishing landmarks and goals for achieving implantable renal tissue.

The future of the field

The future of field requires a fluidic system with an inlet and outlet for vasculature and collecting duct drainage. Not only is this necessary for growth and function of the cultured kidneys, but flow is required for a healthy vascular system. Once flow is properly established, this will allow us to scale-up the organoid culture system and reduce aberrant stroma expansion and organoid quality degradation. Only then will we be able to achieve an artificial kidney that is large enough to hand the filtration requirements for an adult.

CHAPTER SIX MATERIALS AND METHODS

Mice and embryo handling

Experiments were performed in accordance with protocols approved by the UT Southwestern Medical Center IACUC. For each experiment, female mice of 7–8 weeks of age were crossed with a male of 9–10 weeks of age. Plugs were checked and the embryos were collected at the desired time points for further analysis. Noon of the day on which the mating plug was observed was designated embryonic day (E) 0.5. Flk1-GFP endothelial reporter mice were acquired from Dr. Eli Keshet (available from Jackson Laboratory Kdrtm2.1Jrt/J, stock number 017006), (Takahashi et al., 1996). These mice were created by knocking in the eGFP cassette into the first exon of Kdr. The homozygous mice are embryonic lethal and are maintained as heterozygotes in a CD1 background. In addition, the following mice were used in the studies described: Foxd1-Cre (MGI Cat# 4437923, RRID:MGI:4437922 (Humphreys et al., 2010)), Six2Cre (MGI Cat# 3848504, RRID:MGI:3848504 (Kobayashi et al., 2008)), Hoxb7Cre (IMSR Cat# JAX:004692, RRID:IMSR_JAX:004692 (Yu et al., 2002)), Rosa26 YFP (IMSR Cat# JAX:006148, RRID:IMSR_JAX:006148 (Srinivas et al., 2001)), and the RosaDTRflox or terminator mouse was kindly provided by Lloyd Cantley (Guo et al., 2013).

Generation of human ESC organoids

The methods used were adapted from previously published protocols (Takasato et al., 2015, 2016a). H9 ESCs were generously provided by Dr. Jenny Hsieh and Dr. Vanesa Nieto-Estevez at University of Texas at San Antonio. Cells were validated free of mycoplasma with a Universal Mycoplasma Detection Kit (ATCC, 30–1012K). H9 ESCs were cultured on Matrigel-coated plates

in mTeSR plus (STEMCELL, 05825) with 10 μ M Rock inhibitor Y-27632 (ATCC) for the first 24 h of growth to limit cell death. For differentiation, ESCs were split at 1:12 ratio and cultured for 24 h in mTeSR plus and Rock inhibitor. The next day, day 7, the media was replaced with TeSR-E6 (STEMCELL, 05946) with 6 μ M CHIR 99021 (R&D, 4423). Media was changed daily or every other day. On day 3, the media was replaced with TeSR-E6 with 200 ng/ml FGF9 (R&D, 273-F9-025). On day 0, the cells were collected using TrypLE Express (ThermoFisher, 12604013). Cells were distributed into an Ultra-Low Attachment 96 well U bottom plate (Corning, CLS7007-24 EA) with approximately 100,000 cells per well in TeSR-E6 with 200 ng/ml FGF9. Media was changed every 2–3 days. On day 5, FGF9 was no longer added. Organoids were also made by spotting 100,000 cells in 1 μ l onto a 2.4 cm Transwell filter, which required a 1 h 6 μ M CHIR pulse. (Unlike filter organoids, we found that submerged organoids did not require a CHIR pulse to differentiate. Additionally, the submerged format limited user error by accidental flooding of the Transwell which caused the organoids to die. Lastly, the 96 well plate format provided a more efficient use of media than Transwell filters in a 6-well plate (200 μ l media per organoid vs. >300 μ l per organoid) plus the additional media that was required for the 1 h CHIR pulse after aggregation.

Generation of mouse NZC derived kidney organoids

Nephrogenic zone cells (NZCs) were isolated using the protocol from Brown et al. (Brown et al. (2015). Briefly, kidneys were dissected from embryonic day 17.5 (E17.5) mice in PBS. Kidneys were cleaned and capsules were carefully removed ensuring no damage to the kidneys. The kidneys were combined and washed in HBSS (Gibco, 14175) on a nutator (Fisher Scientific, 260 100F) at 37 C for 2 min. HBSS was removed and the kidneys were carefully submerged in a filtered

0.1% collagenase A (Roche, 11,088,793 001)/0.5% porcine pancreatin (Sigma, P1625) solution in PBS without calcium or magnesium (Corning, 20–031 CV). The kidneys were incubated in the collagenase/pancreatin enzyme digest on a nutator at 37 C for 10 min. The enzyme was inactivated using 125 µl of fetal bovine serum (FBS). While avoiding contact with the kidneys, the supernatant was removed and centrifuged at 2000 RPM for 5 min using a microcentrifuge (Eppendorf Centrifuge 5415 D). The supernatant was discarded and the cell pellet was resuspended in 1 ml of AutoMacs buffer (Miltenyi Biotec, 130-091-221) and passed through a 30 µm pre-separation filter (Miltenyi Biotec, 130-041-407) that was previously primed with 4 ml of AutoMacs buffer. The filter was immediately washed with 500 µl of AutoMacs buffer and cells were counted from the resulting filtrate. If cells were to be plated in monolayer, cells were seeded onto a tissue culture plate pre-coated in 25% Matrigel (Fisher Scientific, 08-774-553)/DMEM F12 (Gibco, 11,320,033) at a cell density of between 5000 and 25,000 cells per cm² similar to the method used by Brown et al. (Brown et al. (2015)). Cells were cultured in APEL2 (STEMCELL, 05270) with 1% Penicillin-Streptomycin supplemented with 200 ng/ml FGF9 (R&D, 273-F9-025) and 10 µM Rock inhibitor Y27632 (Millipore, 688001). Media was changed every two days and the cells were passaged when after reaching 70% confluency using TrypLE dissociation solution (Life Technologies, 12,563,029). Cells can be maintained in monolayer no more than two passages.

If the collected NZCs were to be aggregated into organoids, cells were resuspended in AutoMacs buffer at a concentration of 500,000 cells/2 µl, accounting for the volume of the cells. 2 µl of the cell solution was carefully pipetted onto a Nuclepore Track-Etch Membrane (Whatman, #110409) which was floating in 1 ml APEL 2 (StemCell, 05270) with 1% Penicillin-Streptomycin and 8 µM CHIR. Organoids were incubated for in 37 C at 5% CO₂ for 1 h after which the 8 µM CHIR media was removed and replaced with 1 ml APEL 2 with 1% Penicillin-Streptomycin and

200 ng/ml human recombinant FGF9 (R&D, 273-F9-025). Except for Fig. 4J, where the organoid was treated with CHIR overnight. Organoids were cultured for 5 days after which the media was removed and replaced with 1 ml APEL 2 with 1% Penicillin-Streptomycin without any additional growth factors and cultured for an additional 5 days for a total of 10 days of growth. Throughout the culture period, media was replaced every two days.

For hypoxia experiments, organoids were cultured at 37°C in 3% O₂ and 5% CO₂. Media was placed in the hypoxia chamber at least 8 hours before media changes in order to equilibrate oxygen levels. Organoids were fixed in the hypoxia chamber.

Explant culture of embryonic kidneys

Flk1-GFP embryos were dissected at E12.5. Kidneys were cultured on Nuclepore Track-Etch Membranes (Whatman, 110409) floating on DMEM/F12 medium with 10% FBS and 1% Penicillin-Streptomycin. For live imaging, kidneys were cut with a tungsten wire and cultured cut-side down on fibronectin-coated, glass-bottom plates (MatTek, P35G-1.5-14- C).

Histology and immunohistochemistry on sections

Kidneys and organoids isolated at the desired time points were fixed using 4% paraformaldehyde at 4 C overnight (kidneys and NZC organoids) or 20 min at room temperature (hESC organoids) with gentle agitation. For paraffin histology, tissue was washed 3 times in PBS for 5 min, dehydrated in an ethanol series, xylene cleared, and embedded in paraffin. 10 µm sections from paraffin-embedded kidneys were stained by haematoxylin and eosin or immunofluorescence. Alternatively, tissue was processed through cryosectioning, where tissue was washed 3 times in PBS for 5 min, incubated overnight in 30% sucrose, and embedded in OCT (ThermoFisher

Scientific, 23-730-571). OCT-embedded tissue was sectioned on a cryostat into 10 μm sections. Paraffin and frozen sections were baked at 60 C for 10 min. Paraffin sections were deparaffinized in xylene then hydrated in an ethanol series to water. Both paraffin and frozen sections were then washed in 0.1% Triton-X/PBS and blocked in 5% normal donkey serum/0.1% Triton-X/PBS for a minimum of 1 h at room temperature. Sections were incubated in a variety of primary antibodies in blocking solution overnight at 4 C (for dilutions, see Table S1) followed by 3 washes in 0.1% Triton-X/PBS. Sections were then incubated in secondary antibody at 1:500 in blocking solution for 1 h at room temperature, washed 3 times in PBS, incubated in DAPI, and mounted with anti-fade mounting media (Vectashield, H1000) or Prolong Gold Mounting Medium (Cell Signaling, 8961). Tissue was viewed and imaged by scanning laser confocal microscopy (NIKON A1R).

Whole-mount immunofluorescence

Fixed organoids were washed in PBS and permeabilized with 1% Triton-X 100 for 1.5 h before being blocked using CAS-Block (ThermoFisher Scientific, 008120) for 1.5 h. The tissues were incubated in primary antibodies in CAS block (for dilutions, see Table S1) overnight at 4 C. Tissues were washed in PBS at least 5 times for 10 min each and incubated in secondary antibodies in CAS block for 1 h and then washed and subsequently incubated in DAPI for 1 h. Tissues were mounted on slides with ProLong Gold and visualized using a Nikon A1R confocal to take optical sections every 1 μm .

Whole kidneys were additionally cleared by incubating them in a 1:2 mixture of benzyl alcohol/benzyl benzoate (BABB) for at least 10 min. Kidneys were mounted in BABB and visualized using an LSM710 Meta Zeiss confocal to take optical sections every 2.5–3 μm as described in Daniel et al., 2018.

Vascular quantification

Whole mount organoids and embryonic kidneys stained for CD31 and Sox17 (organoids) or CD31 and EMCN (kidneys) were analyzed with Imaris. Volume of the organoids was automatically calculated. For the kidneys, due to extraneous tissue, a surface was created manually by using the contour setting to trace the kidney about every 5 slices through the z-stack. The volume of this surface was used to estimate the kidney volume. Then, the surface was used to create a mask of the CD31/EMCN channel so that blood vessel volume was only calculated within the kidney. Next, a surface of the masked CD31/EMCN channel was created. Surfaces were created automatically using the same parameters across all samples, including the absolute intensity and automatic thresholding. The sum of surface volumes of this channel were used as the estimation of blood vessel volume. Automatic surface calculations with Imaris fail when there is extremely low signal and/or high background. Therefore, the surface was adjusted by hand for quantification of the day 3, VEGF- treated organoid and background subtraction was used for the quantification of day 15 and 18 VEGF treated organoids (Fig. 3). Sox17⁺ nuclei were counted using the spots function on Imaris using a 6 μm estimated diameter with automatic quality thresholding and background subtraction.

Branching of vasculature was quantified with angiotool, a free soft- ware developed by the NIH (Zudaire et al., 2011). The same whole mount organoids and E13.5 embryonic kidneys stained for CD31 and Sox17 (organoids) or CD31 and EMCN (kidneys) analyzed for Fig. 2D–F were analyzed for branching. Every 5th virtual slice was analyzed and the number of junctions and junction density were automatically calculated. For epithelial-endothelial contact, EC contact with E-Cad⁺ epithelial structures were counted by hand using FIJI. 10 μm sections of E15.5 kidneys

stained by immunofluorescence for Flk1-GFP and E-Cad as well as 10 μm virtual sections of whole mount organoids stained for CD31 and E-Cad were analyzed. Brightness/contrast adjustments made for representative images were equally applied to all images in that set. To analyze NZC organoid vascularity and variability, we visually assessed (two observers, one blinded) by EC whole mount antibody stain. We classified organoids into Class I (little), II, and III (lot) depending on the area of EC staining.

Quantitative PCR

At least 8 organoids were collected and RNA was isolated using the RNeasy Micro Plus kit (Qiagen, 74034). Up to 2 μg of total RNA was used to make cDNA with the SuperScriptTM III Reverse Transcriptase kit (Invitrogen, 18080). Primers were selected from published sources and are available in Table S2. qPCR was performed in triplicate using SYBR green master mix (Applied Biosystems, 4,309,155) and 1 μl diluted cDNA (~ 2 ng) with an annealing temperature of 60 C. The reaction was run with the QuantStudio 3 Real-Time PCR system (Applied Biosystems/Thermo Fisher, A28567). Gene expression levels were determined by PCR reactions (15 s at 95 C and 1 min at 60 C for 40 cycles). GAPDH was used as an internal control for gene expression and the $\Delta\Delta\text{Ct}$ method was used to calculate fold change compared to day 0.

Organoid engraftment under the kidney capsule

hPSC organoids for engraftment were developed according to the protocol in Kumar Gupta et al. (2020) where two days after organoid aggregation, organoids cells are collected and mixed with newly differentiated kidney progenitor cells then reaggregated. 18 days after the initial

differentiation began, organoids were implanted under the kidney capsule of an immunocompromised NOD SCID gamma (NSG) mouse. Organoids were harvested 3 weeks after engraftment. 100 μ l of 1 μ g/ μ l of Isolectin B4-FITC (Sigma) was injected into the retroorbital sinus of the host mouse 30 min before harvest in order to visualize perfused vasculature. Tissue was sectioned with a vibratome and analyzed by immunofluorescent staining. More detailed methods in (Kumar Gupta et al., 2020).

Single cell data analysis

Mouse embryonic kidney datasets published (Combes et al., 2018; England et al., 2020) are curated in the Gene Expression Omnibus (GEO) database under accession numbers GSE108291 and GSE155794, respectively. The GEO accession numbers for each human embryonic and organoid single cell RNA-seq dataset analyzed can be found in Tables S3 and S4, respectively. In addition, sequencing data for 8- and 9-week embryos published by (Young et al., 2018) was included.

Each batch was processed independently using the scran Bio-conductor package (Lun et al., 2016b). Unfiltered feature-barcode matrices were generating by running the CellRanger count pipeline for data provided in this format. Otherwise, provided gene expression matrices were used directly. Cells were called from empty droplets by testing for deviation of the expression profile for each cell from the ambient RNA pool (Lun et al., 2018). Cells with large mitochondrial proportions, i.e., more than 3 mean-absolute deviations away from the median, were removed. Cells were pre-clustered, a deconvolution method was applied to compute size factors for all cells (Lun et al., 2016a) and normalized log-expression values were calculated. Variance was partitioned into technical and biological components by assuming technical noise was Poisson-

distributed and attributing any estimated variance in excess of that accounted for by a fitted Poisson trend to biological variation. The dimensionality of the data set was reduced by performing principal component analysis and discarding the later principal components for which the variance explained was less than variance attributable to technical noise.

A single set of features for batch correction were obtained by computing the average biological component of variation across batches and retaining those genes with a positive biological component. The batches were rescaled, and log-normalized expression values recomputed after the size factors were adjusted for systemic differences in sequencing depth between batches. Batch effects were corrected by matching mutual nearest neighbors in the high-dimensional expression space (Haghverdi et al., 2018). The resulting reduced-dimensional representation of the data was used for all subsequent embeddings including UMAP's and diffusion maps.

Cells were clustered by building a shared nearest neighbor graph (Xu and Su, 2015) and executing the Walktrap algorithm (Pons and Matthieu., 2006). Differential gene expression analysis was performed using the two-part generalized linear model that concurrently models expression rate above background and expression mean implemented in MAST (Finak et al., 2015). A one-versus-all strategy was employed comparing each cluster to all other identified interstitial clusters.

Cell type labels were transferred from embryonic mouse to embryonic human cells as follows. First, the mouse and human embryonic cells were integrated and embedded together in a 50-dimensional diffusion map (Haghverdi et al., 2016). Next, the TensorFlow platform (Abadi et al., 2015) was utilized to train a sequential neural network with two hidden layers each containing 512 nodes, with dropout layers following each hidden layer, to classify the mouse embryonic cells

by cell type as either epithelium, interstitium, endothelium, erythrocyte or leukocyte. The Adam optimizer was used with a focal sparse categorical cross entropy loss (Lin et al., 2017). Graph regularization (Bui et al., 2018) was employed. Five-fold cross validation was used during training. Next, clusters of the human embryonic cells, obtained independently as above, were assigned to one of the above cell types by a voting process where each cell's mapped cell type determined its vote. These assigned cell types were then used to classify the human organoid cells in the same way.

Microfluidics

Two fluidics devices were used. The microfluidics chip developed by the Lewis Lab may be found in Homan et al., 2018. In brief, a gelbrin mixture was made by mixing PBS, gelatin, fibrinogen, sodium chloride and transglutaminase. Thrombin was added to polymerize the mixture, which was poured into the mold. With a cut 200 μ l pipette, organoids were transferred onto the gelbrin and the cover was screwed onto the top and attached to pump system. The pump used for this experiment was the Ibidi Perfusion System (Ibidi, 10902). Flow rates used were around 2.8 ml/minute.

The second microfluidics device was designed by Kevin Lam using AutoCAD, based on Wang et al., 2016 (Lam et al., 2019). The CAD design was used as a mask in contact photolithography, creating a silicon wafer so the pattern is raised. Sylgard 184 Silicon Elastomer was mixed with curing agent to create polydimethylsiloxane (PDMS), which was poured into the wafer. Once cured, the PDMS mold was removed and holes were stamped out with a biopsy punch at the various ports. The PDMS mold was plasma treated and adhered onto plasma-treated glass,

creating the microfluidics channels. Detailed methods may be found in Lam et al., 2019 and Duffy et al., 1998). In order to seed the microfluidics chips, the methods from Wang et al., 2016 and 2017. In brief, HUVECs and normal lung human fibroblasts were mixed together in fibrinogen at a concentration of 10^7 cells/ml. Thrombin was added to the cell/fibrinogen mixture and quickly seeded into the cell port. EGM2 media was added to the top two media reservoirs at a 3:1 ratio and the chip was placed to culture in the incubator. Media was changed daily.

Table 1. Select clinical trials in CKD

Trial number	Title	Drug/Treatment	Delivery	Biologic activity	Primary outcome	Sponsor	Phase	Enrollment	Start date	Estimated end date	Other indications	Status
NCT02841280	Chlorthalidone in Chronic Kidney Disease (CLCK)	Chlorthalidone	Oral	Diuretic	Change from baseline to 12 weeks in systolic ambulatory blood pressure	Indiana University	2	160	2016	2022	Hypertension	Active, not recruiting
NCT02848131	Senescence, Frailty, and Mesenchymal Stem Cell Functional in Chronic Kidney Disease: Effect of Senolytic Agents	Dasatinib and Quercetin	Oral	tyrosine-kinase inhibitor, leukemia therapy; antioxidant	Assessment of senescence markers in skin, fat, and/or blood	Mayo Clinic	2	16	2016	2022		Enrolling by invitation
NCT02915601	Bicarbonate Administration in CKD	Sodium bicarbonate	Oral	Base	Change in Brachial Artery Flow Mediated Dilation and Aortic Pulse Wave Velocity	University of Colorado, Denver	N/A	108	2017	2021	Metabolic Acidosis	Recruiting
NCT02946034	Safety, Efficacy, and Changes in Traditional and Novel Biomarkers of Kidney Function in Patients With Hepatitis C and Advanced Chronic Kidney Disease Treated With Abbvie Viekira Pak or Mavyret Regimen	paritaprevir/ritonavir, ombitasvir, dasabuvir (referred to as Viekira Pak) ± ribavirin	Oral	Antiviral	Reduction in biomarkers of CKD progression	Abbvie	4	24	2017	2021	Chronic Hepatitis C	Active, not recruiting
NCT02947750	Neurovascular Regulation During Exercise in Humans With Chronic Kidney Disease	6R-BH4	Oral	phenyletonuria treatment	Change in functional sympatholysis; Changes in vascular diameter in response to phenylephrine, blood pressure and sympathetic responses during exercise	Emory University	2	150	2016	2022		Recruiting
NCT03055598	Effect of Auryxia on ESA Utilization in ESRD Patients With High Ferritin & Low Transferrin Saturation: A Pilot Project	Ferric Citrate	Oral	iron-based phosphate binder, decreases phosphate, increases iron		Keryx Biopharmaceuticals	4	30	2019	2020	End Stage Renal Disease	Active, not recruiting
NCT03223883	Curcumin Supplementation for Improving Vascular and Cognitive Function in Chronic Kidney Disease	Curcumin (Longvida)	Oral	natural polyphenol with anti-inflammatory and antioxidant characteristics	Vascular endothelial function, Brachial artery flow-mediated dilation	Diana Lalai, Stanford, University of Colorado	2	88	2018	2023	Cognitive decline	Recruiting
NCT03325322	Frailty, Inflammation, and Stem Cell Functionality in Chronic Kidney Disease	Fisetin	Oral	Antioxidant	Change in inflammatory markers, Effect on Mesenchymal stem cell function	Mayo Clinic	2	30	2018	2025	Diabetes Mellitus, Diabetic Nephropathies	Recruiting

NCT03380962	A Phase I/II Trial to Evaluate the Safety and Tolerability of Cazakizumab (Anti-IL-6 Monoclonal) to Eliminate Donor Specific HLA Antibodies (DSAs) and Improve Transplant Rates in Highly-HLA Sensitized Patients Awaiting Renal Transplant	Cazakizumab	Infusion	Anti-IL-6 Monoclonal antibody	Change in donor specific antibodies and adverse events	Stanley Jordan, MD	1/2	20	2018	2023	Kidney Transplant Failure and Rejection	Active, not recruiting
NCT03471117	Targeting ADMA With Pioglitazone to Reduce Sympathetic Overactivity in CKD Patients	Pioglitazone	Oral	typically used to improve glucose control	Muscle sympathetic nerve activity (MSNA) will be reduced	The University of Texas at Arlington	4	28	2018	2021		Recruiting
NCT03565913	Potential Therapeutic Role of Effervescent Calcium-Magnesium Citrate in Chronic Kidney Disease Stage V	EffCaMgCit	Oral	(hypohthesis) retard the formation of calciprotein particles (CPP) in CKD Stage V, thereby reducing the degree of coronary artery and peripheral artery calcification and cardiac hypertrophy-fibrosis.	Serum T50 for CPP	University of Texas Southwestern Medical Center	2/3	125	2017	2023		Active, not recruiting
NCT03574363	A Phase 2, Randomized, Double-Blind, Placebo-Controlled, Multi-Center Study to Assess the Efficacy, Safety, and Pharmacokinetics of KBP-5074 in Patients With Moderate-to-Severe Chronic Kidney Disease and Uncontrolled Hypertension	KBP-5074	Oral	mineralocorticoid receptor antagonist	Systolic blood pressure	KBP Biosciences	2	165	2018	2020	Hypertension	Active, not recruiting
NCT03579693	Cross-over Randomized Controlled Trial of Coenzyme Q10 or Nicotinamide Riboside in Chronic Kidney Disease	COQ10	Oral	reduce oxidative stress	Maximal Aerobic Capacity and work efficiency	University of Washington	2	30	2018	2021	Sarcopenia Frailty	Recruiting
NCT03579693	Controlled Trial of Coenzyme Q10 or Nicotinamide Riboside in Chronic Kidney Disease	Nicotinamide riboside	Oral	restore substrate delivery to mitochondria	Maximal Aerobic Capacity and work efficiency	University of Washington	2	30	2018	2021	Sarcopenia Frailty	Recruiting
NCT03594110	A Multicentre International Randomized Parallel Group Double-blind Placebo-controlled Clinical Trial of EMPagliflozin Once Daily to Assess Cardio-renal Outcomes in Patients With Chronic KIDNEY Disease	Empagliflozin	Oral	SGLT2 Inhibitor	Time to first occurrence of kidney disease progression or cardiovascular death	Boehringer Ingelheim	3	6609	2019	2022		Active, not recruiting

NCT03602261	A Multi-Center, Randomized, Two-Cohort Phase 2 Study to Evaluate the Safety, Efficacy, Pharmacokinetics and Pharmacodynamics of CTAP101 (Calcitriol) Extended-Release Capsules to Treat Secondary Hyperparathyroidism in Subjects With Vitamin D Insufficiency and Chronic Kidney Disease Requiring Regular Hemodialysis.	Calcitriol	Oral		Change of mean plasma intact parathyroid hormone (iPTH), Severity of Treatment- Emergent Adverse Events as assessed by CTCAE, Maximum serum concentration of Calcitriol, Increase mean serum total 25-hydroxyvitamin D	OPKO Health, Inc.	2	256	2018	2023	Secondary Hyperparathyroidism Due to Renal Causes, Vitamin D deficiency	
NCT03649711	A Mechanistic Study in Patients With Non-Dialysis Chronic Kidney Disease to Investigate Altered Platelet Response to Antiplatelet Therapy (KID-Platelet Study)	Ticagrelor (Brilinta) + aspirin	Oral	Blood thinners	ADP induced platelet aggregation	University of Arkansas	3	81	2018	2022	Heart Attack Stroke, Ischemic	Recruiting
NCT03649711	A Mechanistic Study in Patients With Non-Dialysis Chronic Kidney Disease to Investigate Altered Platelet Response to Antiplatelet Therapy (KID-Platelet Study)	Clopidogrel (Plavix) + aspirin	Oral	Blood thinners	ADP induced platelet aggregation	University of Arkansas	3	81	2018	2022	Heart Attack Stroke, Ischemic	Recruiting
NCT03710291	A Phase 3b, Randomized, Double-blind, Placebo-controlled Study to Evaluate the Efficacy and Safety of TRC101 in Delaying Chronic Kidney Disease Progression in Subjects With Metabolic Acidosis	TRC101	Oral	polymeric hydrochloric acid binder	Progression of chronic kidney disease	Tricida, Inc.	3	1600	2018	2024	Metabolic Acidosis	Recruiting
NCT03781089	Patromer Efficacy to Reduce Episodic Hyperkalemia in End Stage Renal Disease Patients Treated With Hemodialysis (PEARL-HD)	Patromer	Oral		Number of episodes of serum K \geq 5.5 mEq/L	Duke University	4	40	2019	2022	Hyperkalemia, ESRD	Enrolling by invitation
NCT03787368	An Observer-blind, Multi-center, Placebo-controlled, Parallel Group Study to Assess the Safety and Tolerability and to Characterize the Pharmacokinetics and the Pharmacodynamics of Different Doses of BAY1213790 in Patients With End-stage Renal Disease Undergoing Hemodialysis	BAY1213790	Infusion		Number of major and CRNM bleeding events	Bayer	1	55	2019	2021	ESRD/dialysis	Active, not recruiting

NCT03810911	Mechanisms of Erythropoietin Induced Hypertension	Darbepeetin		Stimulates RBC production	Change in diastolic blood pressure, flow mediated dilatation, Oxygen-induced change in forearm blood flow, Predictors of change in flow mediated dilatation	VA Office of Research and Development	2	160	2021	2025	Blood pressure, anemia	recruiting
NCT03840343	Intra-arterially Delivered Autologous Mesenchymal Stem/Stromal Cell Therapy in Patients With Diabetic Kidney Disease: A Phase I Study	Autologous adipose derived mesenchymal stem/stromal cells (MSC)	Infusion	Stem cells	Safety trial. Adverse events and/or serious adverse events	Mayo Clinic	1	30	2019	2025	Diabetes Mellitus 1 and 2, Diabetic Nephropathies, kidney failure, kidney insufficiency	
NCT03934736	An Open-label, Single Arm Study, Evaluating the Immunogenicity and Safety of HEPISAV-B® in Adults With End-Stage Renal Disease (ESRD) Undergoing Hemodialysis	HEPLISAV-B	Injection	Hepatitis B vaccine	Safety evaluation of clinically significant adverse events, Evaluation of seroprotection rate (SPR)	Dynavax Technologies Corporation	1	119	2019	2021	ESRD/dialysis	Active, not recruiting
NCT03982160	Role of Decreased Nitric Oxide in the Tonic Elevation of Resting Sympathetic Nerve Activity in Chronic Kidney Disease Patients	L-Arginine	Infusion	nitric oxide production	Muscle sympathetic nerve activity (MSNA)	The University of Texas at Arlington	4	15	2018	2022		Recruiting
NCT03988920	A Long-Term, Open Label Study to Evaluate the Ability of Tenapanor Alone or in Combination With Sevelamer to Treat to Goal Serum Phosphorus in Patients With End-Stage Kidney Disease on Dialysis (NORMALIZE)	Tenapanor	Oral	inhibitor of the sodium-proton exchanger NHE3	Achieving normal serum phosphorus level	Ardelyx	4	150	2019	2021	Hypophosphatemia	
NCT03990363	A Phase 2b, Multicentre, Randomised, Double-blind, Placebo-controlled Study of Verinurad and Allopurinol in Patients With Chronic Kidney Disease and Hyperuricaemia	Verinurad + Allopurinol	Oral	URAT1 inhibitor, xanthine oxidase (XO)inhibitor	Ratio of urinary albumin to urinary creatinine	AstraZeneca	2	861	2019	2021		Active, not recruiting
NCT04040959	Nicotinamide Riboside Supplementation for Treating Arterial Stiffness and Elevated Systolic Blood Pressure in Patients With Moderate to Severe CKD	Nicotinamide riboside	Oral	naturally occurring vitamin B3 derivative	carotid-femoral pulse wave velocity	University of Colorado, Denver	2	118	2019	2024	Vascular disease, Blood Pressure, Oxidative Stress	Recruiting

NCT04053764	A Phase II, Multicenter, Randomized, Open Label Two Arm Study Comparing the Effect of Crizanlizumab + Standard of Care to Standard of Care Alone on Renal Function in Sickle Cell Disease Patients ≥ 16 Years With Chronic Kidney Disease Due to Sickle Cell Nephropathy	Crizanlizumab	Infusion		Percentage of patients with ≥ 30% decrease in albuminuria (ACR)	Novartis Pharmaceuticals	2	148	2019	2024	Sickle Cell Disease (SCD)	Recruiting
NCT04115345	A Phase 1 Open-Label Safety, Tolerability, and Early Efficacy Study of a Renal Autologous Cell Therapy (REACT) in Patients With Chronic Kidney Disease From Congenital Anomalies of the Kidney and Urinary Tract (CAKUT) (REGEN-004)	Biological: REACT - renal autologous cell therapy	Injection into renal cortex	May augment renal structure/function	Assess change in eGFR and adverse events	ProKidney	1	15	2019	2023	Congenital Anomalies of Kidney and Urinary Tract	Recruiting
NCT04123613	A Multi-Center Open-label Investigation to Assess the Safety and Efficacy of Multiple Doses of DM199 in Patients With Chronic Kidney Disease	DM199	Injection	recombinant human tissue kallikrein-1 (rhKLK-1)	Incidence of treatment emergent adverse events; Change in renal function (eGFR); Change in urine albumin to creatinine ratio; Plasma measurements of DM199	DiaMedica Therapeutics Inc	2	90	2019	2021		Recruiting
NCT04258397	Trial of Pirfenidone to Prevent Progression in Chronic Kidney Disease (TOP-KD)	pirfenidone	Oral		Change from baseline in kidney fibrosis, MRI and urinary markers	Genentech	2	200	2020	Jul-05		Recruiting
NCT04365218	A Phase I Randomized, Blinded, Placebo-controlled Study to Evaluate the Safety and Pharmacokinetics of MEDI8367 Administered as Single Ascending Doses in Healthy Subjects, and as a Single Dose in Healthy Subjects of Japanese-descent and in Subjects With Chronic Kidney Disease	MEDI8367	Injection	Antibody, inhibits TGFb activation	Safety trial. Adverse events and/or serious adverse events	AstraZeneca	1	70	2020	2022		Active, not recruiting
NCT04492722	A Phase 2b Randomised, Double Blind, Placebo-Controlled, Multi-Centre, Dose-Ranging Study of AZD5718 in Participants With Proteinuric Chronic Kidney Disease	AZD5718	Oral		Change from baseline in urine ACR to Week 20	AstraZeneca	2	632	2020	2022		Recruiting

NCT04500665	Anti-Inflammatory Treatment of Uremic Cardiomyopathy With Colchicine	Colchicine	Oral	Anti-inflammatory	Change in left ventricular global longitudinal strain by transthoracic echocardiography	Brigham and Women's Hospital	2	20	2020	2021		Not yet recruiting
NCT04510844	A Phase IV, Double-Blind, Placebo-Controlled, Multi-Center Trial To Study The Effects Of Evolocumab In Stage IV-V Chronic Kidney Disease: The Cardiovascular and Lipid-Lowering Effects Of Evolocumab In Advanced Chronic Kidney Disease Trial	Evolocumab	Injection	Biologic, monoclonal antibody that inhibits proprotein convertase subtilisin/kexin type 9	LDL cholesterol concentration	NYU Langone Health	4	115	2021	2023	High cholesterol	Recruiting
NCT04511338	A Randomized, Open Label, Cross-over Feasibility Study for Heparin-free Hemodialysis With the Dialyzer With Endexo™ in End-Stage Renal Disease (ESRD) Subjects	Dialyzer with Endexo	Infusion	Anti thrombotogenic	Successful heparin-free HD sessions	Fresenius Medical Care North America	N/A	16	2020	2021		Recruiting
NCT04534114	Factor XI UCLA to Reduce Thrombotic Events in End-Stage Renal Disease Patients on Hemodialysis: A Phase 2, Randomized, Double-Blind, Placebo-Controlled Study of the Safety, Pharmacokinetics, and Pharmacodynamics of Multiple Doses of BAY 2976217	BAY2976217	Injection	Prevention of thrombosis	Incidence of major bleeding and clinically-relevant non-major bleeding	Bayer	2	305	2020	2022	ESRD requiring hemodialysis	Active, not recruiting
NCT04542304	Efficacy of Diuretics in Kidney Disease	Metolazone	Oral	Diuretic	Change in urine output	Stanford University	2	50	2021	2024	End Stage Renal Disease	Recruiting
NCT04549597	Randomized Open-Label Study to Evaluate Tenapanor as the Core Therapy in the Treatment of Hyperphosphatemia in Patients With Chronic Kidney Disease Who Are Phosphate Binder Naive or on Phosphate Binders to Optimize Phosphorus Management	Tenapanor	Oral	Inhibitor of the sodium-proton exchanger NHE3	achieve target s-p levels of less than or equal to 5.5 mg/dL	Ardelyx	4	330	2020	2021	Hyperphosphatemia	Recruiting
NCT04595370	Efficacy, Safety and Tolerability of AZD9977 and Dapagliflozin in Participants With Heart Failure and Chronic Kidney Disease (MIRACLE)	AZD9977	Oral		Percent change from baseline in urinary albumin to creatinine ratio (UACR)	Astrazeneca	2	540	2021	2022	Heart failure	Recruiting

NCT04600323	Bicarbonate Administration and Cognitive Function in Midlife and Older Adults With CKD	Sodium Bicarbonate Tablets	Oral	Base	Cognitive function	University of Colorado, Denver	1	50	2021	2022	Metabolic Acidosis	Recruiting
NCT04622709	Pilot Study of Loop Diuretics Among Individuals Receiving Hemodialysis	Furosemide	Oral	change in urine volume, serum potassium, serum magnesium + others	Change in 24-hour urine volume	University of North Carolina, Chapel Hill	2	36	2020	2021		Recruiting
NCT04696146	A Phase I/II, Double-Blind, Placebo-Controlled Study: Assessing Safety and Efficacy of Preoperative Renal Allograft Infusions of C1 Inhibitor (Berinert®) (Human) (C1INH) vs. Placebo Administration in Recipients of a Renal Allograft From Deceased High Risk Donors and its Impact on Delayed Graft Function (DGF) and Ischemia/Reperfusion Injury (IRI)	Berinert	Infusion	C1 esterase inhibitor, involved in swelling and inflammation	Need for Dialysis in the first 30 days post-transplant	Cedars-Sinai Medical Center	1/2	40	2021	2022	End Stage Renal Disease	Recruiting
NCT04699032	A Phase 1, Open-Label Evaluation of the Pharmacokinetics and Safety of a Single Dose of Apraglutide in Subjects With Normal and Impaired Renal Function.	Apraglutide	Injection	Peptide GLP-2 analogue	Maximum Plasma Concentration	VectivBio AG	1	16	2020	2021		Recruiting
NCT04702997	A Phase 2 Trial to Evaluate Safety, Tolerability, and Efficacy of Bardoxolone Methyl in Patients With Chronic Kidney Disease at Risk of Rapid Progression	Bardoxolone methyl	Oral		Change in eGFR from baseline	Reata Pharmaceuticals, Inc.	2	70	2021	2021		Recruiting
NCT04707768	A Randomized, Open-Label, Active-controlled Study Evaluating the Efficacy and Safety of Dose Conversion From a Long-acting Erythropoiesis-stimulating Agent (Mircera®) to Three Times Weekly Oral Vadadustat for the Maintenance Treatment of Anemia in Hemodialysis Subjects	Vadadustat, Micera (Micera IV)	Oral		Mean change in hemoglobin	Akebia Therapeutics	3	450	2021	2022	Anemia Associated With Chronic Kidney Disease (CKD)	Recruiting

NCT04724837	A Phase 2b Multicentre, Randomised, Double-Blind, Placebo-Controlled, Parallel Group Dose-Ranging Study to Assess the Efficacy, Safety and Tolerability of Zibotentan and Dapagliflozin in Patients With Chronic Kidney Disease With Estimated Glomerular Filtration Rate (eGFR) Between 20 and 60 mL/Min/1.73 m ²	Zibotentan and Dapagliflozin	Oral		Change in Log-transformed Urinary Albumin to Creatinine Ratio (UACR)	Astrazeneca	2	660	2021	2022		Recruiting
NCT04727840	Combined Dietary Intervention in Hyperkalemic CKD Patients With Potassium Binder (With Hyperkalemia) (Dipo Trial)	Sodium Zirconium Cyclosilicate Oral Product	Oral	cation exchanger that selectively binds potassium in the intestine		Brigham and Women's Hospital	1	20	2021	2022	Hyperkalemia	Not yet recruiting
NCT04736628 v	Randomised, Double-blind (Within Dose Groups), Placebo Controlled and Parallel Group Trial to Investigate the Effects of Different Doses of Oral BI 685509 Given Over 20 Weeks on UACR Reduction in Patients With Non-diabetic Kidney Disease	BI 685509	Oral		Change from baseline in log transformed Urine Albumin Creatinine Ratio (UACR)	Boehringer Ingelheim	2	240	2021	2022		Recruiting
NCT04849650	An Open Label Study of the Pharmacokinetics of Intravenous and Oral Amisulpride in Adults With Severe Renal Impairment and Healthy Control Subjects	Amisulpride	Infusion and oral		Amisulpride plasma exposure (AUC) after a single IV dose	Acadia Pharma Ltd	1	12	2021	2021	ESRD	Recruiting
NCT04865770	Renal Mode of Action of Semaglutide in Patients With Type 2 Diabetes and Chronic Kidney Disease	Semaglutide	Injection		Change in kidney oxygenation, perfusion, and inflammation	Novo Nordisk	3	105	2021	2023		Recruiting
NCT04869761	Allogeneic Mesenchymal Stem Cell Therapy in Patients With Chronic Kidney Disease: A Phase I Study	Allogeneic adipose-derived mesenchymal stem cells (MSC) infusion	Infusion	Stem cells	Safety trial. Adverse events and/or serious adverse events	Mayo Clinic	1	40	2021	2027	Diabetes Mellitus 1 and 2, Diabetic Nephropathies	Not yet recruiting
NCT04985383	An Open Label Phase 1 Study to Compare the Safety and Tolerability of the AKST1210 Column at Different Blood-Flow Rates in Patients With End-Stage Renal Disease Undergoing Hemodialysis	AKST 1210	Device, Hemodialysis		Safety and tolerability of each column size at each blood-flow rate	Alkermest, Inc.	N/A	15	2021	2021		Recruiting

Table 2. Human organoid EC GEO accession

Experiment	Sample	Species	Stage	Tissue	Cell line	Platform
GSE124472	GSM3534660	Homo sapiens	d16d	organoid	ESC	10x
GSE124472	GSM3534661	Homo sapiens	d16d	organoid	ESC	10x
GSE124472	GSM3534662	Homo sapiens	d28d	organoid	ESC	10x
GSE124472	GSM3534663	Homo sapiens	d28d	organoid	ESC	10x
GSE132023	GSM3834523	Homo sapiens	d10d	organoid	ESC	10x
GSE132023	GSM3834524	Homo sapiens	d10d	organoid	ESC	10x
GSE132023	GSM3834525	Homo sapiens	d12d	organoid	ESC	10x
GSE132023	GSM3834526	Homo sapiens	d14d	organoid	ESC	10x
GSE132023	GSM3834527	Homo sapiens	d14d	organoid	ESC	10x
GSE114802	GSM3150499	Homo sapiens	d25d	organoid	iPSC	10x
GSE114802	GSM3150500	Homo sapiens	d25d	organoid	iPSC	10x
GSE114802	GSM3150501	Homo sapiens	d25d	organoid	iPSC	10x
GSE114802	GSM3150502	Homo sapiens	d25d	organoid	iPSC	10x
GSE109718	GSM2949337	Homo sapiens	d21d	organoid	iPSC	Drop-Seq
GSE109718	GSM2949339	Homo sapiens	d21d	organoid	iPSC	Drop-Seq
GSE108291	GSM2914997	Homo sapiens	d25d	organoid	iPSC	10x
GSE108291	GSM2914998	Homo sapiens	d25d	organoid	iPSC	10x
GSE108291	GSM2914999	Homo sapiens	d25d	organoid	iPSC	10x
GSE108291	GSM2915000	Homo sapiens	d25d	organoid	iPSC	10x
GSE118184	GSM3320174	Homo sapiens	d26d	organoid	iPSC	Drop-Seq
GSE118184	GSM3320175	Homo sapiens	d26d	organoid	iPSC	Drop-Seq
GSE118184	GSM3320176	Homo sapiens	d26d	organoid	iPSC	Drop-Seq
GSE118184	GSM3320177	Homo sapiens	d26d	organoid	iPSC	Drop-Seq
GSE118184	GSM3320178	Homo sapiens	d26d	organoid	ESC	Drop-Seq
GSE118184	GSM3320179	Homo sapiens	d26d	organoid	ESC	Drop-Seq
GSE118184	GSM3320180	Homo sapiens	d26d	organoid	ESC	Drop-Seq
GSE118184	GSM3320181	Homo sapiens	d26d	organoid	ESC	Drop-Seq
GSE118184	GSM3320182	Homo sapiens	d26d	organoid	ESC	Drop-Seq
GSE118184	GSM3320183	Homo sapiens	d26d	organoid	ESC	Drop-Seq
GSE118184	GSM3320184	Homo sapiens	d26d	organoid	ESC	Drop-Seq
GSE118184	GSM3320185	Homo sapiens	d26d	organoid	iPSC	Drop-Seq
GSE118184	GSM3320186	Homo sapiens	d26d	organoid	iPSC	Drop-Seq
GSE118184	GSM3320187	Homo sapiens	d26d	organoid	iPSC	Drop-Seq
GSE118184	GSM3320188	Homo sapiens	d26d	organoid	iPSC	Drop-Seq
GSE118184	GSM3320189	Homo sapiens	d26d	organoid	ESC	Drop-Seq
GSE118184	GSM3320190	Homo sapiens	d26d	organoid	ESC	Drop-Seq
GSE118184	GSM3320191	Homo sapiens	d0d	organoid	iPSC	Drop-Seq
GSE118184	GSM3320192	Homo sapiens	d7d	organoid	iPSC	Drop-Seq
GSE118184	GSM3320193	Homo sapiens	d12d	organoid	iPSC	Drop-Seq
GSE118184	GSM3320194	Homo sapiens	d19d	organoid	iPSC	Drop-Seq

GSE118184	GSM3320195	Homo sapiens	d26d	organoid	iPSC	Drop-Seq
GSE118184	GSM3320196	Homo sapiens	d34d	organoid	iPSC	Drop-Seq

Table 3. Human embryonic kidney EC GEO accession

Experiment	Sample	Species	Stage	Tissue	Cell type	Platform
GSE112570	GSM3073088	Homo sapiens	e17w	kidney	cortex	10x
GSE112570	GSM3073089	Homo sapiens	e17w	kidney	cortex	10x
GSE114530	GSM3143601	Homo sapiens	e16w	kidney	kidney	10x
GSE114530	GSM3509837	Homo sapiens	e9w	kidney	kidney	10x
GSE114530	GSM3509838	Homo sapiens	e11w	kidney	kidney	10x
GSE114530	GSM3509839	Homo sapiens	e13w	kidney	kidney	10x
GSE114530	GSM3509840	Homo sapiens	e18w	kidney	kidney	10x
GSE124472	GSM3534656	Homo sapiens	e17w	kidney	outer cortex	10x
GSE124472	GSM3534657	Homo sapiens	e17w	kidney	inner cortex	10x
GSE124472	GSM3534658	Homo sapiens	e15w	kidney	outer cortex	10x
GSE124472	GSM3534659	Homo sapiens	e15w	kidney	inner cortex	10x
GSE102596	GSM2741551	Homo sapiens	e16w	kidney	cortex	10x

Table 4. Antibodies

Antibody	Host	Reactivity	Antibody Product ID	Dilution
SMA-Cy3	Mouse	Mouse & human	Sigma Aldrich, Cat# C6198, RRID:AB_476856	1:200
Aqp1	Rabbit	Mouse & human	Abcam, Cat#ab15080, RRID:AB_2056839	1:500
Aqp3	Rabbit	Mouse	Millipore, Cat# AB3276, RRID:AB_2059552	1:500
CD31/PECAM1	Rat	Mouse	BD Biosciences, Cat# 550274, RRID: AB_393571	1:500
CD31/PECAM1	Rat	Mouse	BD Pharmingen, Cat# 550274, RRID:AB_393571	1:50
CD31/PECAM1	Mouse	Human	Cell signaling Tech., RRID:AB_2160882	1:50
CD31/PECAM1	Mouse	Human	BD Biosciences Cat# 555444, RRID:AB_395837	1:250
CD31/PECAM1	Sheep	Human	R&D Systems, Cat# AF806, RRID:AB_355617	1:250
Cleaved Caspase3	Rabbit	Mouse & human	Cell signaling technologies, Cat# 9661, RRID:AB_2341188	1:250
E-Cadherin	Mouse	Mouse & human	Invitrogen, Cat# 13-1900, RRID:AB_2533005	1:250
E-Cadherin	Mouse	Mouse & human	BD Biosciences Cat# 610182, RRID:AB_397581	1:250
Endomucin	Rat	Mouse	Santa Cruz, Cat# sc-65495, RRID:AB_2100037	1:500
Endomucin	Rat	Human	Abcam, Cat# ab45771, RRID:AB_869629	1:100
GFP/YFP	Chicken		Aves Labs Cat# GFP-1020, RRID:AB_10000240	1:500
HuNu	Mouse	Human	Millipore, Cat# MAB1281B, RRID:AB_94090	1:50
Icam2	Rat	Mouse	BD Pharmingen, Cat# 553326, RRID:AB_394784	1:100
LTL		Mouse & human	Vector Laboratories, Cat# B-1325, RRID:AB_2336558	1:500
Meis1	Rabbit	Mouse & human	Abcam , Cat# ab19867, RRID:AB_776272	1:100
Meis1/2/3	Mouse	Mouse & human	Active Motif, Cat# 39795, RRID:AB_2750570	1:100

NPHS1 (Nephrin)	Goat	Mouse	R&D Systems, Cat# AF3159, RRID:AB_2155023	1:750
pan Cytokeratin (CK)	Mouse	Mouse & human	Sigma-Aldrich, Cat# C2562, RRID:AB_476839	1:500
Pdgfrb	Rabbit	Mouse & human	CST, Cat# 3169, RRID:AB_2162497	1:100
Podocalyxin	Goat	Mouse	R&D Systems, Cat# AF1556, RRID:AB_354858	1:100
Podocalyxin	Mouse	Human	R&D Systems, Cat# MAB1658, RRID:AB_2165984	1:100
Six2	Rabbit	Mouse & human	Proteintech, Cat# 11562-1-AP, RRID:AB_2189084	1:500
Sox17	Goat	Mouse & human	R&D Systems, Cat# AF1924, RRID:AB_355060	1:500
THP/Umod	Rabbit	Mouse	Alfa Aesar, Cat# J65429	1:500
VEGFR2	Rabbit	Mouse & human	Cell signaling, Cat# 55B11, RRID:AB_2212507	1:100

Table 5. qPCR primers

Gene	Forward Primer 5'-3'	Reverse Primer 5'-3'	Source
MEIS1	GCGCAAAGGTACGACGATCT	GGTACTGATGCGAGTGCAGA	(Phipson et al., 2019)
VEGFR2	AGGACTTCCAGGGAGGAAATAA	AAAGTAATTCAGGACCCCTGG	(Homan et al., 2019)
PECAM1	TCATTACGGTCACAATGACGA	GAGTATCTGCTTCCACGGC	(Homan et al., 2019)
Ecad	ACTCGTAACGACGTTGCACCA	GGTCAGTATCAGCCGCTTTCAG	(Taguchi and Nishinakamura, 2017)
Six2	CGCCCATGTGGGTCAGTGGG	AGCCGGGAGCGCTGTAGTCA	(Bantounas et al., 2018)
Podxl	TCATCATCACCATCGTCTGC	CCACCTTCTTCTCTGCATC	(Bantounas et al., 2018)
GAPDH	AGCCACATCGCTCAGACAC	GCCCAATACGACCAAATCC	(Bantounas et al., 2018)
COL3A1	GGAGCTGGCTACTTCTCGC	GGGAACATCCTCCTCAACAG	(Yuan et al., 2017)

BIBLIOGRAPHY

- 7 Things to Know About Kidney Function | National Kidney Foundation. (n.d.). Retrieved August 23, 2021, from <https://www.kidney.org/kidneydisease/howkidneyswrk>
- 10 Signs You May Have Kidney Disease | National Kidney Foundation. (n.d.). Retrieved August 23, 2021, from https://www.kidney.org/news/ekidney/august14/10_Signs_You_May_Have_Kidney_Disease
- Abadi, M., Agarwal, A., Barham, P., Brevdo, E., Chen, Z., Citro, C., Corrado, G. S., Davis, A., Dean, J., Devin, M., Ghemawat, S., Goodfellow, I., Harp, A., Irving, G., Isard, M., Jia, Y., Jozefowicz, R., Kaiser, L., Kudlur, M., ... Research, G. (n.d.). *TensorFlow: Large-Scale Machine Learning on Heterogeneous Distributed Systems*. Retrieved August 31, 2021, from www.tensorflow.org.
- Adam, M., Potter, A. S., & Potter, S. S. (2017). Psychrophilic proteases dramatically reduce single-cell RNA-seq artifacts: A molecular atlas of kidney development. *Development (Cambridge)*, *144*(19), 3625–3632. <https://doi.org/10.1242/dev.151142>
- Aird, W. C. (2007). Phenotypic heterogeneity of the endothelium: I. Structure, function, and mechanisms. *Circulation Research*, *100*(2), 158–173. <https://doi.org/10.1161/01.RES.0000255691.76142.4a>
- Alon, T., Hemo, I., Itin, A., Pe'er, J., Stone, J., & Keshet, E. (1995). Vascular endothelial growth factor acts as a survival factor for newly formed retinal vessels and has implications for retinopathy of prematurity. *Nature Medicine*, *1*(10), 1024–1028. <https://doi.org/10.1038/nm1095-1024>
- Amato, A., Baldassano, S., & Mulè, F. (2016). GLP2: an underestimated signal for improving glycaemic control and insulin sensitivity. *Journal of Endocrinology*, *229*(2), R57–R66. <https://doi.org/10.1530/JOE-16-0035>
- Ando, J., & Yamamoto, K. (2009). Vascular Mechanobiology Endothelial Cell Responses to Fluid Shear Stress. In *Circulation Journal* (Vol. 73).
- Armulik, A., Abramsson, A., & Betsholtz, C. (2005). Endothelial/Pericyte Interactions. *Circulation Research*, *97*(6), 512–523. <https://doi.org/10.1161/01.RES.0000182903.16652.D7>
- Bantounas, I., Ranjzad, P., Tengku, F., Silajdžić, E., Forster, D., Asselin, M. C., Lewis, P., Lennon, R., Plagge, A., Wang, Q., Woolf, A. S., & Kimber, S. J. (2018). Generation of Functioning Nephrons by Implanting Human Pluripotent Stem Cell-Derived Kidney Progenitors. *Stem Cell Reports*, *10*(3), 766–779. <https://doi.org/10.1016/j.stemcr.2018.01.008>
- Barry, D. M., McMillan, E. A., Kunar, B., Lis, R., Zhang, T., Lu, T., Daniel, E., Yokoyama, M., Gomez-Salinerio, J. M., Sureshbabu, A., Cleaver, O., di Lorenzo, A., Choi, M. E., Xiang, J., Redmond, D., Rabbany, S. Y., Muthukumar, T., & Rafii, S. (2019). Molecular determinants of nephron vascular specialization in the kidney. *Nature Communications*, *10*(1). <https://doi.org/10.1038/s41467-019-12872-5>
- Benjamin, L. E., Hemo, I., & Keshet, E. (1998). *A plasticity window for blood vessel remodelling is defined by pericyte coverage of the preformed endothelial network and is regulated by PDGF-Band VEGF*.

- Betônico, C. C. R., Titan, S. M. O., Correa-Giannella, M. L. C., Nery, M., & Queiroz, M. (2016). Management of diabetes mellitus in individuals with chronic kidney disease: therapeutic perspectives and glycemic control. *Clinics*, *71*(1), 47. [https://doi.org/10.6061/CLINICS/2016\(01\)08](https://doi.org/10.6061/CLINICS/2016(01)08)
- Brown, A. C., Gupta, A. K., & Oxburgh, L. (2019). Long-Term Culture of Nephron Progenitor Cells Ex Vivo. *Methods in Molecular Biology*, *1926*, 63–75. https://doi.org/10.1007/978-1-4939-9021-4_6
- Brown, A. C., Muthukrishnan, S. D., & Oxburgh, L. (2015). A Synthetic Niche for Nephron Progenitor Cells. *Developmental Cell*, *34*(2), 229–241. <https://doi.org/10.1016/j.devcel.2015.06.021>
- Bruno, S., Remuzzi, G., & Ruggenenti, P. (2004). Transplant Renal Artery Stenosis. *Journal of the American Society of Nephrology*, *15*(1), 134–141. <https://doi.org/10.1097/01.ASN.0000099379.61001.F8>
- Bui, T. D., Ravi, S., & Ramavajjala, V. (2018). Neural Graph Learning: Training Neural Networks Using Graphs. *Proceedings of the Eleventh ACM International Conference on Web Search and Data Mining*. <https://doi.org/10.1145/3159652>
- Cakir, B., Xiang, Y., Tanaka, Y., Kural, M. H., Parent, M., Kang, Y.-J., Chapeton, K., Patterson, B., Yuan, Y., He, C.-S., Raredon, M. S. B., Dengelegi, J., Kim, K.-Y., Sun, P., Zhong, M., Lee, S., Patra, P., Hyder, F., Niklason, L. E., ... Park, I.-H. (2019). Engineering of human brain organoids with a functional vascular-like system. *Nature Methods*, 1–7. <https://doi.org/10.1038/s41592-019-0586-5>
- Chatterjee, S., & Naik, U. P. (2012). Pericyte-endothelial cell interaction: A survival mechanism for the tumor vasculature. *Cell Adhesion & Migration*, *6*(3), 157. <https://doi.org/10.4161/CAM.20252>
- Chronic Kidney Disease (CKD) | NIDDK*. (n.d.). Retrieved August 23, 2021, from <https://www.niddk.nih.gov/health-information/kidney-disease/chronic-kidney-disease-ckd>
- Cleaver, O., & Melton, D. A. (2003). Endothelial signaling during development. *Nature Medicine*, *9*(6), 661–668. <https://doi.org/10.1038/nm0603-661>
- Combes, A. N., Wilson, S., Phipson, B., Binnie, B. B., Ju, A., Lawlor, K. T., Cebrian, C., Walton, S. L., Smyth, I. M., Moritz, K. M., Kopan, R., Oshlack, A., & Little, M. H. (2018). Haploinsufficiency for the Six2 gene increases nephron progenitor proliferation promoting branching and nephron number. *Kidney International*, *93*(3), 589–598. <https://doi.org/10.1016/J.KINT.2017.09.015>
- Czerniecki, S. M., Cruz, N. M., Harder, J. L., Menon, R., Annis, J., Otto, E. A., Gulieva, R. E., Islas, L. v., Kim, Y. K., Tran, L. M., Martins, T. J., Pippin, J. W., Fu, H., Kretzler, M., Shankland, S. J., Himmelfarb, J., Moon, R. T., Paragas, N., & Freedman, B. S. (2018). High-Throughput Screening Enhances Kidney Organoid Differentiation from Human Pluripotent Stem Cells and Enables Automated Multidimensional Phenotyping. *Cell Stem Cell*, *22*(6), 929-940.e4. <https://doi.org/10.1016/J.STEM.2018.04.022>
- Daniel, E., Azizoglu, D. B., Ryan, A. R., Walji, T. A., Chaney, C. P., Sutton, G. I., Carroll, T. J., Marciano, D. K., & Cleaver, O. (2018). Spatiotemporal heterogeneity and patterning of developing renal blood vessels. *Angiogenesis*. <https://doi.org/10.1007/s10456-018-9612-y>

- Diabetic Kidney Disease* | NIDDK. (n.d.). Retrieved August 23, 2021, from <https://www.niddk.nih.gov/health-information/diabetes/overview/preventing-problems/diabetic-kidney-disease>
- Dickson, M. C., Martin, J. S., Cousins, F. M., Kulkarni, A. B., Karlsson, S., & Akhurst, R. J. (1995). Defective haematopoiesis and vasculogenesis in transforming growth factor-beta 1 knock out mice. *Development*, *121*(6), 1845–1854. <https://doi.org/10.1242/DEV.121.6.1845>
- DiMasi, J. A., Hansen, R. W., & Grabowski, H. G. (2003). The price of innovation: new estimates of drug development costs. *Journal of Health Economics*, *22*(2), 151–185. [https://doi.org/10.1016/S0167-6296\(02\)00126-1](https://doi.org/10.1016/S0167-6296(02)00126-1)
- Ding, B. sen, Nolan, D. J., Guo, P., Babazadeh, A. O., Cao, Z., Rosenwaks, Z., Crystal, R. G., Simons, M., Sato, T. N., Worgall, S., Shido, K., Rabbany, S. Y., & Rafii, S. (2011). Endothelial-derived angiocrine signals induce and sustain regenerative lung alveolarization. *Cell*, *147*(3), 539–553. <https://doi.org/10.1016/j.cell.2011.10.003>
- Drake, C. J., & Fleming, P. A. (2000). Vasculogenesis in the day 6.5 to 9.5 mouse embryo. *Blood*, *95*(5), 1671–1679. https://doi.org/10.1182/BLOOD.V95.5.1671.005K39_1671_1679
- Dumas, S. J., Meta, E., Borri, M., Goveia, J., Rohlenova, K., Conchinha, N. v, Falkenberg, K., Teuwen, L.-A., de Rooij, L., Kalucka, J., Chen, R., Khan, S., Taverna, F., Lu, W., Parys, M., de Legher, C., Vinckier, S., Karakach, T. K., Schoonjans, L., ... Carmeliet, P. (2020). *Single-Cell RNA Sequencing Reveals Renal Endothelium Heterogeneity and Metabolic Adaptation to Water Deprivation*. <https://doi.org/10.1681/ASN.2019080832>
- England, A. R., Chaney, C. P., Das, A., Patel, M., Malewska, A., Armendariz, D., Hon, G. C., Strand, D. W., Drake, K. A., & Carroll, T. J. (2020). Identification and characterization of cellular heterogeneity within the developing renal interstitium. *Development*, *147*(15). <https://doi.org/10.1242/DEV.190108>
- Filippatos, G., Anker, S. D., Agarwal, R., Pitt, B., Ruilope, L. M., Rossing, P., Kolkhof, P., Schloemer, P., Tornus, I., Joseph, A., Bakris, G. L., & Investigators, F. the F.-D. (2021). Finerenone and Cardiovascular Outcomes in Patients With Chronic Kidney Disease and Type 2 Diabetes. *Circulation*, *143*, 540–552. <https://doi.org/10.1161/CIRCULATIONAHA.120.051898>
- Finak, G., McDavid, A., Yajima, M., Deng, J., Gersuk, V., Shalek, A. K., Slichter, C. K., Miller, H. W., McElrath, M. J., Prlic, M., Linsley, P. S., & Gottardo, R. (2015). MAST: a flexible statistical framework for assessing transcriptional changes and characterizing heterogeneity in single-cell RNA sequencing data. *Genome Biology*, *16*(1). <https://doi.org/10.1186/S13059-015-0844-5>
- Finkbeiner, S. R., Freeman, J. J., Wieck, M. M., El-Nachef, W., Altheim, C. H., Tsai, Y.-H., Huang, S., Dyal, R., White, E. S., Grikscheit, T. C., Teitelbaum, D. H., & Spence, J. R. (2015). Generation of tissue-engineered small intestine using embryonic stem cell-derived human intestinal organoids. *Biology Open*, bio.013235-. <https://doi.org/10.1242/bio.013235>
- Francipane, M. G., Han, B., Oxburgh, L., Sims-Lucas, S., Li, Z., & Lagasse, E. (2019). Kidney-in-lymph node: a novel organogenesis assay to model human renal development and test nephron progenitor cell fates. *Journal of Tissue Engineering and Regenerative Medicine*, term.2924. <https://doi.org/10.1002/term.2924>
- Fraser, S. T., Hadjantonakis, A.-K., Sahr, K. E., Willey, S., Kelly, O. G., Jones, E. A. V., Dickinson, M. E., & Baron, M. H. (2005). Using a Histone Yellow Fluorescent Protein Fusion for Tagging

- and Tracking Endothelial Cells in ES Cells and Mice. *Genesis (New York, N.Y. : 2000)*, 42(3), 162. <https://doi.org/10.1002/GENE.20139>
- Freedman, B. S., Brooks, C. R., Lam, A. Q., Fu, H., Morizane, R., Agrawal, V., Saad, A. F., Li, M. K., Hughes, M. R., Werff, R. vander, Peters, D. T., Lu, J., Baccei, A., Siedlecki, A. M., Valerius, M. T., Musunuru, K., McNagny, K. M., Steinman, T. I., Zhou, J., ... Bonventre, J. v. (2015). Modelling kidney disease with CRISPR-mutant kidney organoids derived from human pluripotent epiblast spheroids. *Nature Communications*, 6(1), 1–13. <https://doi.org/10.1038/ncomms9715>
- Garlanda, C., & Dejana, E. (1997). Heterogeneity of endothelial cells. Specific markers. *Arteriosclerosis, Thrombosis, and Vascular Biology*, 17(7), 1193–1202. <https://doi.org/10.1161/01.ATV.17.7.1193>
- Gerecht-Nir, S., Ziskind, A., Cohen, S., & Itskovitz-Eldor, J. (2003). Human Embryonic Stem Cells as an in Vitro Model for Human Vascular Development and the Induction of Vascular Differentiation. *Laboratory Investigation*, 83(12), 1811–1820. <https://doi.org/10.1097/01.LAB.0000106502.41391.F0>
- Glossary of Common Site Terms - ClinicalTrials.gov*. (n.d.). Retrieved August 23, 2021, from <https://www.clinicaltrials.gov/ct2/about-studies/glossary>
- Grune, J., Beyhoff, N., Smeir, E., Chudek, R., Blumrich, A., Ban, Z., Brix, S., Betz, I. R., Schupp, M., Foryst-Ludwig, A., Klopffleisch, R., Stawowy, P., Houtman, R., Kolkhof, P., & Kintscher, U. (2018). Selective Mineralocorticoid Receptor Cofactor Modulation as Molecular Basis for Finerenone's Antifibrotic Activity. *Hypertension*, 71(4), 599–608. <https://doi.org/10.1161/HYPERTENSIONAHA.117.10360>
- Guo, J.-K., Shi, H., Koraihy, F., Marlier, A., Ding, Z., Shan, A., & Cantley, L. G. (2013). The Terminator mouse is a diphtheria toxin–receptor knock-in mouse strain for rapid and efficient enrichment of desired cell lineages. *Kidney International*, 84(5), 1041–1046. <https://doi.org/10.1038/KI.2013.202>
- Gupta, A. K., Coburn, J. M., Davis-Knowlton, J., Kimmerling, E., Kaplan, D. L., & Oxburgh, L. (2019). Scaffolding kidney organoids on silk. *Journal of Tissue Engineering and Regenerative Medicine*, 13(5), 812–822. <https://doi.org/10.1002/TERM.2830>
- Guyton, A. C., & Hall, J. E. (2006). *Textbook of Medical Physiology* (W. Schmitt & R. Gruliow, Eds.; 11th ed.). Elsevier.
- Habib, N., Avraham-Davidi, I., Basu, A., Burks, T., Shekhar, K., Hofree, M., Choudhury, S. R., Aguet, F., Gelfand, E., Ardlie, K., Weitz, D. A., Rozenblatt-Rosen, O., Zhang, F., & Regev, A. (2017). Massively-parallel single nucleus RNA-seq with DroNc-seq. *Nature Methods*, 14(10), 955. <https://doi.org/10.1038/NMETH.4407>
- Hagedorn, M., Balke, M., Schmidt, A., Bloch, W., Kurz, H., Javerzat, S., Rousseau, B., Wilting, J., & Bikfalvi, A. (2004). VEGF Coordinates Interaction of Pericytes and Endothelial Cells During Vasculogenesis and Experimental Angiogenesis. *Developmental Dynamics*, 230(1). <https://doi.org/10.1002/dvdy.20020>
- Haghverdi, L., Büttner, M., Wolf, F. A., Buettner, F., & Theis, F. J. (2016). Diffusion pseudotime robustly reconstructs lineage branching. *Nature Methods* 2016 13:10, 13(10), 845–848. <https://doi.org/10.1038/nmeth.3971>

- Haghverdi, L., Lun, A. T. L., Morgan, M. D., & Marioni, J. C. (2018). Batch effects in single-cell RNA-sequencing data are corrected by matching mutual nearest neighbors. *Nature Biotechnology* 2018 36:5, 36(5), 421–427. <https://doi.org/10.1038/nbt.4091>
- Harding, S. D., Armit, C., Armstrong, J., Brennan, J., Cheng, Y., Haggarty, B., Houghton, D., Lloyd-MacGilp, S., Pi, X., Roochun, Y., Sharghi, M., Tindal, C., McMahon, A. P., Gottesman, B., Little, M. H., Georgas, K., Aronow, B. J., Potter, S. S., Brunskill, E. W., ... Davidson, D. (2011). The GUDMAP database - an online resource for genitourinary research. *Development*, 138(13), 2845–2853. <https://doi.org/10.1242/dev.063594>
- He, L., Vanlandewijck, M., Mäe, M. A., Andrae, J., Ando, K., del Gaudio, F., Nahar, K., Lebouvier, T., Laviña, B., Gouveia, L., Sun, Y., Raschperger, E., Segerstolpe, Å., Liu, J., Gustafsson, S., Räsänen, M., Zarb, Y., Mochizuki, N., Keller, A., ... Betsholtz, C. (2018). Single-cell RNA sequencing of mouse brain and lung vascular and vessel-associated cell types. *Scientific Data* 2018 5:1, 5(1), 1–11. <https://doi.org/10.1038/sdata.2018.160>
- Hemodialysis - Definition, procedure, and types | National Kidney Foundation.* (n.d.). Retrieved August 23, 2021, from <https://www.kidney.org/atoz/content/hemodialysis>
- Hickson, L. J., Abedalqader, T., Ben-Bernard, G., Mondy, J. M., Bian, X., Conley, S. M., Zhu, X., Herrmann, S. M., Kukla, A., Lorenz, E. C., Kim, S. R., Thorsteinsdottir, B., Lerman, L. O., & Murad, M. H. (2021). A systematic review and meta-analysis of cell-based interventions in experimental diabetic kidney disease. *STEM CELLS Translational Medicine*. <https://doi.org/10.1002/SCTM.19-0419>
- Hoeffel, G., Chen, J., Lavin, Y., Low, D., Almeida, F. F., See, P., Beaudin, A. E., Lum, J., Low, I., Forsberg, E. C., Poidinger, M., Zolezzi, F., Larbi, A., Ng, L. G., Chan, J. K. Y., Greter, M., Becher, B., Samokhvalov, I. M., Merad, M., & Ginhoux, F. (2015). C-Myb+ Erythro-Myeloid Progenitor-Derived Fetal Monocytes Give Rise to Adult Tissue-Resident Macrophages. *Immunity*, 42(4), 665–678. <https://doi.org/10.1016/J.IMMUNI.2015.03.011>
- Holloway, E., Wu, J., Czerwinski, M., Sweet, C., Wu, A., Tsai, Y.-H., Huang, S., Stoddard, A., Capeling, M., Glass, I., & Spence, J. (2020). Differentiation of human intestinal organoids with endogenous vascular endothelial cells. *Developmental Cell*, 54(4), 516-528.e7. <https://doi.org/10.1101/2020.03.15.991950>
- Homan, K. A., Gupta, N., Kroll, K. T., Kolesky, D. B., Skylar-Scott, M., Miyoshi, T., Mau, D., Valerius, M. T., Ferrante, T., Bonventre, J. v., Lewis, J. A., & Morizane, R. (2019). Flow-enhanced vascularization and maturation of kidney organoids in vitro. *Nature Methods*, 1. <https://doi.org/10.1038/s41592-019-0325-y>
- Home - ClinicalTrials.gov.* (n.d.). Retrieved August 23, 2021, from <https://www.clinicaltrials.gov/ct2/home>
- Humphreys, B. D., Lin, S.-L., Kobayashi, A., Hudson, T. E., Nowlin, B. T., Bonventre, J. v., Valerius, M. T., McMahon, A. P., & Duffield, J. S. (2010). Fate Tracing Reveals the Pericyte and Not Epithelial Origin of Myofibroblasts in Kidney Fibrosis. *The American Journal of Pathology*, 176(1), 85. <https://doi.org/10.2353/AJPATH.2010.090517>
- Ihermann-Hella, A., & Kuure, S. (n.d.). *Chapter 2 Mouse Ex Vivo Kidney Culture Methods*. https://doi.org/10.1007/978-1-4939-9021-4_2

- ISH Data :: Allen Brain Atlas: Developing Mouse Brain.* (n.d.). Retrieved August 25, 2021, from <http://developingmouse.brain-map.org/>
- Jakab, M., & Augustin, H. G. (2020). *Understanding angiodiversity: insights from single cell biology.* <https://doi.org/10.1242/dev.146621>
- Jiayi Yao,¹ Pierre J. Guihard,¹ Xiuju Wu,¹ Ana M. Blazquez-Medela,¹ Melissa J. Spencer,² Medet Jumabay,¹ & Peter Tontonoz,^{3,5,6} Alan M. Fogelman,⁴ Kristina I. Boström,^{1,6} and Yucheng Yao^{1, 7}. (2017). Vascular endothelium plays a key role in directing pulmonary epithelial cell differentiation. *The Rockefeller University Press J. Cell Biol.* <https://doi.org/10.1083/jcb.201612122>
- Kidney Disease | NIDDK.* (n.d.). Retrieved August 23, 2021, from <https://www.niddk.nih.gov/health-information/kidney-disease>
- Kim, G. D., Kim, G. J., Seok, J. H., Chung, H. M., Chee, K. M., & Rhee, G. S. (2008). Differentiation of endothelial cells derived from mouse embryoid bodies: A possible in vitro vasculogenesis model. *Toxicology Letters*, *180*(3), 166–173. <https://doi.org/10.1016/J.TOXLET.2008.05.023>
- Kloth, S., Aigner, J., Brandt, E., Moll, R., & Minuth, W. W. (1993). Histochemical markers reveal an unexpected heterogeneous composition of the renal embryonic collecting duct epithelium. *Kidney International*, *44*, 527–536. <https://doi.org/10.1038/ki.1993.277>
- Know Your Kidney Numbers: Two Simple Tests | National Kidney Foundation.* (n.d.). Retrieved August 23, 2021, from <https://www.kidney.org/atoz/content/know-your-kidney-numbers-two-simple-tests>
- Kobayashi, A., Valerius, M. T., Mugford, J. W., Carroll, T. J., Self, M., Oliver, G., & McMahon, A. P. (2008). Six2 Defines and Regulates a Multipotent Self-Renewing Nephron Progenitor Population throughout Mammalian Kidney Development. *Cell Stem Cell*, *3*(2), 169–181. <https://doi.org/10.1016/J.STEM.2008.05.020>
- Korn, C., & Augustin, H. G. (2015). *Mechanisms of Vessel Pruning and Regression.* <https://doi.org/10.1016/j.devcel.2015.06.004>
- Kumar Gupta, A., Sarkar, P., Wertheim, J. A., Pan, X., Carroll, T. J., & Oxburgh, L. (2020). Asynchronous mixing of kidney progenitor cells potentiates nephrogenesis in organoids. *Communications Biology*, *3*(1), 231. <https://doi.org/10.1038/s42003-020-0948-7>
- L. Lun, A. T., Bach, K., & Marioni, J. C. (2016). Pooling across cells to normalize single-cell RNA sequencing data with many zero counts. *Genome Biology* *2016 17:1*, *17*(1), 1–14. <https://doi.org/10.1186/S13059-016-0947-7>
- Lancaster, M. A., Renner, M., Martin, C., Wenzel, D., Bicknell, L. S., Hurles, M. E., Homfray, T., Penninger, J. M., Jackson, A. P., & Knoblich, J. A. (2013). Cerebral organoids model human brain development and microcephaly. *Nature*, *501*(7467), 373–379. <https://doi.org/10.1038/nature12517>
- Langille, B. L., & O'Donnell, F. (1986). Reductions in arterial diameter produced by chronic decreases in blood flow are endothelium-dependent. *Science*, *231*(4736), 405–407. <https://doi.org/10.1126/science.3941904>
- Lin, T.-Y., Goyal, P., Girshick, R., He, K., & Dollár, P. (n.d.). *Focal Loss for Dense Object Detection.*

- Little, M. H., McMahon, A. P., Bhatt, S., Diaz, R., Trainor, P. a, Ochoa-espinoza, A., Affolter, M., Fedoriw, A., Mugford, J., & Tam, P. L. (2013). *Mammalian Kidney Development : Principles , Progress , and Projections Mammalian Kidney Development : Principles , Progress , and Projections*. 1–18. <https://doi.org/10.1101/cshperspect.a008300>
- Loughna, S., Yuan, H. T., & Woolf, A. S. (1998). Effects of oxygen on vascular patterning in Tie1/LacZ metanephric kidneys in vitro. *Biochemical and Biophysical Research Communications*, 247(2), 361–366. <https://doi.org/10.1006/bbrc.1998.8768>
- Low, J. H., Li, P., Chew, E. G. Y., Zhou, B., Suzuki, K., Zhang, T., Lian, M. M., Liu, M., Aizawa, E., Rodriguez Esteban, C., Yong, K. S. M., Chen, Q., Campistol, J. M., Fang, M., Khor, C. C., Foo, J. N., Izpisua Belmonte, J. C., & Xia, Y. (2019). Generation of Human PSC-Derived Kidney Organoids with Patterned Nephron Segments and a De Novo Vascular Network. *Cell Stem Cell*, 25(3), 373–387.e9. <https://doi.org/10.1016/j.stem.2019.06.009>
- Lucitti, J. L., Jones, E. A. v., Huang, C., Chen, J., Fraser, S. E., & Dickinson, M. E. (2007). Vascular remodeling of the mouse yolk sac requires hemodynamic force. *Development (Cambridge, England)*, 134(18), 3317. <https://doi.org/10.1242/DEV.02883>
- Lun, A. T. L., McCarthy, D. J., & Marioni, J. C. (2016). A step-by-step workflow for low-level analysis of single-cell RNA-seq data with Bioconductor. *F1000Research 2016 5:2122*, 5, 2122. <https://doi.org/10.12688/f1000research.9501.2>
- Lun, A. T. L., Riesenfeld, S., Andrews, T., Dao, T. P., Gomes, T., & Marioni, J. C. (2019). EmptyDrops: distinguishing cells from empty droplets in droplet-based single-cell RNA sequencing data. *Genome Biology 2019 20:1*, 20(1), 1–9. <https://doi.org/10.1186/S13059-019-1662-Y>
- Magenheim, J., Ilovich, O., Lazarus, A., Klochendler, A., Ziv, O., Werman, R., Hija, A., Cleaver, O., Mishani, E., Keshet, E., & Dor, Y. (2011). Blood vessels restrain pancreas branching, differentiation and growth. *Development*, 138(21), 4743–4752. <https://doi.org/10.1242/dev.066548>
- Marcu, R., Jung Choi, Y., Xue, J., Fortin, C. L., Wang, Y., Nagao, R., Xu, J., MacDonald, J., Bammler, T., Murry, C. E., Muczynski, K., Stevens, K. R., Himmelfarb, J., Schwartz, S. M., & Zheng, Y. (2018). Human Organ-specific Endothelial Cell Heterogeneity. *Science*. <https://doi.org/10.1016/>
- Matsui, T., Kanai-Azuma, M., Hara, K., Matoba, S., Hiramatsu, R., Kawakami, H., Kurohmaru, M., Koopman, P., & Kanai, Y. (2006). Redundant roles of Sox17 and Sox18 in postnatal angiogenesis in mice. *Journal of Cell Science*, 119(17), 3513–3526. <https://doi.org/10.1242/jcs.03081>
- Matsushita, K., Velde, M. van der, Astor, B. C., Woodward, M., Levey, A. S., Jong, P. E. de, Coresh, J., & Gansevoort, R. T. (2010). Association of estimated glomerular filtration rate and albuminuria with all-cause and cardiovascular mortality: a collaborative meta-analysis of general population cohorts. *Lancet*, 375(9731), 2073. [https://doi.org/10.1016/S0140-6736\(10\)60674-5](https://doi.org/10.1016/S0140-6736(10)60674-5)
- McGill, R. L., & Weiner, D. E. (2017). Dialysate Composition for Hemodialysis: Changes and Changing Risk. *Seminars in Dialysis*, 30(2), 112. <https://doi.org/10.1111/SDI.12573>
- McMahon, A. P. (2016). Development of the Mammalian Kidney. In *Current Topics in Developmental Biology* (1st ed., Vol. 117). Elsevier Inc. <https://doi.org/10.1016/bs.ctdb.2015.10.010>
- McMahon, A. P., Aronow, B. J., Davidson, D. R., Davies, J. A., Gaido, K. W., Grimmond, S., Lessard, J. L., Little, M. H., Potter, S. S., Wilder, E. L., & Zhang, P. (2008). GUDMAP: The Genitourinary

- Developmental Molecular Anatomy Project. *Journal of the American Society of Nephrology*, 19(4), 667–671. <https://doi.org/10.1681/ASN.2007101078>
- Meeson, A., Palmer, M., Calton, M., & Lang, R. (1996a). *A relationship between apoptosis and flow during programmed capillary regression is revealed by vital analysis*. 3938, 3929–3938.
- Meeson, A., Palmer, M., Calton, M., & Lang, R. (1996b). *A relationship between apoptosis and flow during programmed capillary regression is revealed by vital analysis*. 3938, 3929–3938. <https://dev.biologists.org/content/122/12/3929.long>
- Molema, G., & Aird, W. C. (2012). Vascular Heterogeneity in the Kidney. *Semin Nephrol*, 32, 145–155. <https://doi.org/10.1016/j.semnephrol.2012.02.001>
- Morita, R., Suzuki, M., Kasahara, H., Shimizu, N., Shichita, T., Sekiya, T., Kimura, A., Sasaki, K., Yasukawa, H., & Yoshimura, A. (2015). ETS transcription factor ETV2 directly converts human fibroblasts into functional endothelial cells. *Proceedings of the National Academy of Sciences*, 112(1), 160–165. <https://doi.org/10.1073/PNAS.1413234112>
- Morizane, R., & Bonventre, J. v. (2017). Generation of nephron progenitor cells and kidney organoids from human pluripotent stem cells. *Nature Protocols*, 12(1), 195–207. <https://doi.org/10.1038/nprot.2016.170>
- Morizane, R., Lam, A. Q., Freedman, B. S., Kishi, S., Valerius, M. T., & Bonventre, J. v. (2015). Nephron organoids derived from human pluripotent stem cells model kidney development and injury. *Nature Biotechnology*, 33(11), 1193–1200. <https://doi.org/10.1038/nbt.3392>
- Moya, M. L., Hsu, Y.-H., Lee, A. P., Hughes, C. C. W., & George, S. C. (2013). In Vitro Perfused Human Capillary Networks. *Tissue Engineering Part C: Methods*, 19(9), 730–737. <https://doi.org/10.1089/ten.tec.2012.0430>
- Müller, S. M., Stolt, C. C., Terszowski, G., Blum, C., Amagai, T., Kessaris, N., Iannarelli, P., Richardson, W. D., Wegner, M., & Rodewald, H.-R. (2008). Neural Crest Origin of Perivascular Mesenchyme in the Adult Thymus. *The Journal of Immunology*, 180(8), 5344–5351. <https://doi.org/10.4049/JIMMUNOL.180.8.5344>
- Munro, D. A. D., Hohenstein, P., & Davies, J. A. (2017). Cycles of vascular plexus formation within the nephrogenic zone of the developing mouse kidney. *Scientific Reports*, 7(1), 3273. <https://doi.org/10.1038/s41598-017-03808-4>
- N., F., K., C.-M., H., C., M., D., L., L., K.S., O., L., P.-B., K.J., H., & M.W., M. (1996). Heterozygous embryonic lethality induced by targeted inactivation of the VEGF gene. *Nature*, 380(6573), 439–442. <http://www.embase.com/search/results?subaction=viewrecord&from=export&id=L26102720%5Cnhttp://dx.doi.org/10.1038/380439a0%5Cnhttp://elvis.ubvu.vu.nl:9003/vulink?sid=EMBASE&issn=00280836&id=doi:10.1038/380439a0&atitle=Heterozygous+embryonic+lethality+induce>
- Nankivell, B. J., & Alexander, S. I. (2010). Rejection of the Kidney Allograft. *New England Journal of Medicine*, 363(15), 1451–1462. <https://doi.org/10.1056/NEJMra0902927>
- National Kidney Foundation. (n.d.). www.kidney.org
- Noble, F., Moyon, D., Pardanaud, L., Yuan, L., Djonov, V., Matthijsen, R., Bréant, C., Fleury, V., & Eichmann, A. (2004). *Flow regulates arterial-venous differentiation in the chick embryo yolk sac*. <https://doi.org/10.1242/dev.00929>

- Nolan, D. J., Ginsberg, M., Israely, E., Palikuqi, B., Poulos, M. G., James, D., Ding, B. sen, Schachterle, W., Liu, Y., Rosenwaks, Z., Butler, J. M., Xiang, J., Rafii, A., Shido, K., Rabbany, S. Y., Elemento, O., & Rafii, S. (2013). Molecular Signatures of Tissue-Specific Microvascular Endothelial Cell Heterogeneity in Organ Maintenance and Regeneration. *Developmental Cell*, 26(2), 204–219. <https://doi.org/10.1016/j.devcel.2013.06.017>
- Obara-Ishihara, T., Kuhlman, J., Niswander, L., & Herzlinger, D. (1999). The surface ectoderm is essential for nephric duct formation in intermediate mesoderm. *Development*, 126(6), 1103–1108. <https://doi.org/10.1242/DEV.126.6.1103>
- Official Journal Of the internatiOnal SOciety Of nephroLOgy KDIGO 2012 Clinical Practice Guideline for the Evaluation and Management of Chronic Kidney Disease*. (n.d.). Retrieved August 23, 2021, from www.publicationethics.org
- O’Flanagan, C. H., Campbell, K. R., Zhang, A. W., Kabeer, F., Lim, J. L. P., Biele, J., Eirew, P., Lai, D., McPherson, A., Kong, E., Bates, C., Borkowski, K., Wiens, M., Hewitson, B., Hopkins, J., Pham, J., Ceglia, N., Moore, R., Mungall, A. J., ... Aparicio, S. (2019). Dissociation of solid tumor tissues with cold active protease for single-cell RNA-seq minimizes conserved collagenase-associated stress responses. *Genome Biology*, 20(1). <https://doi.org/10.1186/s13059-019-1830-0>
- Ottone, C., Krusche, B., Whitby, A., Clements, M., Quadrato, G., Pitulescu, M. E., Adams, R. H., & Parrinello, S. (2014). Direct cell-cell contact with the vascular niche maintains quiescent neural stem cells. *Nature Cell Biology*, 16(11), 1045–1056. <https://doi.org/10.1038/ncb3045>
- Oxburgh, L., Chu, G. C., Michael, S. K., & Robertson, E. J. (2004). TGF β superfamily signals are required for morphogenesis of the kidney mesenchyme progenitor population. *Development*, 131(18), 4593–4605. <https://doi.org/10.1242/DEV.01324>
- Palikuqi, B., Nguyen, D. H. T., Li, G., Schreiner, R., Pellegata, A. F., Liu, Y., Redmond, D., Geng, F., Lin, Y., Gómez-Salineró, J. M., Yokoyama, M., Zumbo, P., Zhang, T., Kunar, B., Witherspoon, M., Han, T., Tedeschi, A. M., Scottoni, F., Lipkin, S. M., ... Rafii, S. (2020). Adaptable haemodynamic endothelial cells for organogenesis and tumorigenesis. *Nature*, 585(7825), 426–432. <https://doi.org/10.1038/s41586-020-2712-z>
- Paredes, I., Vieira, J. R., Shah, B., Ramunno, C. F., Dycow, J., Adler, H., Richter, M., Schermann, G., Giannakouri, E., Schirmer, L., Augustin, H. G., & Ruiz de Almodóvar, C. (2021). Oligodendrocyte precursor cell specification is regulated by bidirectional neural progenitor–endothelial cell crosstalk. *Nature Neuroscience* 2021 24:4, 24(4), 478–488. <https://doi.org/10.1038/s41593-020-00788-z>
- Pham, M. T., Pollock, K. M., Rose, M. D., Cary, W. A., Stewart, H. R., Zhou, P., Nolte, J. A., & Waldau, B. (2018). Generation of human vascularized brain organoids. *NeuroReport*, 29(7), 588–593. <https://doi.org/10.1097/WNR.0000000000001014>
- Phipson, B., Er, P. X., Combes, A. N., Forbes, T. A., Howden, S. E., Zappia, L., Yen, H. J., Lawlor, K. T., Hale, L. J., Sun, J., Wolvetang, E., Takasato, M., Oshlack, A., & Little, M. H. (2019). Evaluation of variability in human kidney organoids. *Nature Methods*, 16(1), 79–87. <https://doi.org/10.1038/s41592-018-0253-2>
- Pons, P., & Latapy, M. (2006). *Journal of Graph Algorithms and Applications Computing Communities in Large Networks Using Random Walks*. 10(2), 191–218. <http://jgaa.info/volhttp://www.liafa.jussieu.fr/>

- Rafii, S., Butler, J. M., & Ding, B. sen. (2016). Angiocrine functions of organ-specific endothelial cells. In *Nature* (Vol. 529, Issue 7586, pp. 316–325). <https://doi.org/10.1038/nature17040>
- Rak-Raszewska, A., Hauser, P. v., & Vainio, S. (2015). Organ in vitro culture: What have we learned about early kidney development? *Stem Cells International*, 2015. <https://doi.org/10.1155/2015/959807>
- Rennert, K., Steinborn, S., Gröger, M., Ungerböck, B., Jank, A. M., Ehgartner, J., Nietzsche, S., Dinger, J., Kiehntopf, M., Funke, H., Peters, F. T., Lupp, A., Gärtner, C., Mayr, T., Bauer, M., Huber, O., & Mosig, A. S. (2015). A microfluidically perfused three dimensional human liver model. *Biomaterials*, 71, 119–131. <https://doi.org/10.1016/J.BIOMATERIALS.2015.08.043>
- Risau, W. (n.d.). *Mechanisms of angiogenesis*.
- Rocha, A. S., Vidal, V., Mertz, M., Kendall, T. J., Charlet, A., Okamoto, H., & Schedl, A. (2015). The Angiocrine Factor Rspodin3 Is a Key Determinant of Liver Zonation. *Cell Reports*, 13(9), 1757–1764. <https://doi.org/10.1016/J.CELREP.2015.10.049>
- Ryan, A. R., England, A. R., Chaney, C. P., Cowdin, M. A., Hiltabidle, M., Daniel, E., Gupta, A. K., Oxburgh, L., Carroll, T. J., & Cleaver, O. (2021). Vascular deficiencies in renal organoids and ex vivo kidney organogenesis. *Developmental Biology*, 477, 98–116. <https://doi.org/10.1016/J.YDBIO.2021.04.009>
- SA, H., PH, S., CV, H., YF, C., & D, van V. (1991). Human intrauterine renal growth expressed in absolute number of glomeruli assessed by the disector method and Cavalieri principle. *Laboratory Investigation; a Journal of Technical Methods and Pathology*, 64(6), 777–784. <https://pubmed.ncbi.nlm.nih.gov/2046329/>
- Sawada, H., Stukenbrok, H., Kerjaschki, D., & Farquhar, M. G. (1986). Epithelial polyanion (podocalyxin) is found on the sides but not the soles of the foot processes of the glomerular epithelium. *The American Journal of Pathology*, 125(2), 309. <https://pubmed.ncbi.nlm.nih.gov/7011111/>
- Shi, Y., Sun, L., Wang, M., Liu, J., Zhong, S., Li, R., Li, P., Guo, L., Fang, A., Chen, R., Ge, W.-P., Wu, Q., & Wang, X. (2020). Vascularized human cortical organoids (vOrganoids) model cortical development in vivo. *PLOS Biology*, 18(5), e3000705. <https://doi.org/10.1371/journal.pbio.3000705>
- Short, K. M., & Smyth, I. M. (2016). The contribution of branching morphogenesis to kidney development and disease. *Nature Reviews Nephrology*, 12(12), 754–767. <https://doi.org/10.1038/nrneph.2016.157>
- Song, J. W., & Munn, L. L. (2011). Fluid forces control endothelial sprouting. *Proceedings of the National Academy of Sciences*, 108(37), 15342–15347. <https://doi.org/10.1073/pnas.1105316108>
- Spence, J. R., Mayhew, C. N., Rankin, S. A., Kuhar, M. F., Vallance, J. E., Tolle, K., Hoskins, E. E., Kalinichenko, V. v., Wells, S. I., Zorn, A. M., Shroyer, N. F., & Wells, J. M. (2010). Directed differentiation of human pluripotent stem cells into intestinal tissue in vitro. *Nature* 2010 470:7332, 470(7332), 105–109. <https://doi.org/10.1038/nature09691>
- Sprague, E. A., Luo, J., & Palmaz, J. C. (1997). Human Aortic Endothelial Cell Migration onto Stent Surfaces under Static and Flow Conditions. *Journal of Vascular and Interventional Radiology*, 8(1), 83–92. [https://doi.org/10.1016/S1051-0443\(97\)70521-9](https://doi.org/10.1016/S1051-0443(97)70521-9)

- Srinivas, S., Watanabe, T., Lin, C.-S., William, C. M., Tanabe, Y., Jessell, T. M., & Costantini, F. (2001). Cre reporter strains produced by targeted insertion of EYFP and ECFP into the ROSA26 locus. *BMC Developmental Biology* 2001 1:1, 1(1), 1–8. <https://doi.org/10.1186/1471-213X-1-4>
- Sumida, K., Molnar, M. Z., Potukuchi, P. K., Hassan, F., Thomas, F., Yamagata, K., Kalantar-Zadeh, K., & Kovesdy, C. P. (2018). Treatment of rheumatoid arthritis with biologic agents lowers the risk of incident chronic kidney disease. *Kidney International*, 93(5), 1207. <https://doi.org/10.1016/J.KINT.2017.11.025>
- Taguchi, A., Kaku, Y., Ohmori, T., Sharmin, S., Ogawa, M., Sasaki, H., & Nishinakamura, R. (2014). Redefining the In Vivo Origin of Metanephric Nephron Progenitors Enables Generation of Complex Kidney Structures from Pluripotent Stem Cells. *Cell Stem Cell*, 14(1), 53–67. <https://doi.org/10.1016/J.STEM.2013.11.010>
- Taguchi, A., & Nishinakamura, R. (2015). Nephron reconstitution from pluripotent stem cells. *Kidney International*, 87(5), 894–900. <https://doi.org/10.1038/KI.2014.358>
- Takahashi, Y., Imanaka, T., & Takano, T. (1996). Spatial and temporal pattern of smooth muscle cell differentiation during development of the vascular system in the mouse embryo. *Anatomy and Embryology* 1996 194:5, 194(5), 515–526. <https://doi.org/10.1007/BF00185997>
- Takasato, M., Er, P. X., Chiu, H. S., & Little, M. H. (2016). Generation of kidney organoids from human pluripotent stem cells. *Nature Protocols*, 11(9), 1681–1692. <https://doi.org/10.1038/nprot.2016.098>
- Takasato, M., Er, P. X., Chiu, H. S., Maier, B., Baillie, G. J., Ferguson, C., Parton, R. G., Wolvetang, E. J., Roost, M. S., Chuva de Sousa Lopes, S. M., & Little, M. H. (2015). Kidney organoids from human iPS cells contain multiple lineages and model human nephrogenesis. *Nature*, 526(7574), 564–568. <http://dx.doi.org/10.1038/nature15695>
- Takasato, M., & Little, M. H. (2017). Making a Kidney Organoid Using the Directed Differentiation of Human Pluripotent Stem Cells. *Methods in Molecular Biology*, 1597, 195–206. https://doi.org/10.1007/978-1-4939-6949-4_14
- Takasato, M., Maier, B., & Little, M. H. (2014). Recreating kidney progenitors from pluripotent cells. *Pediatric Nephrology*, 29(4), 543–552. <https://doi.org/10.1007/s00467-013-2592-7>
- Tuttle, K. R., Brosius, F. C., Cavender, M. A., Fioretto, P., Fowler, K. J., Heerspink, H. J. L., Manley, T., McGuire, D. K., Molitch, M. E., Mottl, A. K., Perreault, L., Rosas, S. E., Rossing, P., Sola, L., Vallon, V., Wanner, C., & Perkovic, V. (2021). SGLT2 Inhibition for CKD and Cardiovascular Disease in Type 2 Diabetes: Report of a Scientific Workshop Sponsored by the National Kidney Foundation. *American Journal of Kidney Diseases*, 77(1), 94–109. <https://doi.org/10.1053/J.AJKD.2020.08.003>
- Tzima, E., Irani-Tehrani, M., Kiosses, W. B., Dejana, E., Schultz, D. A., Engelhardt, B., Cao, G., DeLisser, H., & Schwartz, M. A. (2005). A mechanosensory complex that mediates the endothelial cell response to fluid shear stress. *Nature* 2005 437:7057, 437(7057), 426–431. <https://doi.org/10.1038/nature03952>
- Udan, R. S., Vadakkan, T. J., & Dickinson, M. E. (2013). Dynamic responses of endothelial cells to changes in blood flow during vascular remodeling of the mouse yolk sac. *Development*, 140(19), 4041–4050. <https://doi.org/10.1242/DEV.096255>

US Renal Data System 2019 Annual Data Report: Epidemiology of Kidney Disease in the United States EXECUTIVE SUMMARY. (n.d.).

- van den Berge, K., Perraudeau, F., Soneson, C., Love, M. I., Risso, D., Vert, J.-P., Robinson, M. D., Dudoit, S., & Clement, L. (2018). Observation weights unlock bulk RNA-seq tools for zero inflation and single-cell applications. *Genome Biology* 2018 19:1, 19(1), 1–17. <https://doi.org/10.1186/S13059-018-1406-4>
- Vanlandewijck, M., He, L., Mäe, M. A., Andrae, J., Ando, K., del Gaudio, F., Nahar, K., Lebouvier, T., Laviña, B., Gouveia, L., Sun, Y., Raschperger, E., Räsänen, M., Zarb, Y., Mochizuki, N., Keller, A., Lendahl, U., & Betsholtz, C. (2018). A molecular atlas of cell types and zonation in the brain vasculature. *Nature*, 554(7693). <https://doi.org/10.1038/nature25739>
- Vaughan, M. R., & Quaggin, S. E. (2008). How Do Mesangial and Endothelial Cells Form the Glomerular Tuft? *Journal of the American Society of Nephrology*, 19(1), 24–33. <https://doi.org/10.1681/ASN.2007040471>
- Vittet, D., Prandini, M. H., Berthier, R., Schweitzer, A., Martin-Sisteron, H., Uzan, G., & Dejana, E. (1996). Embryonic stem cells differentiate in vitro to endothelial cells through successive maturation steps. *Blood*, 88(9), 3424–3431. <https://doi.org/10.1182/blood.v88.9.3424.bloodjournal8893424>
- Wakui, S., Yokoo, K., Muto, T., Suzuki, Y., Takahashi, H., Furusato, M., Hano, H., Endou, H., & Kanai, Y. (2006). Localization of Ang-1, -2, Tie-2, and VEGF expression at endothelial-pericyte interdigitation in rat angiogenesis. *Laboratory Investigation* 2006 86:11, 86(11), 1172–1184. <https://doi.org/10.1038/labinvest.3700476>
- Wang, R., Clark, R., & Bautch, V. L. (1992). Embryonic stem cell-derived cystic embryoid bodies form vascular channels: an in vitro model of blood vessel development. In *Development* (Vol. 114).
- Wanner, C., Inzucchi, S. E., Lachin, J. M., Fitchett, D., von Eynatten, M., Mattheus, M., Johansen, O. E., Woerle, H. J., Broedl, U. C., & Zinman, B. (2016). Empagliflozin and Progression of Kidney Disease in Type 2 Diabetes. <https://doi.org/10.1056/NEJMoa1515920>, 375(4), 323–334. <https://doi.org/10.1056/NEJMoa1515920>
- What is peritoneal dialysis?* | National Kidney Foundation. (n.d.). Retrieved August 23, 2021, from <https://www.kidney.org/atoz/content/peritoneal>
- Wiles, M. V., & Keller, G. (1991). Multiple hematopoietic lineages develop from embryonic stem (ES) cells in culture. *Development*, 111(2), 259–267. <https://doi.org/10.1242/DEV.111.2.259>
- Wilting, J., & Christ, B. (n.d.). *NATUR WISSENSCHAFTEN Embryonic Angiogenesis: A Review Origin of Endothelial Cells.*
- Xu, C., & Su, Z. (2015). Identification of cell types from single-cell transcriptomes using a novel clustering method. *Bioinformatics*, 31(12), 1974–1980. <https://doi.org/10.1093/BIOINFORMATICS/BTV088>
- Yamazaki, T., & Mukoyama, Y. (2018). Tissue Specific Origin, Development, and Pathological Perspectives of Pericytes. *Frontiers in Cardiovascular Medicine*, 0, 78. <https://doi.org/10.3389/FCVM.2018.00078>
- Young, M. D., Mitchell, T. J., Vieira Braga, F. A., Tran, M. G. B., Stewart, B. J., Ferdinand, J. R., Collord, G., Botting, R. A., Popescu, D. M., Loudon, K. W., Vento-Tormo, R., Stephenson, E.,

- Cagan, A., Farndon, S. J., Velasco-Herrera, M. D. C., Guzzo, C., Richoz, N., Mamanova, L., Aho, T., ... Behjati, S. (2018). Single-cell transcriptomes from human kidneys reveal the cellular identity of renal tumors. *Science*, *361*(6402), 594–599. <https://doi.org/10.1126/SCIENCE.AAT1699>
- Yu, J., Carroll, T. J., & McMahon, A. P. (2002). Sonic hedgehog regulates proliferation and differentiation of mesenchymal cells in the mouse metanephric kidney. *Development*, *129*(22), 5301–5312. <https://doi.org/10.1242/DEV.129.22.5301>
- Zeng, Z., Huang, B., Parvez, R. K., Li, Y., Chen, J., Vonk, A. C., Thornton, M. E., Patel, T., Rutledge, E. A., Kim, A. D., Yu, J., Grubbs, B. H., McMahon, J. A., Pastor-Soler, N. M., Hallows, K. R., McMahon, A. P., & Li, Z. (2021). Generation of patterned kidney organoids that recapitulate the adult kidney collecting duct system from expandable ureteric bud progenitors. *Nature Communications* *2021 12:1*, *12*(1), 1–15. <https://doi.org/10.1038/s41467-021-23911-5>
- Zhang, Y. S., Pi, Q., & Genderen, A. M. van. (2017). Microfluidic Bioprinting for Engineering Vascularized Tissues and Organoids. *JoVE (Journal of Visualized Experiments)*, *2017*(126), e55957. <https://doi.org/10.3791/55957>
- Zoetis, T., & Hurtt, M. E. (2003). Species comparison of anatomical and functional renal development. *Birth Defects Research Part B: Developmental and Reproductive Toxicology*, *68*(2), 111–120. <https://doi.org/10.1002/BDRB.10013>
- Zudaire, E., Gambardella, L., Kurcz, C., & Vermeren, S. (2011). A Computational Tool for Quantitative Analysis of Vascular Networks. *PLOS ONE*, *6*(11), e27385. <https://doi.org/10.1371/JOURNAL.PONE.0027385>